

# **Low avidity CD8<sup>+</sup> T cells in viral infection: from neuroinflammation to adoptive T cell therapy**

A thesis submitted to attain the degree of  
**DOCTOR OF SCIENCES of ETH ZURICH**  
**(Dr.sc ETH Zurich)**

presented by

**JOVANA CUPOVIC**

Dipl. Mol. Biol. and Physiol.,  
University of Belgrade

born on 30. April 1984

Republic of Serbia

accepted on the recommendation of

Prof. Dr. Wolf-Dietrich Hardt

Prof. Dr. Burkhard Ludewig

Prof. Dr. Annette Oxenius

2014



*To my Dad,*

*I will always miss you!*



# Table of Contents

<b>1</b>	<b>Summary.....</b>	<b>1</b>
<b>2</b>	<b>Zusammenfassung .....</b>	<b>3</b>
<b>3</b>	<b>General Introduction.....</b>	<b>6</b>
3.1	General principles of the immune system .....	6
3.2	T cells biology .....	8
3.2.1	T cell development.....	8
3.2.2	CD8 vs. CD4 lineage commitment .....	12
3.3	$\alpha\beta$ TCR receptor complex .....	13
3.3.1	Structure of $\alpha\beta$ TCR molecular complex .....	13
3.3.2	TCR recombination – diversification of the defense arsenal.....	15
3.3.3	TCR signaling – T cell fate determined by the signal strength.....	18
3.3.3.1	TCR triggering models.....	18
3.3.3.2	Components of the TCR signaling pathway the TCR “signalosome” .....	21
3.3.3.3	Regulation of TCR signaling – implications for TCR sensitivity and specificity .....	25
3.3.4	CD8 <sup>+</sup> T cell activation and effector functions .....	28
3.3.4.1	CD8 <sup>+</sup> T cell activation .....	28
3.3.4.2	CD8 <sup>+</sup> T cell effector mechanisms .....	30
3.3.4.3	Helping the killer – CD8 <sup>+</sup> T cell responses tuned by CD4 <sup>+</sup> T cells and cytokines .....	32
3.3.5	Model systems to study T cell biology.....	34
3.4	Immunity in the CNS - focus on T cell-mediated protection .....	36
3.4.1	Anatomic structure of the brain .....	36
3.4.2	Blood brain barrier and immune privilege .....	38
3.4.3	T cell migration to and regulation of their function within the CNS.....	40
3.5	Neurotropic virus infections .....	43
3.5.1	Coronaviruses - Mouse hepatitis virus (MHV).....	44
3.5.1.1	Coronaviridae .....	44
3.5.1.1.1	Mouse hepatitis virus (MHV).....	46
3.5.1.1.2	Immune responses to MHV .....	47

<b>4 Aims of the study .....</b>	<b>49</b>
<b>5 Characterization of a murine coronavirus spike protein-specific TCR and generation of TCR transgenic mice .....</b>	<b>50</b>
5.1 Abstract.....	50
5.2 Introduction .....	51
5.3 Materials and Methods .....	52
5.4 Results.....	58
5.4.1 Characterization of a MHV A59 spike protein <sub>(598-605)</sub> specific TCR .....	58
5.4.2 Generation of MHV spike protein- specific transgenic mice.....	60
5.4.3 Comparison of transgenic TCR expression in the different founder lines .....	62
5.4.4 Functional assessment of TCR transgenic CD8 <sup>+</sup> T cells .....	63
5.5 Discussion .....	65
5.6 Acknowledgments .....	67
5.7 Data contribution .....	67
<b>6 Extra-lymphatic CCR7-ligand expression controls virus-induced CNS inflammation .....</b>	<b>68</b>
6.1 Abstract.....	68
6.2 Introduction .....	70
6.3 Materials and Methods .....	73
6.4 Results.....	77
6.4.1 CNS-restricted MHV infection drives strong induction of CCR7 ligands within CNS tissue .....	77
6.4.2 Mapping of CCL19 and CCL21 producing cells in the MHV-infected CNS.....	79
6.4.3 CCR7 expression is essential for successful control of neurotropic MHV infection.....	81
6.4.4 CCR7-proficiency of CD8 <sup>+</sup> T cells protects against viral CNS infection .....	83
6.4.5 CNS-restricted expression of CCR7 ligands is sufficient to provide CD8 <sup>+</sup> T cell-mediated immunity .....	86
6.5 Discussion .....	88
6.5.1.1 Supplementary material.....	91
6.6 Acknowledgments .....	93
6.7 Data contribution .....	93
<b>7 Tuning the functional avidity of virus-specific CD8<sup>+</sup> T cells.....</b>	<b>94</b>
7.1 Abstract.....	94

7.2	Introduction.....	96
7.3	Material and Methods .....	98
7.4	Results.....	108
7.4.1	Polyclonal low avidity CD8 <sup>+</sup> T cell responses during MHV infection .....	108
7.4.2	Generation of s598-specific TCR retrogenic CD8 <sup>+</sup> T cells .....	109
7.4.3	Tunable expression of the s598-specific TCR .....	112
7.4.4	TCR density determines T cell activation threshold .....	114
7.4.5	Modeling TCR density-dependent CD8 <sup>+</sup> T cell behavior.....	115
7.4.6	In vivo protective capacity TCR retrogenic CD8 <sup>+</sup> T cells.....	118
7.5	Discussion .....	120
7.6	Acknowledgments .....	124
7.7	Data contribution .....	124
<b>8</b>	<b>Discussion.....</b>	<b>125</b>
8.1	Selecting an appropriate system to study T cell biology.....	125
8.2	Underestimated efficacy of low avidity CD8 <sup>+</sup> T cells.....	126
8.3	CCR7 ligands control CD8 <sup>+</sup> T cells during CNS inflammation.....	128
8.4	Varying the strength of TCR engagement – implications for adoptive T cell therapy 131	
<b>9</b>	<b>Appendix.....</b>	<b>134</b>
9.1	Literature.....	134
9.2	Figure legend.....	155
9.3	Abbreviations .....	156
9.4	Acknowledgments .....	160
9.5	Curriculum Vitae .....	163
9.6	Bibliography .....	<b>Error! Bookmark not defined.</b>





# 1 Summary

CD8<sup>+</sup> T cells play a critical role in antiviral immunity. The type of the functional response elicited upon the activation of the particular CD8<sup>+</sup> T cell is predominantly determined by the strength of the signal received through the T cell receptors (TCR). CD8<sup>+</sup> T cells can be activated by low levels of antigen, hence high avidity CD8<sup>+</sup> T cells have been preferable choice for adoptive T cell therapy. However, low avidity CD8<sup>+</sup> T cells may as well exert potent effector function, albeit with a different activation threshold. Therefore, a better understanding of the biology of low avidity CD8<sup>+</sup> T cell responses is necessary to complement our knowledge on T cell biology in general, and improve T cell-based treatments.

To dissect the role of low avidity CD8<sup>+</sup> T cell during cytopathic viral infection, we have cloned and characterized a MHC I-restricted TCR specific for the spike protein of mouse hepatitis virus (MHV). In the first part of the presented work, we have described the generation of MHV-specific TCR-transgenic mice named Spiky. Analysis of the transgene expression showed that >98% of peripheral CD8<sup>+</sup>T cells express the functional MHV-specific TCR. Functional assays of Spiky transgenic CD8<sup>+</sup> T cells showed that rather high levels of peptide are needed to allow the activation of the cells, indicating low functional avidity.

In the second part of the work, central nervous system (CNS) infection with MHV facilitated dissection of the mechanisms that regulate recruitment of CD8<sup>+</sup>T cell to the inflamed CNS. We found that the expression of the constitutive chemokines CCL19 and CCL21 was dramatically enhanced during MHV-induced neuroinflammation. Both endothelial cells of blood vessels and fibroblastic stromal were major sources of the CCR7 ligands. Importantly, complete abrogation of the CCR7-axis lead to drastic impairment of antiviral T cell responses in the CNS and had fatal consequences. CCR7-proficient Spiky cells provided protection

against the viral CNS infection in CCR7-deficient mice. Furthermore, extra-lymphatic expression of CCR7 ligands was sufficient to allow optimal recruitment of antiviral CD8<sup>+</sup> T cells and control of the virus. Taken together, the second part of the thesis revealed a critical role of CCR7-ligands expressed in the CNS for regulating recruitment and functionality of antiviral CD8<sup>+</sup>T cells in this organ.

In the third part of the thesis, we have addressed the consequences variation of TCR density has on T cell function. To achieve graded expression of the MHV-specific TCR, we utilized retrogenic mouse approach. Combining CFSE-based in vitro proliferation assay with mathematical modeling, and in vivo assays, we have assessed performance of T cells expressing different numbers of structurally the same TCR. Our results indicated the existence of two different TCR density thresholds that critically impinge on T cell activation and performance. While the first threshold was defined by the minimal numbers of expressed TCRs needed to allow activation of T cells, the second threshold defines the maximal numbers of TCR that can still guarantee optimal T cell activation resulting in protective responses. TCR expression above the second threshold level resulted in aberrant behavior of antiviral T cells leading to loss of the protective function. These findings indicate first that adoptive T cell therapy can rely on a rather broad TCR surface density window to secure optimal performance of the T cells. Second, this study shows that the rheostat function of TCR-mediated signals may reach a particular biological limit that must be taken in consideration for the design of successful and safe adoptive T cell therapy.

## 2 Zusammenfassung

Während einer antiviralen Immunantwort spielen  $CD8^+$  T-Zellen eine entscheidende Rolle. Die funktionelle Antwort, welche nach der Aktivierung einer bestimmten T-Zelle ausgelöst wird, ist vor allem über die Stärke des Signals, welches jede einzelne  $CD8^+$  T-Zelle durch ihren T-Zell-Rezeptor erhält, definiert. Bereits geringe Mengen an Antigen können ausreichend sein, um zu einer  $CD8$ -T-Zellaktivierung zu führen. Bei adoptiven T-Zell-Therapien waren daher  $CD8$ -T-Zellen, welche eine hohe Bindungsfähigkeit aufwiesen, die erste Wahl. Dennoch könnten auch  $CD8$ -T-Zellen mit einer niedrigen Bindungsfähigkeit wirksame Effektorfunktionen ausführen, auch wenn sie über einen anderen Aktivierungsschwellenwert verfügen. Auf Grund dessen ist ein tiefer greifendes Verständnis der Biologie von T-Zellantworten ausgehend von  $CD8$ -T-Zellen mit niedriger Bindungsfähigkeit nötig, um das bereits bestehende Wissen der generellen T-Zell-Biologie zu ergänzen und T-Zell-Therapien zu optimieren.

Um die Rolle aufzuschlüsseln, welche  $CD8$ -T-Zellen mit niedriger Bindungsfähigkeit während einer zytopathischen Virusinfektion spielen, wurde von uns ein für das Spike Protein des Maus-Hepatitis-Virus (MHV) spezifischer und auf MHC I beschränkter T-Zell-Rezeptor kloniert und charakterisiert.

Im ersten Teil der vorliegenden Dissertation wird die Erzeugung von transgenen Mäusen, den sogenannten Spikys, welche einen MHV spezifischen T-Zell-Rezeptor besitzen, beschrieben. Die Untersuchung der Transgenexpression zeigte, dass >98% der peripheren  $CD8$ -T-Zellen den MHV spezifischen T-Zell-Rezeptor exprimieren. Funktionelle Untersuchungen der transgenen Spiky  $CD8$ -T-Zellen wiesen darauf hin, dass relativ hohe

Peptidkonzentrationen nötig sind, um die T-Zell-Aktivierung herbeizuführen und die damit eine niedrige funktionelle Bindungsfähigkeit aufweisen.

Im zweiten Teil dieser Arbeit ermöglichte die MHV- Infizierung des Zentralen Nervensystems (ZNS) den Mechanismus aufzuschlüsseln, welcher die Rekrutierung der CD8-T-Zellen in das entzündete zentrale Nervensystem steuert. Während einer MHV induzierten Neuroentzündung, fanden wir eine drastisch erhöhte Expression der konstitutiven Chemokine CCL19 und CCL21. Sowohl die Endothelzellen der Blutgefäße als auch stromale Fibroblasten waren Hauptquellen der CCR7 Liganden. Bemerkenswerterweise führte das Ausserkraftsetzen der CCR7-Achse zu einer drastischen Beeinträchtigung der antiviralen T-Zell-Antworten innerhalb des ZNS; mit fatalen Konsequenzen. In CCR7 defizienten Mäusen vermittelten CCR7 kompetente Spiky Zellen den Schutz gegen virale ZNS-Infektionen. Des Weiteren waren ausser-lymphatische Freisetzungen der CCR7 Liganden ausreichend, um eine optimale Rekrutierung von antiviralen CD8-T-Zellen und die Eindämmung des Virus zu gewährleisten.

Zusammengefasst, legte der zweite Teil dieser Doktorarbeit eine entscheidende Funktion der im ZNS exprimierten CCR7-Liganden offen. Diese steuern die Rekrutierung und Funktionalität der antiviralen CD8-T-Zellen in dieses Organ.

Im dritten Teil dieser Doktorarbeit wurden die Folgen von Dichtevariationen des T-Zell-Rezeptors auf die T-Zell-Funktion untersucht. Um eine gestaffelte Expression des MHV spezifischen T-Zell-Rezeptors zu erreichen, wurde der Retrogene-Maus-Ansatz benutzt. Durch die Kombination von CFSE-basierten in vitro Proliferationsexperimenten mit mathematischen Modellberechnungen und in vivo Experimenten konnte die Effizienz von T-Zellen, mit unterschiedlichen Anzahlen eines strukturell einheitlichen T-Zell-Rezeptors, beurteilt werden.

Das erzielte Resultat offenbarte, dass zwei verschiedene, in Abhängigkeit von der T-Zell-Rezeptor-Dichte stehende, Schwellenwerte existieren, welche sich entscheidend auf die T-Zell-Aktivierung und T-Zell-Effizienz auswirken.

Während sich der erste Schwellenwert durch die minimale Anzahl der exprimierten T-Zell-Rezeptoren auszeichnet, welche für die Aktivierung von T-Zellen nötig sind, definiert der Zweite die maximale Anzahl von T-Zell-Rezeptoren, die benötigt sind, um eine optimale T-Zell-Aktivierung und folglich eine schützende Immunantwort zu garantieren. Eine über dem zweiten Schwellenwert liegende T-Zell-Rezeptoren-Expression führte zum abnormen Verhalten der antiviralen T-Zellen mit einhergehendem Verlust der schützenden Funktion.

Diese Forschungsergebnisse weisen darauf hin, dass erstens der Erfolg der T-Zell-Therapie von einem eher breit gesteckten Rahmen der T-Zell-Rezeptoren-Oberflächendichte abhängt, welche die optimale Effizienz der T-Zellen definiert.

Zweitens zeigt diese Studie, dass die Widerstandsfunktion des T-Zell-Rezeptors abhängigen Signals eine definierte biologische Grenze erreichen könnte, welche bei der Entwicklung einer erfolgreichen und sicheren adoptiven T-Zell-Therapie in Betracht gezogen werden muss.

### **3 General Introduction**

#### **3.1 General principles of the immune system**

Parallel to the evolution of pathogens, the immune system has evolved into a complex network of multiple effectors that exert their action in a synchronized fashion to protect the body from intruders. The immune system consists of two main branches: innate and adaptive. The innate immune system provides the first line of defense activated immediately after the recognition of pathogens. To achieve this, the innate system uses a limited number of germ line-encoded receptors that are able to distinguish between common molecular structures found on pathogens which are termed pathogen associated molecular patterns- PAMPs (e.g. lipopolysaccharide, double stranded RNA) and those present in the body. These receptors belong to three main types of pattern recognition receptors (PRR): endocytic receptors expressed on the cell surface, signaling receptors expressed either intracellularly or on the cell surface and humoral proteins circulating in plasma (Medzhitov and Janeway, 1998). Communication between the innate and the adaptive branch of the immune system is achieved through secretion of inflammatory mediators that enhance the activation of the adaptive immune system and direct its function. The adaptive immunity relies on the usage of polymorphic receptors that cover the broad range of different antigens. The function of the adaptive immune system relies on two types of lymphocytes: T and B lymphocytes. Activation of T cells starts with recognition of peptide fragments processed and presented on major histocompatibility complex (MHC) molecules on the surface of antigen presenting cells (APCs) (Townsend and Bodmer, 1989). Additional signals received during interaction with APCs (Signal 2) and the surrounding inflammatory milieu (signal 3) are necessary to allow proper activation of these cells (Reis e Sousa et al., 1997). Two main

types of T cells are responsible for performing the tasks of the cellular arm of the adaptive system. While  $CD8^+$  T cells facilitate elimination of intracellular pathogens mainly using contact-dependent cytolytic pathways,  $CD4^+$  T cells are able to secrete a wide range of soluble mediators and are involved in regulation and execution of a broad range of functions. Depending on the signature cytokine responsible for their function,  $CD4^+$  T cells are assigned to different lineages. One of the main functions of  $CD4^+$  T cells is to support other cellular components in their functions, thus directing different elements of the immune response. For example,  $CD4^+$  T helper cells contribute substantially to development of successful  $CD8^+$  T cell responses (Bevan, 2004) and are also crucial for the optimal function of humoral immunity (Crotty, 2011). Recognition of antigens in their native structure by the B cell receptor (BCR) leads to activation of B cells that are responsible for production of soluble antibodies (Treanor, 2012). Secreted antibodies exert their effector function via neutralization, opsonization and complement activation. Unlike the innate immune system, the adaptive immune system is able to exhibit memory responses to antigens it had been exposed to. This feature allows higher functionality and faster eradication of pathogens following subsequent encounter. The highly complex network of cellular interactions within the immune system relies on the specific structure of secondary lymphoid organs (SLO) that generate optimal microenvironments for different types of interactions and hence supports development of protective immune responses.

## 3.2 T cells biology

### 3.2.1 T cell development

The arrival of lymphoid progenitor cells to the thymus starts with embryonic day 11.5 (E11.5) in mice and at eighth weeks of gestation in humans (Owen and Ritter, 1969). During the early stage of embryonic development, i.e. before the vascularization of the thymus, settlement of the incoming progenitors relies on chemotactic attraction mainly provided by the chemokines CCL21 and CCL25 (Liu et al., 2005; Wurbel, 2001). Vasculature-dependent immigration takes place during later stages of embryogenesis and in the postnatal phase. Lymphoid progenitors that colonize the postnatal thymus transmigrate from the blood and enter the thymic parenchyma through blood vessels in the cortico-medullary junction (Lind et al., 2001). While the role of chemokines in seeding the postnatal thymus is still unclear, seeding of the adult thymus is regulated by interactions between platelet selectin glycoprotein ligand 1 (PSGL1) expressed on circulating lymphoid progenitor cells and P-selectin expressed by thymic vascular endothelium (Rossi et al., 2005). Once in the thymus, early T cell lineage progenitors (ETP) will start their developmental pathway fostered by extensive interactions with stromal cells of the thymic microenvironment that provide signals to drive the thymocyte differentiation program. Migration of developing thymocytes through the different thymic microenvironments appears to be crucial for establishment an orderly sequence of thymocyte development. The initial 'pro-T-cell' stage of CD4<sup>-</sup>CD8<sup>-</sup> thymocyte development is independent of TCR signaling and covers stages from ETP to double negative stage 3 (DN3) (Rothenberg et al., 2008). 'Pro-T cell' stages of thymocytes are characterized by the differential expression of CD25, CD44 and CD117 with the ETP (DN1) cell being CD25<sup>-</sup>CD44<sup>+</sup>CD117<sup>+</sup>. Transition of ETP to DN2 will take place after cells have spent ~10 days within the perimedullary cortex, going through several rounds of proliferation.



The Notch signaling pathway together with homeostatic feedback signals influence the final decision of ETP transition to the DN2 stage which is associated with chemokine receptor CXCR4, CCR7 and CCR5 mediated translocation to the inner cortex of the thymus (Hernandez-Lopez, 2002; Ara et al., 2003). Thymocytes in development stage DN2 are characterized by the  $CD25^+CD44^+CD117^+$  phenotype and continue with massive proliferation. In this stage, the cells are still highly dependent on Notch signaling. After ~2 days spent within the inner cortical area, DN2 thymocytes will start a CCL25 and CXCL12 chemokine-driven translocation to the area of outer cortex where they will acquire functional and phenotypic characteristics of DN3 stage thymocytes characterized by  $CD25^+CD44^{lo}CD117^{lo}$  expression. Signals received from the cortical microenvironment determine the irreversible commitment of DN3 thymocytes to the T cell lineage. While losing all non-T cell developmental options, thymocytes will reduce their proliferation rate and start the process of TCR $\beta$  rearrangement as a hallmark of DN3 stage. While expression of RAG genes in lymphoid progenitors can contribute to earlier induction of TCR $\gamma$  and TCR $\delta$  rearrangement, the TCR $\beta$  locus will become accessible for rearrangement only at the DN3 stage, therefore allowing for the final commitment to the  $\alpha\beta$  or the  $\gamma\delta$  T cell lineage. The movement of DN3 cells to the subcapsular zone coincides with a critical developmental transition from the DN to  $CD4^+CD8^+$  (double positive, DP) stage. Survival of cells transiting from DN to DP stage depends on successful, in-frame rearrangement of at least one TCR $\beta$  allele. Cells that fail to successfully rearrange either TCR $\beta$  allele die at this point, whereas surviving cells begin to express the immature form of the T cell receptor (preTCR) on their surfaces. Extensive proliferation of preTCR expressing cells accounts for massive increase in population of preDP cells that now highly upregulate expression of CD4 and CD8. At this stage, preT cells will start recombination on  $\alpha$  TCR locus that will lead to expression of a functional  $\alpha\beta$  TCR and subsequent migration to the inner cortex. This stage of intrathymic development is associated with profound changes in developmental program of T cells, i.e. the subsequent stages will not be dependent on Notch signaling. Thymocytes in cortex at

this stage are highly motile while still intensively interacting with stromal cells, such as cTECs or dendritic cells (Bousso et al., 2002).

The nature of the interaction between peptide-MHC presented by non-hematopoietic (radio-resistant) cells in the cortical region of the thymus and the TCR expressed by DP thymocytes decides the fate of developing T cells in a process known as positive selection. Low affinity interaction between the TCR and MHC molecules loaded with self-peptides presented by cTECs will ensure survival of DP thymocytes with potentially useful TCRs. In contrast, those bearing an MHC-independent TCR will be removed and “die by neglect”. Positively selecting signals are received by only 3-5% of developing thymocytes (Goldrath and Bevan, 1999; Egerton et al., 1990). The process of positive selection will result in the generation of single positive (SP) thymocytes with defined CD4 or CD8 lineage commitment. TCR-mediated signals involved in positive selection induce expression of CCR7 on positively selected SP thymocytes that allows these cells to migrate towards CCL19/CCL21-producing epithelial cells of the thymic medullary region (Petrie and Zúñiga-Pflücker, 2007). Within the medulla, maturation of SP thymocytes is accompanied by deletion of potentially self-reactive thymocytes through the process of negative selection that ensures central tolerance to tissue-specific antigens. While positive selection is dependent on a large number of low affinity TCR-pMHC interactions, negative selection depends on low numbers of high-affinity TCR interactions which lead to elimination of thymocytes bearing self-reactive TCRs (Palmer and Naehre, 2009). Medullary thymic epithelial cells (mTECs) play a dominant role in negative selection by allowing ectopic expression of non-thymic tissue antigens under the control of the transcription factor autoimmune regulator (AIRE) (Zuklys et al., 2000). Nevertheless, successful negative selection demands cooperation between mTECs and DCs. Given the function of DCs as professional antigen presenting cells, cross-presentation of tissue-specific self-antigens supplied to DCs by mTECs contributes to fine-tuning of the selection process (Klein et al., 2009). Additionally, mTECs and thymic DCs have been reported to contribute to conversion of potentially self-reactive thymic T cell to natural T regulatory cells (T regs) (Kyewski and Derbinski, 2004).

Finally, emigration of mature thymocytes from the thymus is an active process that depends on the developmental stage of the organism and is regulated by two different G-protein coupled receptors. While thymocyte emigration in newborn mice relies on CCR7-dependent signals, sphingosine-1-phosphate receptor 1 (S1P1) expression is required for emigration of developed SP thymocytes from the adult thymus (Matloubian et al., 2004). Mature thymocytes exit the thymus through the perivascular space and are funneled into post-capillary venules, arterioles and lymphatics.

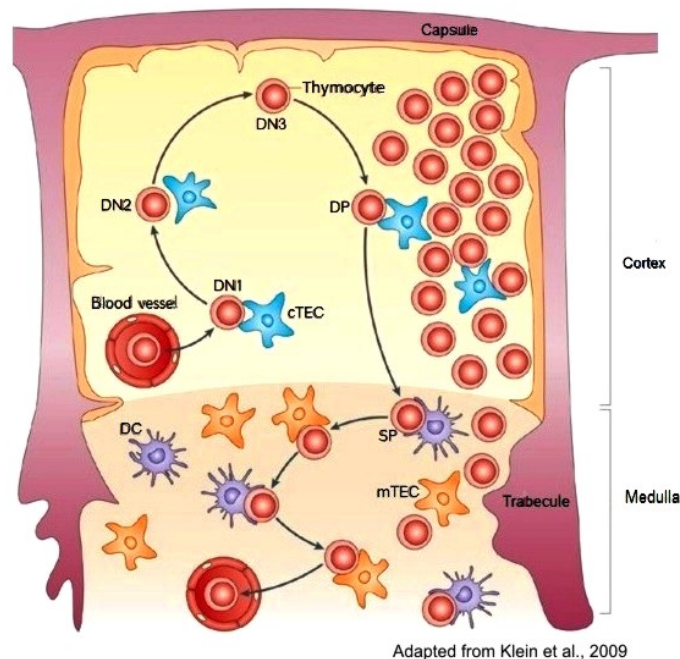


**Figure 1. T cell development.**

T cell progenitors enter the thymus through blood vessels near the cortico-medullary junction. During development double-negative (DN) thymocytes move towards the sub-capsular zone in the outer cortex, where they start rearranging TCR  $\beta$  locus. Following TCR expression, double-positive (DP) cells randomly move through the cortex and scan cortical thymic epithelial cells (cTECs) for positively selecting ligands. Selected thymocytes undergo CD4 or CD8 lineage commitment and relocate to the medulla of the thymus where process of negative selection takes place. Single-positive (SP) thymocytes bearing TCRs that establish high affinity interactions with presented peptide-MHC complexes are deleted from the thymus. Those thymocytes that survive exit the thymus and seed the periphery.

### 3.2.2 CD8 vs. CD4 lineage commitment

The thymic environment not only helps in eliminating the majority of self-reactive T cells, but also determines CD4 vs. CD8 lineage commitment. Over the years, many models have been developed to explain the mechanism of early T cell lineage-fate decision including classical models such as “stochastic selection model” (Leung et al., 2001; Davis et al., 1993), “strength-of-the signal instructional model” (Itano et al., 1996) and “duration-of-signal instructional” (Yasutomo et al., 2000) or “kinetic signaling model” (Brugnera et al., 2000). Currently, the non-classical, kinetic signaling model is considered as the best one to explain the mechanism of CD4/CD8 lineage choice. In short, this model proposes that the lineage choice is made based on two different types of signals where prolonged TCR signaling will result in CD4 lineage differentiation, while signaling through cytokine-receptors will influence CD8 lineage decision (Singer et al., 2008). Indeed, TCR-signaling in DP thymocytes will result in termination of *Cd8* gene transcription, regardless of MHC-restriction specificity of the TCR, while *Cd4* gene transcription remains unchanged (Brugnera et al., 2000). Resulting CD4<sup>+</sup>/CD8<sup>low</sup> cells remain lineage-uncommitted with preserved potential to differentiate to both CD4 and CD8 T cells. At this stage, if there is continued signaling through the TCR after abortion of *Cd8* gene transcription, thymocytes will receive the confirmation that TCR-pMHC interaction is not CD8 dependent and will make the CD4 lineage choice.

Following persistent TCR signaling, CD4<sup>+</sup>CD8<sup>low</sup> cells will upregulate the level of the Th-POK transcriptional factor (T-helper-inducing POZ/Kruppel-like factor) which will ensure differentiation into CD4 T cell lineage by maintaining *Cd4* transcription and further decreasing *Cd8* gene expression. In an alternative scenario, cessation of TCR signaling in the absence of *Cd8* gene transcription will indicate dependency of TCR signaling on CD8 expression and will drive CD8 lineage choice (Sun et al., 2005; He et al., 2005). The final differentiation of CD8-committed CD4<sup>+</sup>CD8<sup>low</sup> thymocytes into CD8<sup>+</sup> T cells involves the process of “co-receptor reversal” which will ensure termination of *Cd4* and reinitiating of *Cd8* gene

transcription (Brugnera et al., 2000). The process of co-receptor reversal crucially relies on signals received through IL-7 and possibly other  $\gamma$ c intrahymic cytokines (Yu et al., 2003; Brugnera et al., 2000). While prolonged TCR signaling prevents intermediate thymocytes from undergoing co-receptor reversal in response to IL-7, only CD8-dependent DP thymocytes that are not able to receive the signal through the TCR will be permissive to IL-7 signaling and therefore undergo co-receptor reversal. During this process signals received through IL-7R will lead to increased activity of the E81 enhancer (transcriptional regulator of *Cd8a* expression) and gene transcription of *Cd8a* (Singer et al., 2008). The transcription factor RUNX3 (runt-related transcriptional factor 3) upregulated in  $CD4^+CD8^{low}$  thymocytes undergoing  $CD8^+$  T cells differentiation has been involved in reinitiation of *Cd8* expression and further silencing of *Cd4* gene translation therefore promoting final differentiation into  $CD8^+$  T cells (Sato et al., 2005; Grueter et al., 2005).

### 3.3 $\alpha\beta$ TCR receptor complex

#### 3.3.1 Structure of $\alpha\beta$ TCR molecular complex

The TCR  $\alpha\beta$  molecule is a dimer composed of two chains, each of them consisting of the N terminal part known as variable (V) region, followed by the non-polymorphic constant (C) region. The variable region contains three hypervariable elements termed complementary-determining regions 1-3 (CDRs) that in large define the specificity of TCR-pMHC interactions. In addition to the constant region, there is a short connecting sequence containing a double cysteine bond that stabilizes the connection between the two chains. A short transmembrane sequence of 21 to 22 amino acids anchors each of the chains into the membrane and is followed by a short intracellular sequence composed of 5-12 amino acids. Transmembrane

regions of both  $\alpha$  and  $\beta$  TCR chains contains amino acids with positive charge that allow for successful interaction with the CD3 complex. This complex consists of five invariant chains that are organized to form three heterodimers:  $\gamma\epsilon$  (gamma-delta),  $\delta\epsilon$  (delta-epsilon) and  $\zeta\eta$  (zeta-eta). The invariant chain  $\eta$  in  $\zeta\eta$  (zeta-eta) heterodimer is frequently replaced with its splicing variant  $\xi$ , leading to homodimer -  $\zeta\zeta$ . Each invariant chain consists of extracellular domain followed by a short transmembrane region composed of negatively charged amino acids and an intracellular tail that contains immunoreceptor tyrosine-based activation motif (ITAM)(Call and Wucherpfennig, 2004). Expression of the CD3 complex is a prerequisite for stable expression of the  $\alpha\beta$  TCR dimer on the surface of the T cell membrane. Finally, the co-receptor molecules CD4 and CD8 represent important members of TCR molecular complex. Mature T cell express one of the co-receptors based on the decision made during intrathymic development that determines final lineage commitment of T cells and sets the stage for its defined behavior as mature  $CD4^+$  or  $CD8^+$  T cell. Although expressed on different cell subsets, the function of the two co-receptors is comparable. Binding of CD8 to conserved regions of MHC I or CD4- binding to conserved regions of MHC II increase the avidity of TCR-pMHC interaction and stabilizes the complex. However, these two molecules are structurally quite distinct. While CD4 is a single molecule with a long extracellular domain composed of four immunoglobulin-like structures, a short transmembrane domain and a short cytoplasmic domain, CD8 is made up of two ( $\alpha\alpha$  or  $\alpha\beta$ ) molecules each with one immunoglobulin (Ig)-like domain and a long stalk, a transmembrane region and short cytoplasmic tail. Overall, the TCR complex represents a multi-molecular structure that has evolved over time to provide distinction of self from non-self structures. Nevertheless, the dependency of TCR signaling on many other molecules present on the membrane of T cells requires fine-tuning of signals received through the TCR for generating the optimal and safe immune responses.

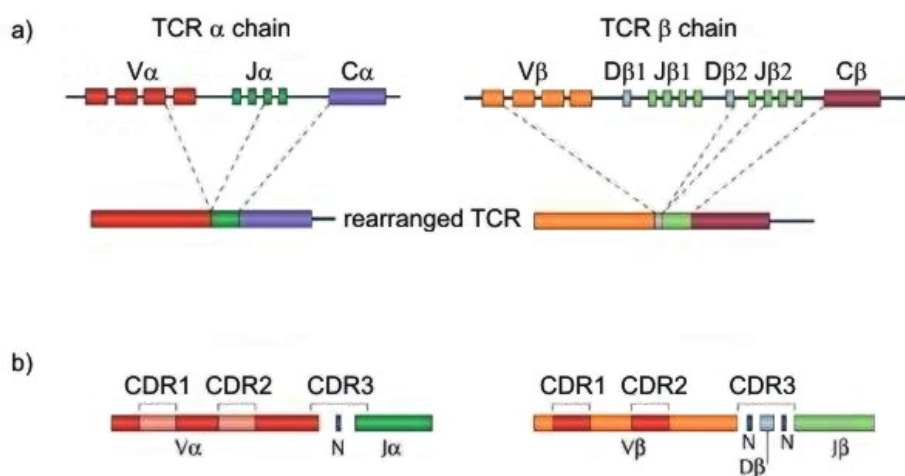
### 3.3.2 TCR recombination – diversification of the defense arsenal

The ability of the immune system to provide protection against the high variability of pathogens relies on the outstanding potential of lymphocytes to convert a limited number of germline-encoded gene fragments into an almost unlimited repertoire of receptor molecules. Through the process of V(D)J recombination that takes place in developing lymphocytes up to  $1 \times 10^{15}$  different  $\alpha\beta$  TCR receptors could be formed (Davis and Bjorkman, 1988). However, as a mouse contains  $\sim 2 \times 10^8$  T cells and at least some T cells that express the same TCR, the number of different TCRs present at one time in a mouse is estimated to  $\sim 2 \times 10^6$  (Casrouge et al., 2000).

Estimated diversity of TCR repertoire in mice relies on the combination of several different mechanisms. The process of V(D)J recombination of 71 variable (V) and 51 joining (J) segments within the  $\alpha$  chain locus on mouse chromosome 14 leads to  $3 \times 10^3$  possible combinations for only the  $\alpha$  chain. Furthermore, 35 different V segments on  $\beta$  chain locus on chromosome 6 can be combined with 2 D (diversity) and 12 J to giving rise to 460 possible combinations (Turner et al., 2006). As the antigen-binding specificity of the TCR depends on the combination of variable regions of both chains, random association of  $\alpha$  and  $\beta$  chains leads to further increase in  $\alpha\beta$  TCRs diversity.

Lack of precision during V(D)J recombination is another mechanism attributing to further diversification of the TCR repertoire. V(D)J recombination is the process that takes place exclusively in developing lymphocytes and relies on the activity of recombination-activating genes (RAG)-1 and -2. Acting synergistically, these two enzymes recognize recombination signal sequences (RSSs) that flank each germ-line V, D or J elements and bring them into proximity. RSS sequences consist of highly conserved palindromic heptamer or AT-rich nonamer that are separated by either 12 (one turn RSS) or 23 base pairs (two turn RSS) (Fugmann et al., 2000). Specific distribution of two types of RSSs and the rule that the same type of the sequences cannot be brought together ensures the sequence of V(D)J

recombination. RAG enzymes catalyze one strand DNA cleavage at the junction of the signal and the coding sequence giving rise to hairpin structures at the ends of two coding sequences. Opening of the hairpin structure achieved through unspecific action of endonucleases leads to generation of uneven DNA ends that are corrected by addition of palindromic P-nucleotides or trimming of the nucleotides by single-strand endonuclease. Cut ends of DNA are then exposed to addition of up to six nucleotides by action of terminal deoxynucleotid transferase (TdT) (Komori et al., 1993). Finally, two coding sequences are connected through normal double strand break repair (NDBR) while noncoding sequences are removed. Imprecise by nature, the process of physical binding of coding elements brought together by gene rearrangement further contributes to TCR diversity. Unspecific addition and removal of nucleotides from the junction regions creates highly polymorphic complementary determining regions (CDR) that determine fine specificity of TCR for pMHC complex.



Adapted from Turner et al., 2006

**Figure 2. Generation of TCR diversity by somatic recombination of TCR gene segments.**

a) Products of somatic gene recombination of variable (V), diversity (D) and junctional (J) gene segments for the  $\beta$  chain, and V and J gene segments for the  $\alpha$  chain are spliced together with the constant region (C) to form the functional  $\alpha\beta$  TCR. b) Regions of



hypervariability, known as complementarity-determining regions (CDRs), are encoded in the V gene segments. Diversification of the TCR  $V\alpha$  and  $V\beta$  gene segments depends on the use of different CDR1 and CDR2 regions. CDR3 is created by the juxtaposition of different V(D)J germline segments after somatic recombination. The lack of precision during V(D)J gene rearrangement results in the addition of non-template-encoded nucleotides (N) at the V(D)J junctions, further increasing the diversity of the naïve TCR repertoire.

Combination of these mechanisms of TCR diversification increases the diversity of the TCR repertoire. Given the fact that majority of processes involved in generation of highly diverse TCR pool are based on random events, the danger of generating potentially self-reactive T cells is high. Therefore, mechanisms of central and peripheral tolerance play important safety mechanism to weed out T cells with undesired specificities and prevent potential autoimmune events.

### 3.3.3 TCR signaling – T cell fate determined by the signal strength

#### 3.3.3.1 TCR triggering models

Signal strength as a function of the affinity of the TCR for pMHC complexes is a predominant factor determining the outcome of T cell – APC interaction. Given the immense diversity of TCRs and pMHC complexes the magnitude of possible TCR-pMHC interactions creates nearly continuum of signals received by T cells. In a given situation, the T cell signaling machinery must precisely compute input signals. Importantly, it is still not completely resolved, how low numbers of foreign peptides presented by MHC molecules are distinguished from the noise of highly abundant self-peptide-MHC complexes and how the differences in signal strength translate into qualitatively different functional responses. Several, not mutually exclusive models have been proposed to answer these questions.

The conformation change model proposes that the binding to pMHC molecule alters the conformation of the  $\alpha\beta$  TCR dimer initiating a cascade of events finally leading to T cell activation (Choudhuri and van der Merwe, 2007). However, the lack of biophysical evidence to support this model and more recent findings involving conformation change of the cytoplasmic region of CD3 molecule upon TCR ligation suggested an alternative scenario. According to the adaptations of the model, the basic residue rich sequence (BRS) of the CD3 $\epsilon$  molecule ITAMs of naïve T cell is buried in the lipid bilayer and therefore protected from phosphorylation. Upon TCR ligation these ITAMs are released from the bilayer and expose to phosphorylation (Aivazian and Stern, 2000; Kuhns and Davis, 2008). Mechanistic forces arising from TCR interaction with pMHC transferred through the rigid structure of CD3 ectodomains are suggested as the major driver of the observed CD3 conformational change. The observation that reagents disrupting actin polymerization abrogate TCR triggering indicates that cytoskeletal changes occur in the area exposed to the active source of force

created by TCR-pMHC interaction (Valitutti et al., 1995). Moreover, pulling or pushing/twisting of the TCR following pMHC engagement is suggested as a second mechanosensing mechanism (Kuhns et al., 2006; Davis, 2002). Pulling or shearing mechanisms are probably more effective than forces created by pushing because only specific interactions can resist pulling or shearing forces (van der Merwe and Dushek, 2011). The mechanical force-based conformation change model is attractive because it can explain how the binding at the structurally variable pMHC binding site of the TCR can induce the same conformation change in all TCR-CD3 complexes leading to T cell activation. Furthermore, the affinity of TCR variable sites for pMHC determines the duration of the contact and thereby the duration of the mechanical force that causes the conformation change.

The second model dealing with molecular details of TCR triggering proposes the mechanism of segregation or redistribution of TCR-CD3 complexes as decisive event in T cell activation (Choudhuri and van der Merwe, 2007). The finding that high levels of phosphorylation of lymphocyte-specific protein tyrosine kinase (Lck) found in naïve T cells does not change upon activation suggested that phosphorylation by constitutively active Lck is kept in check by constitutively active phosphatases (Nika et al., 2010). Therefore, events disturbing this balance would lead to an increase in TCR-CD3 ITAM phosphorylation and T cell activation. Within seconds after TCR ligation TCRs form dynamic TCR microclusters at the initial contact region between the T cell and the APC (Varma et al., 2006). While many small signaling molecules promoting phosphorylation and therefore sustained signaling are being accumulated within the microclusters, molecules with large ectodomains such as inhibitory tyrosine phosphatase CD45 and CD148 are excluded from these structures due to the binding energy created during TCRs ligation. Therefore, binding to pMHC ligand shelters TCR-CD3 complexes within a closed microcluster zone where they are protected from dephosphorylation by inhibitory phosphatases, thus allowing long-lived phosphorylation of CD3 ITAMs and downstream molecules ultimately leading to T cell activation.

Two models of TCR triggering were proposed on the basis of quantitative features of T cell activation and ligand discrimination: 'kinetic proofreading model' and 'serial triggering model'. The kinetic proofreading model proposes that agonists induce phosphorylation of the T cell signaling machinery proportional to the TCR-pMHC interaction time (McKeithan, 1995). Moreover, the model implies that higher affinity interactions would have slower dissociation rates leading to stronger phosphorylation and therefore stronger activation of the cells. Importantly as the model does not take into account regulatory feedback loops, it leaves out the fact that too long interaction times are detrimental for T cell activation. The issue of optimal dissociation times is taken into account in the 'serial triggering model'. This model proposes that the interaction time between TCR and pMHC should last for long enough to allow the signaling to occur, but should also be sufficiently short allowing single agonists to activate multiple TCRs therefore amplifying the signal (Valitutti et al., 1995b). The serial triggering model offers the explanation how small numbers of agonists can allow sustained signaling.

As the two proposed models are not mutually exclusive, the combination of both offers a reasonable theoretical framework to explain T cell activation. However, as they fail to realistically reflect the complexity of the TCR 'signalosome' and its regulation, new molecular models provide a more comprehensive understanding.

### 3.3.3.2 Components of the TCR signaling pathway the TCR “signalosome”

TCR triggering induced by one of the described mechanisms or their combination leads to phosphorylation of ITAMs in the cytoplasmatic tails of the CD3 subunits by LCK, a SRC-family member of protein tyrosine kinases (PTK). For proper regulation, LCK must be anchored into glycolipid-enriched membrane microdomains (GEMs) (Harder and Engelhardt, 2004). Dynamic modules responsible for regulation of LCK activity consists of four elements: the transmembrane protein kinase (PTP) CD45, the cytoplasmic tyrosine kinase CSK (C-terminal SRC kinase), GEM-bound resident scaffold phosphoprotein protein PAG (phosphoprotein associated with GEM) and the adaptor protein TSAD (T-cell-specific adaptor protein). Additional regulation is exerted by cytoplasmic phosphatases PTPN22 (phosphatases protein tyrosine phosphatase non-receptor type 22), SHP1 (SRC homology 2 (SH2)-domain- containing proteintyrosine phosphatase 1) and kinase ERK (extracellular-signal-regulated kinase) (Acuto et al., 2008). This complex LCK regulation results in the generation of three isoforms of LCK: inactive, ‘primed’ and active. In non-stimulated cells one fraction of LCK is anchored in GEMs while the other is associated with co-receptor molecules CD4 and CD8. GEM anchored protein PAG is phosphorylated and recruits CSK, which phosphorylates the inhibitory tyrosine residue of LCK keeping it in an inactive state (Veillette et al., 2002). TCR triggering induces dephosphorylating of PAG that releases CSK, preventing access LCK. Further, PTP CD45 mediated dephosphorylation of LCK’s inhibitory tyrosine deletes inhibitory effects posed by CSK and sets LCK into an active state. TSAD binds to active LCK and positively regulates its function (Acuto et al., 2008). However, the finding that the majority of the LCK molecules in naïve cells is in the active form indicates that phosphorylation of CD3 ITAMs, which is a key step in signal transduction, might be triggered by bringing the TCR into proximity with pre-activated LCK. The fraction of LCK associated with the co-receptors CD4 and CD8 may possibly optimize TCR signaling by delivering active LCK to ligand-bound TCR. Nevertheless, the fact that TCR signaling can

occur in the absence of co-receptors, suggests that proximity of LCK to CD3 ITAMs could be achieved by transient co-localization in GEMs (Drevot et al., 2002). In the next step, LCK mediated phosphorylation of tyrosine residues of one ITAM creates a docking site for ZAP70 ( $\zeta$ -chain-associated protein kinase of 70kD). Following binding of multiple copies of ZAP70 to phosphorylated CD3 ITAMs, a two-stage activation of the enzyme will take place (Deindl et al., 2007; Acuto and Cantrell, 2000). The first stage of activation involves 'unlocking' of ZAP70 by binding to phosphorylated ITAMs and LCK mediated phosphorylation. In the second step autophosphorylation of ZAP70 allows for full catalytic activation of the enzyme. Sustained generation of activated ZAP70 is important to allow connection to the next module of the 'signalosome' making this step one of the most important decision-making points of TCR signaling. While basic levels of non-phosphorylated ZAP70 in association with CD3 $\epsilon$  ITAMs is a signature of self-peptide MHC recognition, accumulation of large numbers of activated ZAP70 molecules for a short time on the ITAMs of a single TCR is a prerequisite for full T cell activation. This mechanism is indicative for the importance of multiple copies of ZAP70 binding sites, i.e. ITAMs, to determine their sensitivity of TCR-pMHC ligands (Love et al., 2000). Connection to the next module of the 'signalosome' is achieved by ZAP70-mediated phosphorylation of several tyrosine residues of GAM-scaffold protein LAT (linker of activation of T cells) and SLP76 (SH2-domain-containing leukocyte protein of 76kDa), which opens the possibility for recruitment of various effector proteins contributing to the diversification of the signal. Highly cooperative interactions between different components of the LAT-SLP76 module allow for fine regulation of the signal diversification influencing the final outcome of TCR ligation. For example, PLC $\gamma$ 1 (phospholipase C $\gamma$ 1) binds to both LAT and SLP76, but requires VAV1 (that is binding to SLP76) for successful interaction with SLP76, while GADS (growth-factor-receptor-binding protein 2 (GRB2)-related adaptor protein) which acts as the bridge between LAT and SLP76, cannot bind to LAT in the absence of SLP76 (Acuto et al., 2008). However, the numbers of the components included in the complex as well as the stoichiometry of the complex formed after single TCR

engagement are still not known. The possibility remains that the composition of the complex assembled at the LAT-SLP76 scaffold is determined by the signal strength of TCR triggering allowing generation of qualitatively different responses reflecting quantitatively different input signals. The outcome of the interdependent relations of the components involved in LAT-SLP76 scaffold is revealed through action of several molecules including ADAP (adhesion- and degranulation-promoting adaptor molecule), NCK (non-catalytic region of tyrosine kinase), VAV1 and PLC $\gamma$ 1 (Smith-Garvin et al., 2009). ADAP mediated activation of integrins upon initial TCR triggering allows for an increase in affinity of T cell integrin LFA1 for its binding partner ICAM1 (Intercellular Adhesion Molecule 1) expressed by APCs resulting in prolonged interaction between the cells allowing full T cell activation to take place (Peterson et al., 2001). NCK and VAV1 are involved in regulation of actin polymerization leading to cytoskeletal rearrangement, the process that strongly supports T cell activation (Faure et al., 2004). Importantly, activation of integrins and cytoskeletal rearrangement have crucial role in organization and regulation of the immunological synapse (IS). While the exact role of the IS in T cell activation remains controversially discussed, it is now clear that this formation develops through merging of peripheral microclusters as areas where initiation of TCR signaling occurs (Smith-Garvin et al., 2009a). Formation of new and translocation of already formed microclusters into the IS is achieved through cytoskeletal rearrangement. Furthermore, integrins play an important structural role in the IS as they represent the major component of its outer ring-peripheral supramolecular activation cluster (pSMAC) (Grakoui, 1999). The inner area of the IS is referred to as central SMAC (cSMAC) and is suggested to be the site of both TCR degradation and signal enhancement, the balance of which is determined by the nature of the ligand (Cemerski et al., 2008).

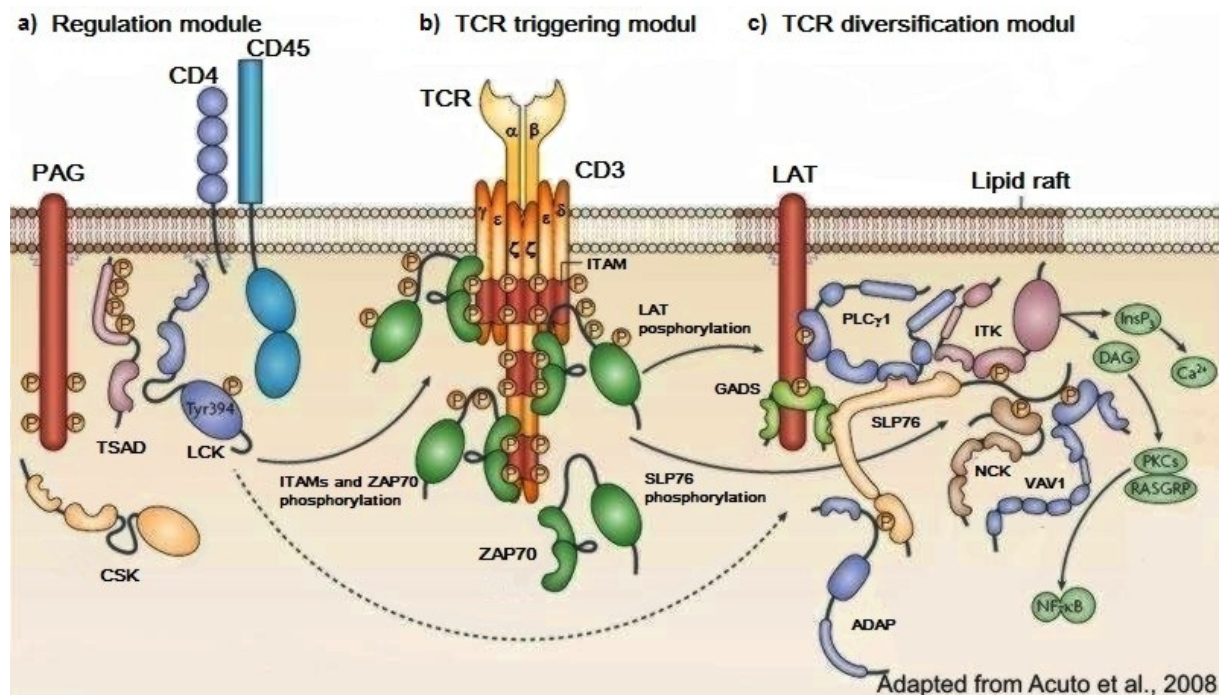


**Figure 3. Components of TCR signalosome and their interactions.**

a) Regulation module includes the lipid-raft-associated proteins LCK and PAG (phosphoprotein associated with glycolipid-enriched membrane domains). A fraction of LCK is associated with the co-receptor CD4 (or CD8, not shown). In unstimulated cells phosphorylated PAG recruits CSK (C-terminal SRC kinase), which is involved in negative regulation of LCK. TCR engagement leads to PAG dephosphorylation causing CSK release. Protein tyrosine phosphatase (PTP) CD45 dephosphorylates LCK, thereby counteracting CSK activity. The adaptor TSAD (T-cell-specific adaptor protein) then binds to and positively regulates LCK. b) Following TCR agonist stimulation, LCK phosphorylates immunoreceptor tyrosine-based activation motifs (ITAMs) of CD3 $\zeta$  chains. ITAM binding and LCK-dependent tyrosine phosphorylation recruits and activates ZAP70 (zeta-chain-associated protein kinase of 70 kDa) that phosphorylates the scaffold proteins LAT (linker for activation of T cells) and SLP76 (SRC homology 2 (SH2)-domain-containing leukocyte protein of 76 kDa). c) Diversification module includes regulators of Ca<sup>2+</sup> signaling and diacylglycerol (DAG) production (which are PLC $\gamma$ 1 (phospholipase C $\gamma$ 1) and ITK (interleukin-2-inducible T-cell kinase)), actin polymerization (which are NCK (non-catalytic region of tyrosine kinase) and VAV1) and integrin activation (ADAP (adhesion- and degranulation-promoting adaptor protein)), all of which are activating signaling pathways that control cell adhesion, cytoskeletal rearrangements and gene expression. In addition to activation of the signal triggering module, LCK may phosphorylate components of the diversification and regulation module (such as ITK and VAV1). GADS, growth-factor-



receptor-bound-protein-2-related adaptor protein; InsP3, inositol-1,4,5-trisphosphate; NF- $\kappa$ B, nuclear factor-kappaB; PKC, protein kinase C.

Finally, ITK (Interleucin-2 –inducible T-cell kinase) dependent PLC $\gamma$ 1 activation results in hydrolysis of the membrane lipids PI(4,5)P<sub>2</sub> (Phosphatidylinositol-4,5-bisphosphate) generating the second messengers DAG (diacyl glycerol) and IP<sub>3</sub> (inositol-1,4,5-trisphosphate) (Smith-Garvin et al., 2009a). These second messengers lead to opening of numerous signaling pathways involving Ras and PKC $\theta$  Ca<sup>2+</sup>/calmodulin-dependent signaling mediated by IP<sub>3</sub>. While Ras is important for unfolding MAPK kinase pathway, PKC $\theta$  and NF- $\kappa$ B pathways result in activation of specific sets of genes responsible for T cell proliferation, survival, differentiation and homeostasis. Ca<sup>2+</sup>/calmodulin dependent signaling will activate the transcriptional factor NFAT (nuclear factor of activated T cells) that can form cooperative complexes with a variety of other transcriptional factors (e.g. transcriptional factors of Ras signaling pathway), therefore integrating different signaling pathways and differential gene expression patterns (Smith-Garvin et al., 2009a).

### 3.3.3.3 Regulation of TCR signaling – implications for TCR sensitivity and specificity

TCR ligand recognition relies on a network of rapid biochemical reactions initiated and propagated in a fashion determined by the fine nature of input signal. Rapid signal amplification is under tight control by both positive and negative feedback mechanisms which are mediated through reversible modifications of signaling molecules, i.e. mainly phosphorylation reactions. Modification of reaction rates of positive and negative feedback loops sets the sensitivity, specificity and signal amplitude of specific TCR-pMHC complex interaction. Tight control of the TCR signaling machinery is achieved by several different mechanisms including early and late steps in the ‘signalosome’, as well as delayed stages of

T cell activation covering hours after the initiation of signaling when the cells have already acquired effector and memory functions.

Negative feedback mechanisms acting on the level of the signalosome are mainly active in naïve T cells and thymocytes. One of the molecules with regulatory function is the PTP SHP1, which in its unbound form is inactive, while phosphorylation of signature tyrosine residues and binding to the ITAMs releases its phosphatase activity (Stefanová et al., 2003; Kilgore et al., 2003). Upon antagonist binding, LCK associates with and phosphorylates SHP1, which in turn dephosphorylates LCK abolishing further signal propagation. In contrast, in response to agonist ligands, SHP1 recruitment to signalosome and activation is delayed. In this situation, a positive feedback loop mediated by ERK allows for LCK phosphorylation, in the same time disabling SHP1 interaction with LCK. Therefore, SHP1 acts as immediate negative feedback mechanism by increasing the activation threshold and thereby allowing for ligand discrimination. Evidence further underlining the importance of SHP1-mediated regulation comes from mice lacking cytoplasmic SHP1 which show increased positive and negative selection, exhibit enhanced T cell activation and develop autoimmunity (Pao et al., 2007). Additional negative feedback regulation of the early signaling events is achieved through adaptor proteins DOK1 (downstream of kinase 1) and DOK2 (Yasuda et al., 2007). TCR signaling triggers rapid phosphorylation of DOK1/DOK2 and allows for their association with LAT, placing the adapters in close proximity to ZAP70. In this location, negative regulation of DOK1/DOK2 can be achieved through competition with ZAP70 for binding to CD3 ITAMs or competition with members of LAT-SLP76 complex for binding to LAT. Development of autoimmunity and impaired T cell homeostasis in mice deficient in DOK1/DOK2 molecules stresses their involvement in negative regulation of the TCR-signalosome. Finally, later stages of TCR signalosome activation are under regulation of HPK1 molecule (hematopoietic progenitor kinase1) that is phosphorylated by ZAP70 and LCK subsequently joins the LAT-SLP76 scaffold. HPK1 seems to be essential for the regulation of TCR-signalosome activity as its deletion or reduction of expression leads to increased TCR-dependent tyrosine phosphorylation of several signaling proteins including

SLP76, PLC $\gamma$ 1, LAT, VAV1 and ZAP70 as well as increased Ca<sup>2+</sup> signaling (Di Bartolo et al., 2007; Shui et al., 2007). While the precise mechanism of HPK1 mediated negative regulation is not fully clarified, experimental evidence suggests a role in destabilization of the signalosome, directly or through recruitment of other negative regulators.

Finally, molecules that are not part of the TCR complex but can influence the outcome of T cell activation by feeding the signal into TCR signalosome are referred to as co-signaling molecules. Most co-signaling molecules are members of immunoglobulin superfamily (IgSF) and tumor necrosis factor receptor superfamily (TNFRSF) (Chen and Flies, 2013). However, depending on the type of the signal they deliver to the signalosome, members of the two families can be further divided to molecules with co-stimulatory and co-inhibitory functions. Co-stimulatory molecules include CD28, OX-40, ICOS, or CD2 which synergize with the TCR signalosome to promote cell cycle progression, cytokine production and T cell survival. A limited number of co-stimulating molecules is expressed on naïve T cell such as CD28 which substantially enhances signals received through the TCR and hence promotes T cell priming. Other co-stimulatory molecules are expressed only following T cell activation and can promote proliferation and survival of effector T cells or shape the behavior of memory T cells (Chen and Flies, 2013).

Co-inhibitory molecules are expressed mainly after initial T cell activation and are involved in regulation of TCR signals. Co-inhibitory molecules include PD-1 (programmed cell death 1), CTLA 4 (Cytotoxic T-Lymphocyte Antigen 4) and CD5. These molecules generally function through recruitment of cytosolic phosphatases that dephosphorylate components of the TCR signalosome (ZAP70 and LAT) thereby inhibiting cell cycle progression and cytokine production (Smith-Garvin et al., 2009a). Co-inhibitory molecules can also regulate distal signaling events by inhibiting phosphorylation of ERK and JUN, leading to further reduction of T cell function (Rudd et al., 2009; Patsoukis et al., 2012).

In summary, the TCR complex is the main trigger for functioning of the highly potent T cell machinery. Development of high-level control mechanisms, covering different temporal and

spatial aspects of TCR signaling permits safe T cells responses through interaction with target cells at high levels of specificity and sensitivity.

### 3.3.4 CD8<sup>+</sup> T cell activation and effector functions

#### 3.3.4.1 CD8<sup>+</sup> T cell activation

The development of cytotoxic T lymphocyte (CTL) responses is a cornerstone in the defense against infection with intracellular bacteria and viruses. The process of CD8<sup>+</sup> T cell activation takes place within secondary lymphoid organs (SLO) that provide structural support for the successful interaction between CD8<sup>+</sup> T cells and antigen presenting cells (APC) (Junt et al., 2008). While all nucleated cells can convert intracellular proteins into peptide fragments and present them in a MHC I-dependent fashion to CD8<sup>+</sup> T cells, dendritic cells are the most successful APC for activating naïve T cells (Steinman, 1991). In order to meet APC that bears cognate antigen, naïve T cell will recirculate many times a day passing from the blood into lymph nodes and then through the lymphatics to the lymph and back through the sub-clavial vein into the blood. To overcome shear forces of blood before entering the lymph nodes, T cells will slow down, tether and roll on the surface of high endothelial venules (HEVs), a specialized type of post-capillary vascular endothelium present within lymph node paracortical region. T cell tethering is mediated through the interaction between T cell expressed CD62L (L-selectin) and various proteins expressed on HEV that are collectively referred to as peripheral node addressins (PNA<sub>d</sub>) (Rosen, 2004). While T cells are tethering on the walls of HEVs, the G-protein coupled receptor CCR7 expressed on their surface will get the opportunity to sample chemokine CCL21 immobilized on the HEV walls, creating the signal that leads to activation of lymphocyte function associated antigen (LFA1) (Bao et al., 2010). Finally, interaction between LFA1 and endothelial cells expressed ICAM1 will allow T

cell arrest and transmigration to the paracortical T cell zone of the lymph node. In absence of antigen, naïve T cells within LNs randomly walk through T cell areas cruising on the CCL19-expressing fibroblastic reticular network (Mempel et al., 2006). Upon infection, with arrival of pathogens and particular antigens to the subcapsular sinus of LNs, T cells and LN-resident DCs will rapidly relocate to the peripheral regions of the T cell zone, i.e. close to the subcapsular sinus where DCs can acquire antigens from infected cells. DCs that have captured the antigen and matured at the site of infection start expressing CCR7 that allows them to enter the subcapsular sinus of the LNs where they can present antigens to the naïve T cells (Dieu et al., 1998; Steinman et al., 2000). Successful priming of naïve T cells depends on the interaction with mature DCs that express ligands B7.1 (CD80) and B7.2 (CD86) therefore allowing binding to T cell expressed co-stimulatory molecule CD28. Signaling through the TCR complex will therefore be enhanced and stabilized further leading to initiation of IL-2 transcription. Binding of T cell-produced IL-2 to its receptor on T cells together with IL-12 signals received from antigen presenting DCs will lead to expression of CD25, the high affinity  $\alpha$  chain of the IL-2 receptor. CD25 expression enhances the affinity of the IL-2 receptor by 100-fold making it more sensitive to this cytokine and further stabilizes its downstream signaling pathways therefore ensuring massive T cell proliferation and differentiation. Badovinac et al. have calculated that naïve T cell can go through as many as 19 cell divisions within seven days upon pathogen stimulation leading to an approximately 500,000-fold expansion (Badovinac et al., 2007). Such extremely high proliferation rates are supported by drastic changes in T cell metabolism leading to increased uptake of glucose, amino acids and iron and a switch from oxidative phosphorylation to aerobic glycolysis that allows faster production of new cells (Michalek and Rathmell, 2010). Signaling through CD28 and further downstream through Akt and mTOR supports T cell proliferation and survival (Chen and Flies, 2013). Failure of T cells to receive stimulation through CD28 results in suboptimal signal strength generating state of T cell unresponsiveness known as anergy (Banchereau and Steinman, 1998). Functional changes arising from clonal expansion and differentiation of naïve T cell to CD8<sup>+</sup> T cells induce downregulation of CD62L and CCR7 and

upregulation of chemokine receptors that will guide activated cells out of lymph nodes to inflamed tissues. While in transit to the site of infection, activated CD8<sup>+</sup> T cells are found to be still in cell cycle. This maintenance of proliferative capacity allows for local regulation of effector T cell numbers through interactions with cells displaying cognate antigen (Bedoui and Gebhardt, 2011). In situ proliferation of activated T cells has been reported even within the immunologically privileged - central nervous system (CNS) (Kang et al., 2011).

### 3.3.4.2 CD8<sup>+</sup> T cell effector mechanisms

During an infection, the main function of CD8<sup>+</sup> T cells is the elimination of infected cells. The high specificity of TCR recognition of antigenic peptides presented on MHC I molecules of infected cell allows for an establishment of firm interactions between effector T cells and target cells through the formation of SMACs. Contact areas between effector CD8<sup>+</sup> T cell and target cells guarantees directional delivery of effector molecule of cytotoxic T cells and therefore ensures specific destruction of infected cells, reducing non-specific killing to the minimum (McGavern and Truong, 2004). Upon establishment of firm contact with target cells, rapid orientation of microtubule-organizing center (MTOC), Golgi apparatus and lytic granules prepares CTLs for performing their lytic functions. Lytic granules contain two kinds of proteins: perforin monomers and several serin proteases called granzymes. Delivery of granules to the extracellular space between two cells occurs in a Ca<sup>2+</sup>-dependent manner. Once released from the granules, perforin molecules polymerize to form pores in the target cell membrane. The pores are subsequently used for the entrance of granzymes into the target cell where they perform their effector functions. Importantly, the uptake of granzymes by target cell can occur in a perforin-independent fashion, e.g. through receptor-mediated endocytosis when mannose-6-phosphate receptor binds and internalize granzyme (Pinkoski et al., 1998). However, it appears that perforin is necessary for the release of granzyme from endosome-like vesicles because in the absence of perforin, internalized granzyme will stay

within vesicles and will not lead cellular toxicity or apoptosis. In addition, granzymes can bind to the surface of target cells and get internalized due to perforin-mediate membrane damage. Which of the pathways will be employed for the delivery of granzymes depends on the amount of perforin and granzyme as well as the characteristics of target cell membrane. Once within the cell the main function of granzymes is to induce apoptosis. Proteolytic activity of granzymes is responsible for cleaving pro-caspase 3 and 8 creating their active apoptotic effectors. A caspase-independent apoptotic pathway can be initiated by granzyme which relies on its ability to cleave the pro-apoptotic molecule BID creating its active form that then translocates to mitochondria and activates BAX and BAK molecules. This finally leads to the opening of mitochondrial permeability transition pore and release of cytochrome c that forms the complex with Apaf 1 (Apoptotic protease activating factor 1) and pro-caspase 9 leading to the activation of terminal effectors of apoptosis. Finally, DNA fragmentation as hallmark of apoptosis is mediated by either endonuclease G released from the mitochondria, or DFF40/CAD (DNA fragmentation factor 40/caspase-activated deoxynuclease). So far 11 different granzymes have been found in human and rodent cytolytic cells of which granzymes A and B are most abundant and best characterized (Barry and Bleackley, 2002).

Another cell contact-dependent mechanism of target cell destruction employed by CTLs relies on the interaction between receptors belonging to the TNF receptor family such as Fas expressed on target cells and its ligand FasL expressed by CTLs (Rouvier et al., 1993). Crosslinking of the two molecules leads to activation of FAS receptor cytosolic domain FADD (Fas-associated protein with death domain) and activation of FADD associated pro-caspase 8 into active form responsible for the initiation of apoptosis.

As both granzyme and Fas-FasL pathways allow direct and immediate elimination of target cells, they need to be highly regulated and specific to prevent off-target killing and therefore rely on direct contact-based interaction between CTL and target cells. However, a third anti-viral mechanism employed by CTLs relies on secretion of cytokines IFN- $\gamma$  and TNF $\alpha$  that although confined to the area of the interaction between two cells, can influence cells in proximity (Sanderson et al., 2012). Bousso and colleagues demonstrated that the effect of

INF- $\gamma$  could reach cells within the radius of 80  $\mu\text{m}$  of the effector cell producing it (Müller et al., 2012). Therefore, by the means of INF- $\gamma$ , CTLs can target distant cells and induce transcription of antiviral genes, enhance phagocytic activity of macrophages and enhance MHC I expression on infected cells increasing their chance to get recognized and destroyed.

### 3.3.4.3 Helping the killer – CD8<sup>+</sup> T cell responses tuned by CD4<sup>+</sup> T cells and cytokines

CD8<sup>+</sup> T cell priming and differentiation can be dependent on CD4<sup>+</sup> T cell help (Castellino and Germain, 2006). Initial studies suggested that both CD8<sup>+</sup> and CD4<sup>+</sup> T cells recognize corresponding pMHC complexes on the same APC (Bennett et al., 1997). However, DCs can be licensed during interaction with CD4<sup>+</sup> T cell and become able to fully activate CD8<sup>+</sup> T cells, even if both cells do not concomitantly interact with the same DC (Smith et al., 2004). The model of DC licensing considers that upon capturing the antigen from dying cells, DCs will process the antigen and present it in a MHC II-dependent fashion to CD4<sup>+</sup> T cells, which in turn upregulate CD40L and can engage CD40 on the DC surface. Although, this model offers an elegant solution for some experimental findings (Cassell and Forman, 1988; Bennett et al., 1997), other data showing that CD8<sup>+</sup> T cells can be successfully primed in the absence of CD4<sup>+</sup> T cells (Buller et al., 1987; Rahemtulla et al., 1991) require an alternative explanation. Noteworthy, CD4<sup>+</sup>-independent CD8<sup>+</sup> T cell mainly occurs during infection with bacterial and viral pathogens (Bevan, 2004). The explanation for this lack on CD4<sup>+</sup> T cell-dependency is a compensation of inflammatory signals (cytokine, surface molecules) induced through the recognition of pathogen associated molecular patterns (PAMPs) ligands derived from pathogens by Toll-like receptors (TLR)(Janeway and Medzhitov, 2002). TLR activation of DCs promotes maturation, upregulation of costimulatory molecules, migration to secondary lymphoid tissues, release of cytokines such as IL-12 and cross-priming of CD8<sup>+</sup> T



cell responses (Schulz and Reis e Sousa, 2002; Janeway and Medzhitov, 2002). Although CD4<sup>+</sup> T cell deficiency might not impair early antiviral CD8<sup>+</sup> T cell responses, experiments from Matloubian and colleagues showed that the lack of CD4<sup>+</sup> T cell help impinges on control of chronic viral infection and results in functional inactivation of CD8<sup>+</sup> T cells (Matloubian et al., 1994). Moreover, other studies have implied a role for CD4<sup>+</sup> T cell help in the maintenance of CD8<sup>+</sup> T cell and antibodies responses during chronic viral infections (Battegay et al., 1994). Overall, while priming of CD8<sup>+</sup> T cells can occur independent of CD4<sup>+</sup> T cell help under conditions of strong inflammation, CD8<sup>+</sup> T cells strongly depend on help provided by CD4<sup>+</sup> T cells for control of persistent pathogens as well as memory formation.

Maximal expansion and differentiation of CD8<sup>+</sup> T cell to full effector CTL often depends on the availability of a 'third signal' which can be provided by different cytokines including IL-2, IL-12, IL-21, and IL-33 (Reis e Sousa, 2006). While IL-2 has an important role in early activation of naïve T cells, effector and memory T cell may regain the ability to produce and respond to this cytokine, which bears important consequences for fine-tuning of T cell responses. Reports have shown that high levels of IL-2 mediated signaling will result in CD8<sup>+</sup> T cell activation with terminally differentiated, short-lived effector phenotype (Kalia et al., 2010; Pipkin et al., 2010). In contrast, in the absence or decreased amounts of IL-2-mediated signaling, CD8<sup>+</sup> T cells exhibit defective effector function and adopt a central memory phenotype with high expression of CD62L. Another set of early signals that can modulate CD8<sup>+</sup> T cell responses comes from type I interferons (IFN $\alpha$  and IFN $\beta$ ) and IL-12 which can signal directly to CD8<sup>+</sup> T cell to promote their survival and effector differentiation (Curtsinger et al., 2005; Kolumam et al., 2005; Pearce and Shen, 2007). Aside from regulation of the early stages of CD8<sup>+</sup> T cell responses, cytokines may play a more important role in supporting effector functions and survival of CD8<sup>+</sup> T cell in the later stages during immune response. Recently, the importance of IL-21 and IL-33 for optimal function of effector CD8<sup>+</sup> T cells during viral infection has been indicated (Bonilla et al., 2012; Fröhlich et al., 2009). In

the absence of IL-33, CD8<sup>+</sup> T cells exhibited a reduction in effector functions with a failure to produce TNF $\alpha$  and IL-2, and severely reduced capacity to produce IFN- $\gamma$ , degranulate and express granzyme B (Bonilla et al., 2012). Moreover, cytokine such as IL-21 can shape CD8<sup>+</sup> T cell responses by restricting differentiation and promoting longevity of the cells (Fröhlich et al., 2009). Nevertheless, effects of IL-21 on the function of virus specific CD8<sup>+</sup> T cells during acute viral infection was shown to be dependent on type of the pathogen.

### 3.3.5 Model systems to study T cell biology

The discovery made by Dembic and colleagues (Dembic et al., 1986) that the specificity of a T cell is determined by T cell receptor and can be transmitted by transferring  $\alpha$  and  $\beta$  TCR genes to other cells has opened a new era in T cell research. This groundbreaking discovery allowed development of new genetic tools that greatly contributed to understanding of fundamental processes in T cell biology and allowed application of this knowledge in clinical settings. Combining  $\alpha$   $\beta$  TCR gene transfer with transgenic mouse technology enabled generation of TCR transgenic mice. From the first TCR transgenic mouse generated 1988 by Uematsu and colleagues (Uematsu et al., 1988) until today, the methodology has greatly improved allowing generation of hundreds of TCR transgenic mice. These tools were instrumental to reveal the concept of thymic selection (Berg et al., 1989; Kisielow et al., 1988), understand basic mechanisms of autoimmunity (Goverman et al., 1993; Pöllinger et al., 2009; Osman et al., 1998), the biochemistry of TCR-pMHC interaction (Udaka et al., 1993) and to study T cell responses against various infectious organisms such as Herpes simplex virus (Mueller et al., 2003), LCMV (Oxenius et al., 1998a; Brändle et al., 1995), MCMV (Torti et al., 2011), Salmonella (Bumann, 2003).

However, development of novel TCR transgenic mice can often be laborious and time consuming. Additionally, crossing of TCR transgenic mice on different genetic backgrounds

often requires complicated breeding schemes. Combining the power of retrovirally mediated stem cell gene transfer with multicistronic 2A – peptide linked retroviral vectors, Dario Vignali and his group introduced novel tool for studying T cell biology named retrogenic mice (“retro” from retrovirus and “genic” from transgenic)(Bettini et al., 2012). This technology has facilitated rapid generation of mice expressing clonotypic TCRs, significantly shortened the time needed to express TCRs on different genetic backgrounds and therefore offered rather inexpensive option for screening, studying and comparing large numbers of TCRs. Given the fact that each retrogenic mouse generated to express the same TCR is independent and hence considered a founder, this methodology has offered the possibility to exclude integration site bias. In an initial study using this approach, the behavior of seven different TCRs expressed either in transgenic or retrogenic mouse models was assessed showing that the two systems are comparable (Holst et al., 2006). Retrogenic mice were further used in studies to compare in vivo performance of large numbers of TCRs (Alli et al., 2008), to rapidly generate new sources of monoclonal T cells (Arnold et al., 2004a) or to study the diversity of the T cell repertoire during autoimmune (Liu et al., 2009) or antiviral responses (Day et al., 2011). Despite the above-mentioned advantage of retrogenic TCR technology, the strong reduction in T cell numbers together with the necessity for constant production of new chimeric mice require a clear choice of the scientific question to justify utilization of this approach.

### **3.4 Immunity in the CNS - focus on T cell-mediated protection**

The central nervous system (CNS) coordinates the interaction of the individual organism with the environment and regulates a plethora of processes within the body. Importantly, the neuronal network that performs these tasks is composed of post-mitotic cells which possess only limited regenerative capacity. Hence, sets of specific immunological guidelines guarantees the surveillance of this organ system to facilitate protection against infection while preventing overshooting immune responses that could cause collateral damage. The balance of these protective mechanisms is achieved by the combination of distinct regulatory mechanisms that impinge on all cellular components and particular anatomical features.

#### **3.4.1 Anatomic structure of the brain**

The brain and the spinal cord are enclosed within the rigid structures of the skull and the vertebrae, while the cerebrospinal fluid (CSF) serves as liquid cushion offering further mechanical protection. CSF is produced within brains ventricles by ependymal cells of the choroid plexus which is composed of a network of fenestrated capillaries and is covered by the monolayer of epithelial cells termed ependymal cells (Dziegielewska et al., 2001). Motion of cilia on the ependymal cells allows the CSF to circulate from the ventricles, through the brain stem exit ports to cover the outer surface of the spinal cord, brain stem, cerebellum and cerebral cortex. Reabsorption of the CSF into venous blood takes place at the arachnoid villi. A small portion of CSF can be derived from CNS interstitial fluids that join the CSF and contribute to the collection of soluble material. Importantly, in addition to being reabsorbed to the blood, CSF also drains along cranial and spinal nerves to local afferent lymphatics, thereby carrying soluble antigens to local draining lymph nodes (Walter et al., 2006). One of the most important draining routes follows the olfactory nerves, draining through the

cribriform plate at the base of the skull towards the nasal mucosa, finally reaching cervical lymph nodes (Ichimura et al., 1991). Since only few areas of the CNS possess a drainage connection to lymph nodes, CNS antigens accumulate mainly in the CSF.

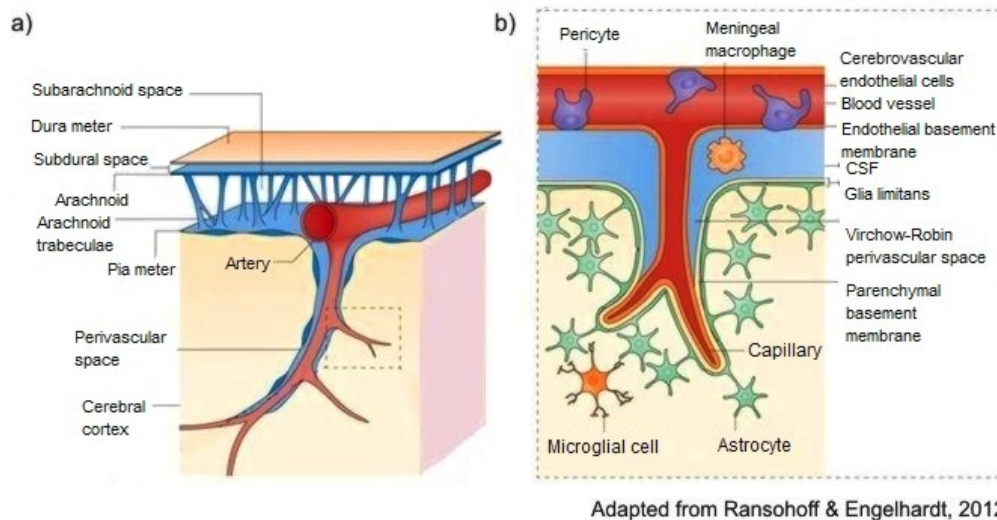


**Figure 4. Structure of the brain meninges and blood vessels.**

a) The meninges comprise a series of three membranes that enclose the CNS parenchymal tissues and the cerebro-spinal fluid (CSF). Tough fibrous dura is positioned directly beneath the inner surface of the skull. Under the dura there are two inner membranes: the arachnoid and the pia, which closely covers the CNS parenchyma. Subarachnoid space is filled by CSF and contains dense stroma and arterial vessels that supply the brain. These vessels penetrate the CNS parenchyma and are lined by the arachnoid and pia giving rise to perivascular spaces. b) CNS perivascular spaces (termed Virchow–Robin spaces) are enclosed and delimited by an endothelial basement membrane on the abluminal side of the vessel wall and the glia limitans on the parenchymal side of the perivascular space. The external surface of the brain is covered by a network of astrocytic processes along with the parenchymal basement membrane, collectively designated the glia limitans.

Additional protection of the CNS is provided by three membranes known as the meninges. The outer fibrous CNS membrane is positioned directly beneath the skull and is known as dura mater. The two inner membranes, arachnoidea and pia matter are separated by the subarachnoid space which is filled with CSF and contains a sponge-like network made by dense stromal cells that are traversed by arterial vessels. From the area of the subarachnoid

space, blood vessels, walled by arachnoidea and pia mater, penetrate the CNS parenchyma. The parenchymal continuation of subarachnoid space that forms the perivascular space is known as Virchow-Robin spaces. These perivascular structures are delimited by an endothelial basement membrane on the abluminal side of the vessel and the glia limitans which is made of astrocytic endfeet on the parenchymal side (Ransohoff and Engelhardt, 2012). Astrocytes that form the glia limitans produce growth factors that enable maturation and maintenance of barrier function of CNS blood vessels (Ge et al., 2005). The space between endothelial cells and glia limitans, in particular around postcapillary venules creates blood vessel sections that exhibit less strict barrier functions. The perivascular space may extend even further around mid-sized veins and arteries accommodating leptomeningeal mesothelial cells that can take up soluble antigens (Owens et al., 2008). Thus, blood vessels in the CNS are highly specialized to very selectively permit access of soluble substances and cells to the CNS parenchyma.

### 3.4.2 Blood brain barrier and immune privilege

Paul Ehrlich had observed that subcutaneous, intravenous or intraarterial injection of dyes stains all organs, but not the brain (Erich, 1885). Lewandowski concluded later that the capillary wall of the brain can block the access of certain molecules which inspired him to coin the term 'Bluthirnschranke' - blood-brain barrier (Lewandowski, 1900). A detailed examination of the nature of the 'barrier' between brain and blood has been performed by Reese and Karnovsky who used injection of horseradish peroxidase and high quality electron microscopy and found the characteristic overlaps between endothelial cells of brain capillaries that contain tight junctions and form 'continuous belts or zonulae occludentes' (Reese and Karnovsky, 1967). The authors have proposed that the barrier functions on the level of subcellular endothelial structures and is not a static physical wall, but rather a dynamic system that utilizes 'metabolic pumps' to maintain ion gradients between blood and

the brain. The special barrier function applies also for antigens that, when exclusively present within the CNS, evade immune recognition (Galea, Bechmann, & Perry, 2007). The finding that CNS antigens presented in the periphery can initiate strong immune responses indicated that the blood-brain barrier excludes not only molecular but also cellular components from the brain parenchyma (Murphy and Sturm, 1923; Medawar, 1948). These and other seminal findings were amalgamated in the concept of 'immune privilege' of the brain (Baker and Billingham, 1977) that implies an 'anatomic barrier, and/or a layer formed by the end processes of neuroglial cell on the capillary walls that restrict leukocyte diapedesis and hence restrains the development of inflammatory responses in the brain. Importantly, not all blood vessels in the CNS are equally tight. Goldmann described in 1913 already that molecules can leave blood vessels and accumulate in cells of the choroid plexus, the leptomeninges and along perivascular spaces, but cannot penetrate into the brain parenchyma (Goldmann, 1913). Later studies confirmed that capillaries in the CNS form a very tight barrier, whereas larger blood vessels such as postcapillary venules are more permissive (Bechmann et al., 2007). Hence, transition of immune cells from the blood occurs mainly in this section and a second control step at the glia limitans secures that only specifically activated immune cells find their way into the brain parenchyma.

Understanding of immune privilege of the brain goes beyond concept of barrier function of brain blood vessels and implies that immune privilege of the brain is not absolute and is confined mainly to the parenchyma (Galea et al., 2007; Bechmann et al., 2007). Hence, immune reactions in the choroid plexus, ventricles, meninges and circumventricular organs follow the same rules as in other peripheral organs (Owens et al., 2008). Moreover, inflammatory reactions mediators can change the "relative" immune privilege of the CNS resulting in immune cells infiltration. Taken together, specific regulatory mechanisms that operate at the level of the blood-brain interface should permit localized and restricted immune reactions in those areas of the CNS which provide the necessary signals for facilitating (i) accumulation of leukocytes in the perivascular space of post-capillary venules

and (ii) maintenance and further activation of immune cells in the perivascular space to permit translocation to the brain parenchyma.

### 3.4.3 T cell migration to and regulation of their function within the CNS

Under physiological conditions T cells are recruited to the CNS mainly through the choroid plexus, entering in a P-selectin dependent manner (Ransohoff et al., 2003). Routine surveillance of the brain by T cells is restricted to the subarachnoid and perivascular spaces. Inflammation leads to upregulation of adhesion molecules and chemokines by endothelial cells fostering tethering and rolling on the walls of endothelium mainly via P-selectin glycoprotein ligand-1 (PSGL-1) expressed on the surface of CD8<sup>+</sup> T cells, while CD4<sup>+</sup> T cells use  $\alpha$ 4-integrin (Engelhardt and Ransohoff, 2005). Depending on the anatomic location of the blood vessels, the binding partner of incoming cells vary, i.e. meningeal vessels express P-selection constitutively and upregulate E-selection during inflammation, while parenchymal blood vessels utilize VCAM- $\alpha$ 4-integrin interactions (Engelhardt, 2008). While rolling on the endothelial walls, T cell will drastically slow their speed and get the chance to collect further signals from the molecules expressed by the endothelium. This step of lymphocyte extravasation is dependent on signals coming through G-protein coupled receptors that collect the signals from chemokines present on the postcapillary endothelium. Signaling through chemokine receptors mediates activation of integrins leading to clustering on the cell surface to increase avidity or changes in integrin conformation improving binding to cell-adhesion molecules (CAMs). For example, studies using blocking antibodies in EAE have clearly indicated importance of  $\alpha$ 4 $\beta$ 1–VCAM-1 interaction in T cell extravasation (Yednock et al., 1992). Signaling through integrin-CAM pairs leads to firm adhesion, arrest and flattening of lymphocytes preparing for the final step of diapedesis. While the molecular mechanisms that decide the type of diapedesis are not fully understood yet, it is likely that lymphocytes in



the CNS use transcellular instead of paracellular diapedesis and thereby preserve tight junctions between endothelial cells (Owens et al., 2008). The perivascular space located between basement membrane of the vascular wall and the basement membrane of the glia limitans contains leptomeningeal mesothelial cells, macrophages and other antigen presenting cells that establish active interaction with incoming T cells. Incoming T cells collect signals from these perivascular APCs which determine whether the T cells will be granted access to the parenchyma. For example, Tran and colleagues have demonstrated that depletion of macrophages did not have the effect on the migration of T cells over the endothelial wall of brain blood vessels, but completely blocked the egress of T cells into the brain parenchyma causing massive cell accumulation within Virchow-Robin spaces (Tran et al., 1998). Furthermore, perivascular phagocytes and APCs can be replaced by blood-derived myeloid cells which can present antigens to T cells and instruct them to egress into the brain parenchyma (Sedgwick et al., 1991). Since the basement membrane of the glia limitans contains laminins 111 and 211 and hence differs from the endothelial basement membrane (containing laminins 411 and 511) (Sixt et al., 2001), T cells have to use a distinct set of matrix metalloproteinase (MMPs) to enter the brain parenchyma. Therefore, broad inhibition of MMPs results in substantial accumulation of T cells in the perivascular space (Toft-Hansen et al., 2006). Crossing of the glia limitans basement membrane requires activity of MMP 2 and 9 which cleave of dystroglycan, i.e. the molecule that anchors astrocyte endfeet to the glia limitans basement membrane (Agrawal et al., 2006). Therefore, while chemokines and integrins direct T cells across the blood vessel endothelial barrier, MMPs are indispensable to allow T cells to cross the second barrier and gain access to the brain parenchyma. Nevertheless, the glia limitans is not only a physical barrier - astrocytes actively participate in the regulation of T cell egress to and function within parenchyma. For example, constitutive expression of CD95L on astrocytic endfeet mediates passage control for T cells as highly activated cells expressing CD95 will die by apoptosis (Pender et al., 1991). Moreover, chemokines produced by astrocytes actively regulate the composition of

perivascular spaces during both homeostasis and inflammation (Farina et al., 2007; Ransohoff et al., 2003).

Once T cells have translocated into the brain parenchyma, their function will be regulated and restricted by microglial cells, neurons and astrocytes. While the level of antigen presentation in the brain is low, inflammation increases MHC expression allowing T cell to be engaged in the interaction with local APCs and infected cells. However, expression of MHC I molecules on infected neurons is strictly regulated (Joly and Oldstone, 1992; Joly et al., 1991) preventing excessive damage of the important neuronal networks. Although, perforin- and Fas- mediated neuronal killing has been reported (Shrestha et al., 2006; Shrestha and Diamond, 2007), CD8<sup>+</sup> T cells are mainly instructed to engage non-cytolytic pathways to destroy infected neuronal cells. Recently, Liu and colleagues have demonstrated that during EAE, neurons that establish cell-to-cell contact with activated T cells produce transforming growth factor (TGF- $\beta$ ) that mediates the conversion of T cells to regulatory T cells irrespective of the antigen specificity (Liu et al., 2006). Additionally, astrocytes can function as efficient APCs (Constantinescu et al., 2005) and direct T cell behavior in a contact-dependent manner. By producing soluble factors, astrocytes can further regulate T cell proliferation and drive induction of regulatory T cells (Trajkovic et al., 2004).

Another cell type that is involved in regulation of T cell behavior within the brain are microglial cell that serve as important sentinel cells. Microglial cell are excellent APCs and produce a wide variety of factors promoting or inhibiting T cell function. For example, expression of B7-H1 molecules on the surface of microglial cells allows engagement of PD-1 co-inhibitory molecule expressed by T cell resulting in inhibition of T cell function (Magnus et al., 2005). Additionally, upregulation of indoleamine2,3-dioxygenase by microglial cells results in production of immunoregulatory tryptophan metabolites that create an immunosuppressive environment (Kwidzinski et al., 2005). In sum, all cells involved in the regulation of T cell function within the CNS create complex network of interactions that maintains the delicate balance between protective response and immunopathology which is critical for optimal CNS function.

### 3.5 Neurotropic virus infections

Several cytopathic and non-cytopathic viruses cause severe diseases in humans that are associated with typical CNS symptoms such as encephalitis or meningoencephalitis. Viruses have acquired strategies to enter the CNS and establish infection invasion via peripheral nerves or via directly crossing vascular barriers. Infection of peripheral sensory or motor nerves and axonal anterograde transport allows viruses such as Theiler's murine encephalomyelitis virus (TMEV), rabies virus, measles virus, Borna disease virus (BDV), poliovirus and alphaherpesviruses (McGavern and Kang, 2011) to reach CNS parenchyma, but depends on the cellular receptors present in nerve endings in peripheral tissues. For example poliovirus, adenovirus and rabies virus bind to neurons at the neuromuscular junction, herpes virus infects sensory nerves, whereas the murine coronavirus can enter the CNS via olfactory nerve endings in the nasal mucosa (Lane and Hosking, 2010).

Other strategies utilized by viruses to enter the CNS include infection of CNS endothelial cells or hijacking of immune cells to sneak into the CNS. Viruses that directly infect endothelial cells are JC, poliovirus, Epstein-Barr (EBV), West Nile and mouse adenovirus (MAV-1) (McGavern and Kang, 2011). Once within the cells, these viruses cause changes in endothelial cell function leading to increased vessel permeability, further promoting viral entrance.

CNS intrusion by hijacking of immune cells is employed by immunodeficiency viruses such as HIV which infect peripheral monocytes and macrophages and use these cells as a vehicle to get past CNS barriers (Alexaki and Wigdahl, 2008). As monocytes travel to the CNS as part of the normal turnover of the perivascular macrophage populations, the virus will be brought into this area where the production of viral proteins induces dysfunction of the barrier causing increased permeability and therefore higher rate of virus entry. Once within the CNS, neurotropic viruses will establish their infection cycle that depends on viral kinetics, particular

properties of viral proteins and the overall immune responsiveness of the host which all together result either in viral clearance or persistence. Failure of the immune system to rapidly eliminate the virus from the CNS will lead either to viral persistence without severe disease or, in case of too strong immune responses to immunopathology.

### 3.5.1 Coronaviruses - Mouse hepatitis virus (MHV)

#### 3.5.1.1 Coronaviridae

The family Coronaviridae is represented by viruses that are large, pseudospherical in shape and contain long, helical nucleocapsid surrounded by an envelope bearing both virus- and host-derived glycoproteins (Lee et al., 2004). The genome of Coronaviridae consists of one single-strand, positive-sense RNA molecule that is the largest among the known RNA viruses. Due to a feature of their replication cycle, coronaviruses produce a nested set of subgenomic RNA (Weiss and Navas-Martin, 2005). Therefore, this family, together with arteriviruses, mesoniviruses and roniviruses, has been classified under the order Nidovirales ('nido' meaning 'nest'). Within the virion, coronaviruses possess several structural proteins including spike glycoprotein (S), transmembrane (M) glycoprotein, nucleocapsid (N), envelope (E) and in some members of the family, hemagglutinin-esterase (HE) protein. The spike glycoprotein is expressed on the surface of the virion and crucially determines the tropism and the virulence of the virus. This protein is formed by three subunits of which S1 forms a globular head structure and the two S2 subunits form transmembrane stalks. Three domains of the spike protein have been shown to influence pathogenicity: (i) the receptor-binding domain (RBD) comprised of 330 amino acids on the N-terminal end of the protein, (ii) the hypervariable region (HVR) within S1 and (iii) the heptad repeated domains (HR1 and HR2) within S2. Small changes within either of the three domains can have drastic consequences for viral tropism, virulence and therefore pathogenesis in vivo (Bender and

Weiss, 2010). The M protein is the most abundant of all structural proteins in the virion and is important for virus assembly. The nucleocapsid (N) protein tightly interacts with the viral genome as it complexes with viral RNA to form the capsid, but also facilitates replication. The envelope (E) protein is integral part of viral membrane and has important role in viral assembly. Finally, hemagglutinin-esterase (HE) is a non-essential glycoprotein that forms a second, smaller spike on the membrane of some members of the family. It has been suggested that HE might function as a second receptor-binding protein, therefore regulating virus spread and infectivity (Bender and Weiss, 2010).

Members of Coronaviridae infect a wide range of species including humans, cows, pigs, chickens, dogs, cats, bats, and mice. While Coronavirus infections in cows, chickens, and pigs can cause great economic burden for farms and industry, infections in humans vary in their severity depending on the virus type and can range from mild respiratory problems caused by HCoV-229E and HCoV-OC43 (McIntosh et al., 1967) to severe acute respiratory syndrome caused by SARS-CoV (Ksiazek et al., 2003) or Mers-CoV (Raj et al., 2013).

Infection of host cells relies on the binding of Spike protein subunit S1 to the receptor expressed on the targeted cells followed by conformational change between S1 and S2 subunits. This conformational change triggers fusion of virus and host cell membranes leading to uncoating and release of viral RNA into the cytoplasm. Replicase/transcriptase complexes are generated upon translation of positive stranded RNA genome and located within double membrane vesicles within the cytoplasm. Replication of genomic RNA that takes place within the vesicles, gives rise to a negative-strand copy of the genome that serves as template for generation of positive-stranded progeny RNAs. Newly generated genomic RNA forms complexes with structural and accessory proteins at the levels of ERGIC (endoplasmic reticulum Golgi intermediate complex) and assembled viral particles leave the cell most likely by using host cell secretory mechanisms (Stanley Perlman and Noah Butler 2008).

### 3.5.1.1.1 Mouse hepatitis virus (MHV)

The mouse hepatitis virus (MHV) belongs to the beta-coronavirus genera and is known as a naturally occurring mouse pathogen, normally infecting cells in liver, gastrointestinal tract and CNS. Hence, this viral infection causes variable diseases including hepatitis, gastroenteritis and acute and chronic encephalomyelitis (Martin P. Hosking and Thomas E. Lane, 2010). Under experimental conditions, the different diseases can be elicited by simple variation of the route of infection. Moreover, pathogenesis of MHV is determined by several factors including presence or absence of pathogenicity factors, dose and immunocompetence of the host. MHV enters host cells upon recognition and binding of spike protein to carcinoembryonic antigen-related cell adhesion molecule 1 (CEACAM1a) that is highly expressed by epithelia, endothelial cells and cells of hematopoietic origin (Godfraind et al, 1995), while in the CNS only epithelial cells and microglia express this protein (Godfraind et al, 1997). However, the recognition that highly neurovirulent strains of MHV (MHV.SD) is able to cause CNS disease in the absence of CEACAM1 (Hemmina et al, 2004) and in vitro identification of psg16 (bCEA) (protein related to pregnancy-specific glycoprotein family) as optional receptor of MHV A59 but not MHV JHM strain (Chen et al 1995) indicated the possibility that other receptors or mechanism might be involved.

The extent of pathology induced by different MHV strains varies significantly. While intracerebral infection with the highly pathogenic MHV.SD (also known as MHV-4) and MHV-JHM cause fatal acute encephalitis, attenuated MHV-J2.2v-1 variant induces less severe encephalomyelitis that results in chronic demyelination (Wiess and Navas-Martin 2005). Unlike other variants of MHV-JHM, MHV A59 has the ability to infect different tissues, mainly depending on the route of infection. While intranasal or intracranial inoculation with MHV A59 virus leads to CNS infection, intraperitoneal or intravenous inoculation results in infection of hepatocytes and induction of severe hepatitis. CNS infection with MHV-J2.2v-1 and MHV A59 leads to acute encephalitis and, if the virus is not cleared efficiently, to viral persistence

in this organs ultimately leading to demyelinating disease (Steven P. Templeton and Stanley Perlman, 2007). Due to clinical and histological similarities between MHV-induced demyelination and human demyelinating diseases such as multiple sclerosis (MS), CNS infection with MHV represents a relevant experimental mouse model for dissection of mechanisms underlying this inflammatory condition.

#### 3.5.1.1.2 Immune responses to MHV

Following intranasal infection of immunocompetent mice with MHV A59, the virus spreads via olfactory nerves to reach the olfactory bulb and spread subsequently within the brain and the spinal cord; other organs, except the cervical lymph nodes are not affected (Lane and Hosking, 2010). In contrast, systemic application of the virus targets internal organs such as liver and spleen, but spares the CNS (Cervantes-Barragan et al., 2007). Irrespective of the route of infection, early control of the virus strongly depends on type I interferon system (IFN-I) as mice deficient in IFN receptor (IFNAR) are highly susceptible to disease and succumb early upon infection (Cervantes-Barragan et al., 2009, 2007). While antiviral effects of IFN type I are necessary to control initial virus replication, successful clearance of the virus strongly depends on adaptive immunity, particularly virus specific CD8<sup>+</sup> T cells. Lack of CD8<sup>+</sup> T cells after either systemic or intranasal MHV A59 infection results in a loss of control of viral replication and has fatal consequences. In immunocompetent mice, the strongest accumulation of virus-specific CD8<sup>+</sup> T cells is observed shortly after the peak virus replication. Large numbers of virus-specific CD8<sup>+</sup> T cells strongly restrict viral spread and reduce viral titers hence ameliorating virus-induced pathology (Eriksson et al., 2008). Likewise, in case of intranasal infection, CD8<sup>+</sup> T cells contribute to clearance of infection virus (Bergmann et al., 1999, 2003). However viral RNA and viral antigens can persist in oligodendrocytes leading to chronic immune activation ultimately resulting in immune-mediated demyelination (Bergmann et al., 2006). Effector mechanisms of CD8<sup>+</sup> T cell-

mediated viral clearance within the CNS depends on the infected cell type, i.e. oligodendroglia respond to IFN- $\gamma$  (Parra et al., 1999; González et al., 2006), while perforin-mediated cytotoxicity eliminates MHV from astrocyte and microglia (Lin et al., 1997). Importantly, in addition to astrocytes, microglia and oligodendrocytes, MHV A59 can establish infection in neurons (Bender and Weiss, 2010). However, the mechanisms responsible for control of MHV within these cells are poorly understood.

While CD8<sup>+</sup> T cell responses to a certain extent independent of CD4<sup>+</sup> T cell during systemic infection, CD8<sup>+</sup> T cell cytotoxicity and survival within the CNS heavily depends on the presents of CD4<sup>+</sup> T cells (Zhou et al., 2005; Stohlman et al., 1998). Furthermore, CD4<sup>+</sup> T cells help to B cell is necessary to allow for neuroprotective IgM and IgG responses (Gil-Cruz et al., 2012). Indeed, neutralizing antibodies represent an additional important line of defense during CNS restricted MHV infection as they prevent the reactivation of the virus in oligodendrocytes and microglia during the chronic phase (Ramakrishna et al., 2002). However, clearance of the virus from MHV A59 infected liver seems to be B cell independent process (Matthews et al., 2001). Taken together, MHV infection represents a well-established experimental system to probe the immune system with a pathogen that leads to distinct pathologies which closely resemble human disease.



## 4 Aims of the study

Defense against viral infections critically depends on CD8<sup>+</sup> T cells. Optimal strength of CD8<sup>+</sup> T cell responses is essential for successful viral clearance. While overshooting CD8<sup>+</sup> T cell responses can be detrimental, particularly in fragile tissues such as the CNS, weak responses fail to control viral replication and lead to viral persistence or death of the host. Therefore, understanding the fine balance of signals that regulate optimal CD8<sup>+</sup> T cell recruitment and performance is of critical importance for development of T cell-based therapies. The major aim of the thesis was to determine the role of low avidity CD8<sup>+</sup> T cells during CNS infection and explore their potential to prevent viral induced pathology in adoptive therapy settings.

The first specific aim of the thesis was to clone and characterize a MHC I restricted TCR specific for the spike protein of MHV and to generate transgenic mice that would allow detailed investigation of CD8<sup>+</sup> T cell responses against the virus.

The second aim was to determine whether and to which extent constitutive chemokines contribute to the control of antiviral CD8<sup>+</sup> T cell recruitment and function within MHV-infected CNS.

The third aim was to determine the consequences of variation in TCR signal strength through tuning TCR density on the surface of antiviral CD8<sup>+</sup> T cells.

## **5 Characterization of a murine coronavirus spike protein-specific TCR and generation of TCR transgenic mice**

Jovana Cupovic<sup>1</sup>, Veronika Nindl<sup>1</sup>, Thomas Rüllicke<sup>2</sup> and Burkhard Ludewig<sup>1</sup>

<sup>1</sup>Institute of Immunobiology, Cantonal Hospital St. Gallen, St. Gallen, Switzerland

<sup>2</sup>Institute of Laboratory Animal Science and Biomodels Austria, University of Veterinary Medicine Vienna, Vienna, Austria

### **5.1 Abstract**

T cell receptor transgenic mice are frequently used tools that facilitate assessment of T cell development and function. Important insight into the nature of T cell responses against pathogens has been gained by tracking monoclonal T cell populations with specificity for immunodominant epitopes. Here, we have analyzed a novel TCR with specificity for the H2-K<sup>b</sup>-binding s598 epitope of the mouse hepatitis virus (MHV). Using hybridoma technology, we have generated stable CD8<sup>+</sup> monoclonal T cell populations expressing the MHV-specific TCR facilitating molecular characterization of the rearranged TCR  $\alpha$  and  $\beta$  chains. Microinjection of two separate cassette vectors containing the cloned TCR  $\alpha$  and  $\beta$  chains into fertilized oocytes of C57BL/5 (B6) mice gave rise to three founder lines. Based on the pattern and stability of transgene expression, founder line #22, named Spiky (TCR-S) has been selected for further characterization. Spiky mice were crossed with B6 mice expressing either the congenic marker CD90.1 (Thy1.1) or CD45.1 (Ly5.1) to allow tracking of the transgenic cells following adoptive transfer. Thorough in vitro and in vivo characterization of Spiky TCR transgenic CD8<sup>+</sup> T cells revealed that this novel tool is well suited to dissect T cell responses directed against a cytopathic coronavirus.

## 5.2 Introduction

The T cell receptor (TCR) critically impinges on the development and differentiation of individual T cells. Since the quality of signals received through the TCR determines the destiny of a T cell, pathogen-specific immune responses can be best studied when instead of surrogates such as ovalbumin, true pathogen-derived epitopes are investigated. Such TCR transgenic T cells can be used in adoptive transfer systems to overcome the limitation of the generally very low frequency of single epitope-specific T cell populations in the naïve state (Butz and Bevan, 1998; Stetson et al., 2002; Blattman et al., 2002). The major prerequisite for the generation of monoclonal T cells is the identification and characterization of a TCR with specificity for the epitope of interest. Technologies that facilitate rapid identification of TCR genes include somatic cell nuclear transfer (Kirak et al., 2010), TCR-gene capture (Linnemann et al., 2013) and MHC multimer-based single cell TCR identification (Dössinger et al., 2013). In addition, isolation of epitope-specific T cells can be achieved by generating T cell clones or T cell hybridomas followed by molecular characterization of rearranged TCR genes. This sequence information can be used to introduce DNA sequences into optimized cassette vectors (Kouskoff et al., 1995). Following microinjection of plasmid vectors containing information of TCR  $\alpha$  or  $\beta$  chains into fertilized oocyte, TCR transgenic mice can be obtained. TCR transgenic mice with specificity for MHC I or II-restricted epitopes have been generated using the latter methodology (Lafaille, 2004). These tools have greatly contributed to our understanding of T cell development and selection (Kisielow et al., 1988; Sha et al., 1988), TCR structure and biochemistry (Udaka et al., 1993), autoimmunity (Goverman et al., 1993; Pöllinger et al., 2009; Osman et al., 1998) and infection biology (Oxenius et al., 1998; Torti et al., 2011; Mueller et al., 2003).

Here, we have employed the hybridoma technology to obtain a stable T cell population expressing a MHC I-restricted TCR specific for the MHV spike protein. Following sequence characterization and molecular cloning into the cassette vector described by Kouskoff et al.

(Kouskoff et al., 1995) , TCR transgenic mice expressing the MHV s598-specific TCR on >98% of their CD8<sup>+</sup> T cells have been generated. Due to the specificity for the spike protein, the novel transgenic mouse line has been named Spiky.

### 5.3 Materials and Methods

#### *Mice and ethical statement*

C57BL/6 (B6) mice were purchased from Charles River Laboratories (Sulzfeld, Germany). Experiments were performed in accordance with federal and cantonal guidelines under permission number SG 11/03 following review and approval by the Cantonal Veterinary Office (St. Gallen, Switzerland).

#### *Generation of s598-605-specific T cell hybridomas*

Six weeks old C57BL/6 (B6) mice were infected intraperitoneally (i.p) with  $5 \times 10^4$  pfu of the molecularly defined MHV A59 strain (Coley et al., 2005). On day 8 post infection, mice were sacrificed and immediately perfused with PBS. Single-cell suspensions from spleen were prepared by mechanical disruption of the organ. Lymphocytes from liver were isolated using mechanical disruption of the organ followed by enrichment based on 70–30% Percoll gradient (GE Healthcare) centrifugation for 25 min at 800xg. Lymphocytes obtained from spleen and liver were used for fusion with BW5147 lymphoma cell line (Hill et al., 1976) (kindly provided by Prof. Dr. Annette Oxenius). Prior to fusion, BW5147 lymphoma cells were cultured in DMEM (Gibco) supplemented with 10% FCS (Lonza), 100 U penicillin-streptomycin (Lonza), 0.02 mM  $\beta$ -mercapthoethanol (Gibco), 1xMEM non-essential amino acids (NEAA; Gibco) and 1 mM sodium pyruvate (Gibco). Fusion of lymphocytes and BW5147 lymphoma cells was performed using polyethylene glycol 1500 (PEG 1500; Roche) at a ratio of 1:5 ( $2 \times 10^7$  BW 5147 cells:  $10^8$  lymphocytes) following the manufacturer's instructions.

Fused cells were seeded in 96-well flat-bottom plates in DMEM 20% (DMEM (Gibco) supplemented with 20% FCS (Lonza), 100 U penicillin-streptomycin (Lonza), 0.02 mM  $\beta$ -mercapthoethanol (Gibco), 1xMEM non-essential amino acids (NEAA; Gibco) and 1mM sodium pyruvat (Gibco) and cultured at 37°C. Twelve to twenty four hours later, the selection medium containing 2xHAT (hypoxanthine-aminopterin-thymidine; Gibco)/DMEM 20% was added and cells were incubated for one week at 37°C. Proliferating hybridoma cell populations were selected, expanded and subjected to flow cytometric analysis. To generate monoclonal populations, positive clones were subcloned using single cell dilutions.

#### *Flow cytometric analysis of hybridoma clones*

Screening of hybridoma clones was performed using surface staining with the following antibodies: anti-CD3-PE, anti-V $\beta$ 7-PE, anti-V $\beta$ 8-PE, anti-V $\beta$ 11-PE, anti-V $\alpha$ 3-FITC, anti-V $\alpha$ 11-FITC, anti-V $\beta$ 3-FITC, anti-V $\beta$ 5-FITC (eBioscience), anti-CD4-FITC, anti-CD8-APC, anti-V $\beta$ 7-PE, anti-V $\beta$ 9-PE (BioLegend). Specificity of hybridoma cells was confirmed using PE-conjugated MHV S598/H-2Kb tetramers (Sanquin, Amsterdam, The Netherlands). Peptide-specific cytokine production of hybridoma clones was assessed using intracellular cytokine staining. To this end,  $10^6$  of hybridoma cells were incubated with  $10^5$  bone marrow-derived DCs loaded with  $10^{-5}$  M s598-605 peptide ((RCQIFANI), Neosystem (Strasbourg, France)) in the presence of brefeldin A (5  $\mu$ g/ml) for 5 h at 37°C. Cells were stimulated with PMA (50 ng/ml) and ionomycin (500 ng/ml; both purchased from Sigma-Aldrich) as positive control or left untreated as negative control. For intracellular staining, restimulated cells were surface stained and fixed with Cytofix-Cytoperm (BD Biosciences) for 20 min. Fixed cells were incubated at 4°C for 40 min with permeabilization buffer (2% FCS/0.5% saponin/PBS) containing anti-IFN- $\gamma$ -PE (Pharmingen). Samples were analyzed by flow cytometry using FACSCalibur flow cytometer (BD Biosciences); data were analyzed using FlowJo software (Tree Star).

### *RNA isolation and cDNA synthesis, DNA isolation, sequencing*

RNA isolation was performed using TRIzol reagent (Invitrogen) following the manufacturer's instructions. In brief, cells were disrupted in TRIzol, RNA was extracted with chloroform and precipitated with isopropanol. The RNA pellet was washed with 75% ethanol and dissolved in RNase-free water (Braun). cDNA synthesis was performed using Super Script II Reverse Transcriptase (Invitrogen) and oligo (dT) primers (purchased from Microsynth) and a standard amplification protocol (25°C 10 min, 37°C 2 h, 85°C 20 s).

For DNA isolation, hybridoma cells were disrupted using Proteinase K (AppliChem). DNA was extracted using a combination of phenol-chloroform-isoamyl alcohol and chloroform. DNA was precipitated using 100% ethanol and the pellet was washed using 70% ethanol. Finally, DNA was dissolved in RNase-free water (Braun).

Sequencing reactions were performed on purified PCR samples (QIAquick PCR purification kit (Qiagen)) using BigDye Terminator v3.1 Cycle Sequencing Kit (Applied Biosystems) following the manufacturer's protocol. Products were purified using SigmaSpin Sequencing Reaction Clean-up columns (Sigma), Hi-Di Formamide denatured (Applied Biosystems) and read with a 4 capillary Genetic Analyzer 3110 (Applied Biosystem). Sequences were analyzed using Geneious software (Biomatters, New Zealand).

### *Identification of TCRV $\alpha$ and TCRV $\beta$ variable region genes and generation of TCR transgenic mouse lines*

Identification of  $\alpha$  and  $\beta$  chain variable elements was performed using PCR reactions with primer sets described previously (Baker et al.). Positive PCR reactions were sequenced as described and aligned to the mouse genome using databases IMGT (<http://www.imgt.org/>) and Ensemble ([http://www.ensembl.org/Mus\\_musculus](http://www.ensembl.org/Mus_musculus)). The full sequence of identified gene segments V $\alpha$ 2J $\alpha$ 7 and V $\beta$ 16J $\beta$ 2-1 was further analyzed on the DNA level to include upstream leader sequences and the intron region. For this purpose additional primer pairs

were designed and generated by Microsynth (Balgach, Switzerland), covering the upstream region of V $\alpha$  chain leader sequence (fwd (5'-GAGCAGGAAGTGCTTCCTATGTCAG-3');

rev (5'-GGGTTCCCTTCCCCAAAGTAAGTC-3'),

leader sequence upstream of V $\beta$  chain (fwd (5'-GAGTCTGCAAAGCAGCAGCTTTGACTTGAG-3')

rev (5'-CACAGAAGTACACAGCTGAGTCCTCC-3'))

and downstream sequence of V $\alpha$  chain constant region

(fwd (5'-GACTCTCAGCCTGGAGACTCAGCTACC-3')

rev 5'-GGTCCCTTCCAGCACTTATTTCTGTGATCC-3')

and downstream sequence of  $\beta$  chain constant region (fwd (5'-

GGCAGATGGTGACCCTCAATTGTGACCCAG-3'), rev (5'-CCCAGCACTGTCAGCTTTGAGCCTTC-3')

The full sequence of the V $\alpha$  chain reads as follows:

CAAGCTTCAGTCTAGGAGGAATGGACAAGATCCTGACAGCATCGTTTTACTCCTAGGCCTTCACCTAGCTG  
GTGAGTCATGAAGGAGAAACCTGAGAATGTGGGATTAATGTGGAGGCATGAGAGACTTGGGGCACCAGGCA  
AGTCATGATATCTAAGCAGGAAGTATATTCCTGGGAACCTAACAAACAGTTGCTATTTCTCTACACAGGGGTGA  
GTGGCCAGCAGCAGGAGAAACGTGACCAGCAGCAGGTGAGACAAAGTCCCCAATCTCTGACAGTCTGGGAA  
GGAGAGACAGCAATTCTGAACTGCAGTTATGAGGACAGCACTTTTGACTACTTCCCATGGTACTGGCAGTTC  
CCTAGGGAAAGCCCTGCACTCCTGATAGCCATACGTCCAGTGTCCTAATAAAAAGGAAGATGGACGATTCACA  
ATCTTCTTCAATAAAAGGGAGAAAAAGCTCTCCTTGACATCACAGACTCTCAGCCTGGAGACTCAGCTACCT  
ACTTCTGTGCAGCAAGTCCGGACTACAGCAACAACAGACTTACTTTGGGGAAGGGAACCCAGGTGGTGGTG  
TTACCAAGTAAGTGAGCTATGTCCTCTGCCACAAGTG.

The full sequence of the V $\beta$  chain reads as follows:

ATTCTGCCGTGACCCTACTATGGATATCTGGCTTCTAGGTTGGATAATTTTAGTTTCTTGGAAGCAGGTGA  
GTTCTTAGAAATTCTAGAGTTTTCAATTCATATTGAGACAATTTAAAGTATTCCATTAATCTTTTTCTCTTTCT  
ACAGGACACACAGGACCCAAAGTCTTACAGATCCCAAGTCATCAAATAATAGATATGGGGCAGATGGTGACC  
CTCAATTGTGACCCAGTTTCTAATCACCTATATTTTATTGGTATAAACAGATTTTAGGACAGCAGATGGAGTT  
TCTGGTTAATTTCTACAATGGTAAAGTCATGGAGAAGTCTAAACTGTTTAAGGATCAGTTTTAGTTGAAAGAC  
CAGATGGTTCATATTTCACTCTGAAAATCCAACCCACAGCACTGGAGGACTCAGCTGTGTACTTCTGTGCCA

## Results

---

GCAGCTTCCTGGGGGGTCATGCTGAGCAGTTCTTCGGACCAGGGACACGACTCACCGTCCTAGGTAAGAAG  
GCAGAGGCCATACAGGTGGGAG)

Plasmids containing sequences of the specific TCR V $\alpha$  and V $\beta$  chains were synthesized by GenScript USA containing Xma I ( $\alpha$  chain) or Xho I ( $\beta$  chain) restriction sites on the 5' end and Not I ( $\alpha$  chain) and Sac II ( $\beta$  chain) restriction sites on the 3' end. The inserts were provided in pUC57 vectors which were digested and linearized sequences were cloned into TCR expression vectors (Kouskoff et al., 1995). Resulting vectors pTS alfa V $\alpha$ 2J $\alpha$ 7 and pTS beta V $\beta$ 16J $\beta$ 2-1 were digested using Sall and KpnI to remove prokaryotic vector DNA and to obtain linearized plasmid DNA. The transgene DNA fragments were co-injected in equimolar ratios into fertilized C57BL/6N oocytes according to the standard method in the Institute of Laboratory Animal Science in Vienna. Based on standardized genetic nomenclature for mice, the resulting TCR transgenic founder lines expressing functional  $\alpha\beta$  TCRs were designated: C57BL/6N Tg (Tcra, Tcrb) 556biat, C57BL/6N Tg (Tcra, Tcrb) 577biat (Spiky) and C57BL/6N Tg (Tcra, Tcrb) 578biat.

### *Generation of BM-derived DCs*

Bone marrow was flushed from femurs and tibias of C57BL/6 mice and erythrocytes were lysed by osmotic shock with 1 ml lysis buffer (0.15 M NH<sub>3</sub>Cl, 1 mM KHCO<sub>3</sub>, 0.1 mM EDTA) for 1 min at room temperature. Cells were washed twice with BSS and cultured in 5% RPMI 1640 (Sigma) supplemented with 5% FCS (Lonza), 100 U penicillin-streptomycin (Lonza) and 5% GM-CSF (supernatant of X63 GM-CSF cells). Medium was replenished on days 2 and 4 of culturing. Non-adherent cells were harvested on day 6.

### *In vitro CFSE proliferation assay*

Single-cell suspensions obtained from spleen were subjected to erythrocyte lysis and labeled using 10  $\mu$ l 5 mM carboxyfluorescein succinimidyl ester (CFSE, Molecular Probes, Leiden,



Netherlands) according to the manufacturer's protocol.  $10^5$  splenocytes and  $2 \times 10^4$  bone marrow-derived DCs were seeded in a 96-well round-bottom plate and s598 peptide was added at indicated concentrations. After 72 h of incubation at 37°C, cells were analyzed by flow cytometry.

### *Phenotyping of TCR transgenic lines*

Single-cell suspensions from spleens were obtained as described above. Blood samples were collected in 3 ml of FACS buffer to prevent coagulation and subsequently treated with BD FACS Lysing Solution (BD Bioscience). Characterization of the cells was performed using surface staining with antibodies against CD4-FITC, CD8-APC (BioLegend), CD3-PE (eBioscience) and PE-conjugated MHV S598/H-2Kb tetramers (Sanquin, Amsterdam, The Netherlands). For PCR phenotyping, ear punch biopsies were digested with Viagen DirectPCR Lysis Reagent (Peqlab) supplemented with 0.2 mg/ml Proteinase K (AppliChem) following the manufacturer's instructions. PCR reactions were performed using primer pairs generated by Microsynth (Balgach, Switzerland):

fwd 5'-(CCTTGCAGCTCTCAGAAGTGCAGTTG)-3'

rev 5'-(GGGTTCCCTTCCCCAAAGTAAGTC)-3' for Va chain and

fwd 5'-(GGCTGAGACTAGGTCCAGTACTACAGAG)-3'

rev 5'-(CACAGAAGTACACAGCTGAGTCCTCC)-3' for Vβ chain

at conditions: 95°C 10min; 39 cycles - 95°C 45 sec, 56°C 45 sec, 72°C 60 sec; 72°C 10 min.

### 5.4 Results

#### 5.4.1 Characterization of a MHV A59 spike protein<sub>(598-605)</sub> specific TCR

We have utilized the hybridoma technology to isolate and characterize a H-2K<sup>b</sup>-restricted TCR recognizing the MHV A59 spike protein-derived epitope s598-605. T cells isolated from livers and spleens of MHV infected mice were fused with TCR<sup>+</sup>/CD4<sup>+</sup>/CD8<sup>+</sup> BW5147 cell line to generate stable hybridoma clones. Proliferating hybridoma clones were initially screened for CD3/CD4/CD8 expression and antigen specificity. Two polyclonal hybridoma populations showed antigen specificity by responding to s598 peptide stimulation *in vitro* as detected by IFN- $\gamma$  production in intracellular cytokine staining and by binding to H2-K<sup>d</sup>/s598 tetramers (result not shown). Polyclonal population 1C3 (Fig. 5a) was selected for further analyses and was subcloned to obtain monoclonal cells. Investigation of antigen specificity of monoclonal hybridoma populations revealed specific IFN- $\gamma$ -production following stimulation with s598 peptide-loaded DCs (Fig. 5b) and specific H2-K<sup>d</sup>/s598 tetramer binding (Fig. 5c). The TCR complex was stably expressed on the surface of the monoclonal population, as shown by CD3 expression (Fig. 5d). FACS screening of the monoclonal clones revealed that the TCR  $\alpha$  chain utilizes the variable segment 2, and is therefore designated V $\alpha$ 2 (according to Wilson et al.,1988) (Fig. 5e).

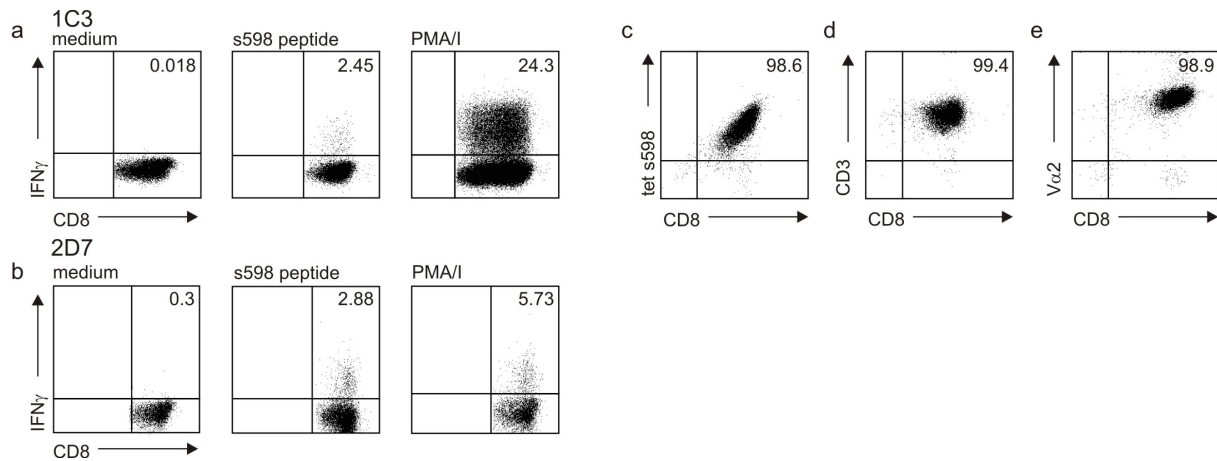


**Figure 5. Generation of MHV s598-specific hybridoma cells.**

Antigen specificity of polyclonal hybridoma population a) 1C3 b) and monoclonal hybridoma clone 2D7 was confirmed by the ability to produce IFN- $\gamma$  upon incubation with s598 peptide-loaded DCs. Flow cytometric analysis of monoclonal hybridoma populations revealed c) binding to H2-K<sup>d</sup>/s598 tetramer, d) stable expression of TCR on the surface determined by CD3 expression and e) usage of variable segment 2 by the  $\alpha$  chain of the TCR. Data are representative of two independent experiments.

Full characterization of the TCR on the molecular level was performed using sets of PCR primers amplifying the majority of genomic V $\alpha$  and V $\beta$  genes of the rearranged TCR (Baker et al., 2002). Pooling the primers in groups of 5 simplified screening for the TCR  $\alpha$  chain (positive PCR signal detected in group composed of V $\alpha$ 1 – V $\alpha$ 5, Fig. 6a) and the TCR  $\beta$  variable region (positive PCR signal detected in group composed of V $\beta$ 12 - V $\beta$ 16, Fig. 6b). Separation of the primers from the pools confirmed V $\alpha$ 2 positivity (Fig. 6c) that had been found by flow cytometry (Fig. 5e). Moreover, we found V $\beta$ 16 (according to Wilson et al., 1988) as a variable segment of the TCR  $\beta$  chain (Fig. 6d). Due to the lack of an antibody against V $\beta$ 16, FACS confirmation of  $\beta$  chain variable segment used by MHV A59-specific TCR is not possible at this moment. Therefore, further characterization and description of surface expression of the TCR has to be addressed using combination of H2-K<sup>d</sup>/s598 tetramer and V $\alpha$ 2-specific antibody.

## Results

The databases IMGT (Bosc and Lefranc, 2000) and Ensembl (Flicek et al., 2014) were used for alignment of sequencing data obtained from PCR products which confirmed the usage of the identified V segments. Identification of the highly variable regions (CDR3), one intron element downstream of the leader region as well as controlling elements on 5' end of leader and 3' end of J regions allowed the characterization of the entire  $\alpha$  ( $V\alpha 2J\alpha 7$ ) and  $\beta$  ( $V\beta 16J\beta 2-1$ ) chains necessary for cloning of the full MHV A59-specific TCR (Fig. 6e).

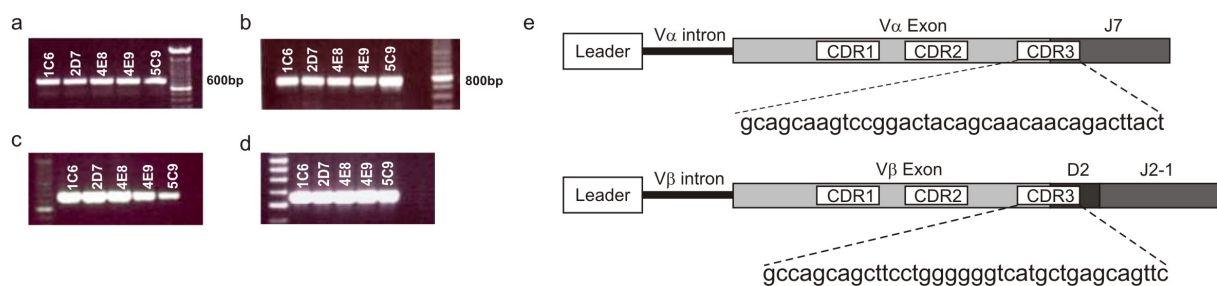


**Figure 6. Characterization of the s598-specific TCR.**

RT-PCR analysis of the variable genes used by a)  $\alpha$  and b)  $\beta$  chains (pooled primer sets). Separating positive primer pool allowed c) confirmation of the variable segment 2 used by TCR  $\alpha$  chain and d) the identification of segment 16 used by  $\beta$  chain in all 5 subclones. e) Schematic illustration of the DNA sequence of the s598-specific TCR. The sequence of the CDR3 region with the highest influence on the TCR specificity is displayed in details.

### 5.4.2 Generation of MHV spike protein- specific transgenic mice

In order to create transferable and traceable T cells allowing characterization of antiviral T cell responses, we made use of the system previously described by Kouskoff et al. (Kouskoff et al., 1995). The full sequence of the MHV spike protein-specific TCR was cloned into cassette vectors and linearized plasmids were microinjected into the male pronucleus of freshly fertilized oocytes. This procedure gave rise to 24 potential founder lines. Initial

screening was performed on the DNA level using PCR that identified three potential founder mice (founder #9, #23 and #22) (Fig. 7a). Surface expression of a functional s598-specific TCR from the integrated constructs was evaluated by FACS analysis of blood samples. Staining for the transgenic  $V\alpha 2$  chain revealed expression of the transgenic TCR on 99.6 % of  $CD8^+$  T cells in founder line #22 and 85.8% of  $CD8^+$  T cell in founder line #23 (Fig. 7b). Initially, no transgenic TCR expression has been detected on  $CD8^+$  T cells from the founder line #9 (data not shown). These data showed that the sequences identified in our screening encode for a productively rearranged TCR that can be expressed in vivo.

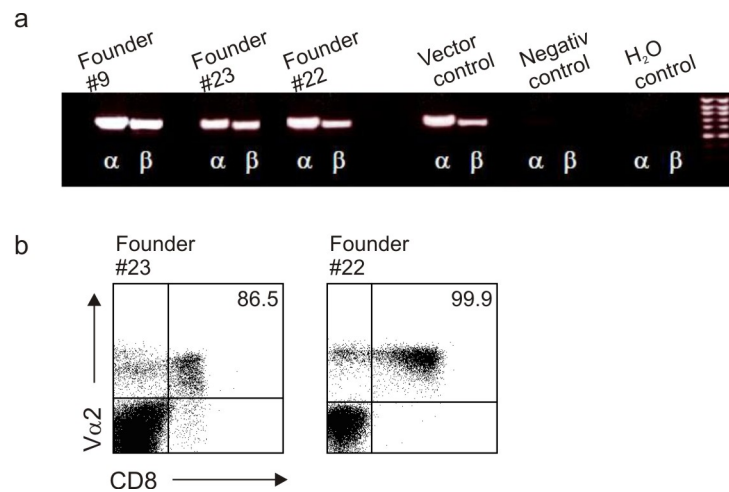


**Figure 7. Analysis of s598-specific transgenic founder mice.**

a) PCR analysis using primers binding to the construct and within the variable regions of the TCR. Founder #9, #22 and #23 were positive for the  $\alpha$  and  $\beta$  constructs. Original cassette vectors were used as positive control. b) The expression of integrated constructs was assessed from the blood of founder mice using flow cytometric analysis for transgenic  $V\alpha 2$  chain expression on  $CD8^+$  T cells. Values in the upper right quadrant indicate the percentage of  $V\alpha 2^+$  of  $CD8^+$  T cells.

### 5.4.3 Comparison of transgenic TCR expression in the different founder lines

Further analysis of the founder lines indicated differences in the pattern of transgenic TCR expression among three different lines. Interestingly, F1 offsprings of the initially negative founder line #9 exhibited expression of transgenic V $\alpha$ 2 on 92.4 $\pm$ 8.4% CD8<sup>+</sup> T cells and high K<sup>d</sup>/s598 tetramer binding (91.6 $\pm$ 7.8%) (Fig. 8a). Expression of the transgenic V $\alpha$ 2 chain was detected on 74.8 $\pm$ 5.9% of CD8<sup>+</sup> T cells from offsprings of founder line #23, which also bound the K<sup>d</sup>/s598 tetramer (Fig. 8b). Highest and most stable transgene expression was detectable in line #22 exhibiting 99.1 $\pm$ 0.7% V $\alpha$ 2-positive CD8<sup>+</sup> T cells and 97 $\pm$ 0.4% K<sup>d</sup>/s598 tetramer binding (Fig. 8c). Assessment of peripheral T cell frequencies revealed a pronounced reduction in CD4<sup>+</sup> T cell compartment in all three founder lines as compared to the control mice (Fig. 8a,b,c,d). Since a major aim of this project has been the generation of potential donors of TCR transgenic splenocytes, we determined which of the lines provided highest yield of virus-specific, TCR transgenic splenocytes (Fig. 8e,f,g). Comparable to the results obtained from blood, the highest frequency of transgene positive and K<sup>d</sup>/s598 tetramer-binding CD8<sup>+</sup> T cells (97.2 $\pm$ 0.7%, 97.2 $\pm$ 0.9%, respectively) could be found in line #22 (Fig. 8g). Therefore, line #22 has been chosen to be utilized for further analysis and has been designated Spiky (TCR-S).

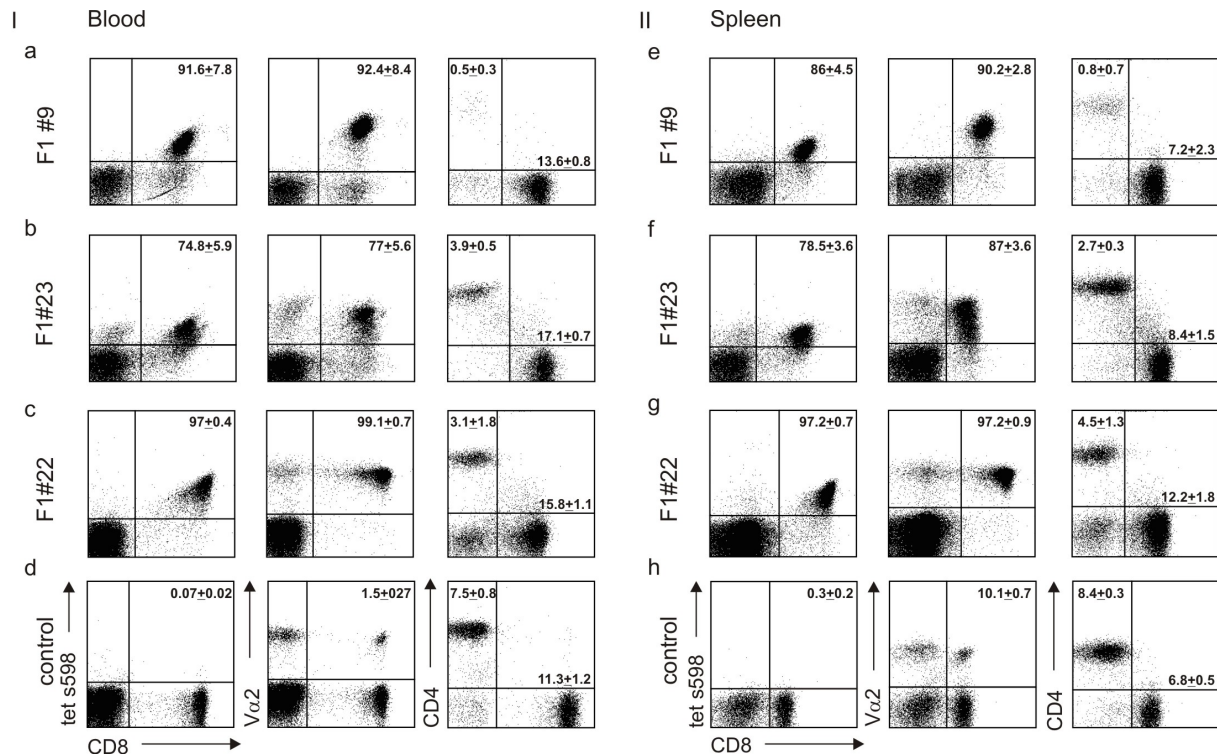


**Figure 8. Comparison of transgenic TCR expression in three different founder lines.**

Analysis of the transgene expression in the offspring of three different founder lines was performed on T cells derived from (I) blood (II) and spleen. The values indicate the mean percentage $\pm$ SD of the frequencies of H2-K<sup>d</sup>/s598 tetramer-binding CD8<sup>+</sup> T cells, V $\alpha$ 2<sup>+</sup> of CD8<sup>+</sup> T cells and CD3<sup>+</sup>CD4<sup>+</sup>, CD3<sup>+</sup> CD8<sup>+</sup> lymphocytes. The plots are representative of 2 independent experiments, n=4 mice.

#### 5.4.4 Functional assessment of TCR transgenic CD8<sup>+</sup> T cells

Antigen responsiveness and proliferation capacity of TCR transgenic CD8<sup>+</sup> T cells was assessed by dilution of the dye CFSE as described previously (Quah et al., 2007). To this end, splenocytes from Spiky transgenic mice were labeled with CFSE and co-incubated with s598 peptide-loaded DCs ( $10^{-4}$ M -  $10^{-7}$ M). Substantial CFSE dilution was detected after 72 h of peptide stimulation (Fig. 9a) and indicated high responsiveness of the TCR transgenic T cells. Functional avidity of a particular T cell population can be determined from the dose-

## Results

response behavior following exposure to the cognate peptide (Hesse et al., 2001; Nauerth et al., 2013). These revealed that TCR Spiky cells require peptide concentrations of around  $10^{-6}$  M to start proliferation. Using CFSE dilution at 72 h after stimulation, we found that Spiky T cells exhibit rather low functional avidity demonstrated by high peptide concentration ( $3 \times 10^{-7}$  M) needed to achieve half-maximal level of the proliferative response (EC50) (Fig. 9b). Further analysis of Spiky mice spleen and lymph node cellular composition revealed, beside a reduction in CD4<sup>+</sup> T cell numbers, no major differences in frequencies and absolute numbers of B cells, NK cells, macrophages, neutrophils or DCs (data not shown). Taken together, we have generated a new TCR transgenic mouse model that possesses CD8<sup>+</sup> T cells of rather modest functional avidity for the MHV A59 spike protein-derived immunodominant epitope s598-605.

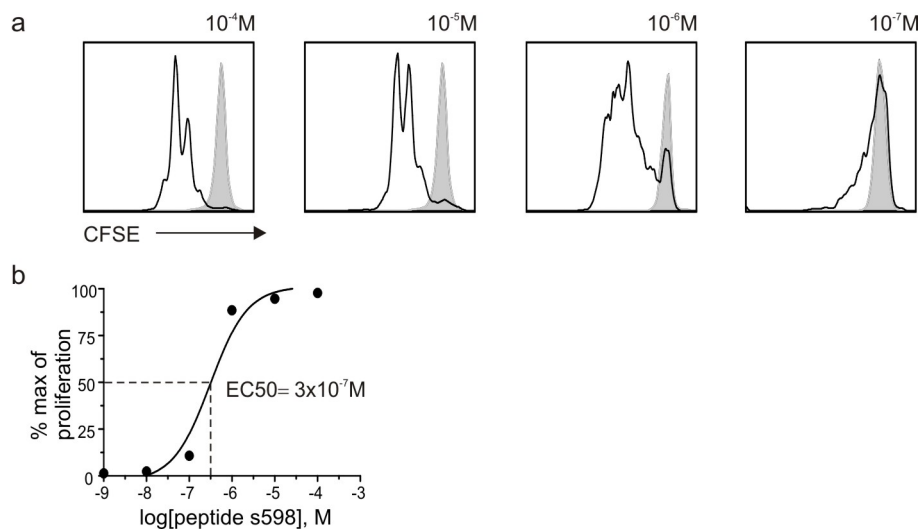


**Figure 9. In vitro functionality of Spiky transgenic splenocytes.**

Functionality of the Spiky transgenic splenocytes assessed by *in vitro* proliferation assay.

a) Proliferative response assessed by CFSE dilution at 72 h of stimulation (black lines-peptide stimulated cells, gray shaded lines - untreated cells).

b) Percent of proliferated cells upon stimulation with indicated amounts of s598 peptide as determined by CFSE dilution after 72 h. The percentage of proliferated CD8<sup>+</sup> T cells was normalized to the maximum, and peptide concentration for half-maximal proliferative response (EC50) was calculated after fitting a nonlinear regression curve.



## 5.5 Discussion

The nature of an invading pathogen impinges on the pattern of T cell activation. Hence, the analysis of pathogen-specific T cell responses depends on the availability of analytical tools and routines to reveal basic mechanisms of infectious disease pathogenesis and to assess efficacy of potential vaccination approaches against infectious diseases. Since the numbers of epitope-specific T cells in the naïve state (Blattman et al., 2002; Butz and Bevan, 1998; Whitmire et al., 2006) and frequently in the memory phase of an infection (Blattman et al., 2002) are rather low, systems that permit T cell analysis at higher resolution are required. To circumvent time-consuming characterization of pathogen-specific TCRs and generation of TCR transgenic mice, surrogate antigens, such as ovalbumin, recognized by OT-I or OT-II TCR transgenic T cells are widely used (Gerlach et al., 2010; King et al., 2012; Prlic, Hernandez-Hoyos, & Bevan, 2006; Sun, Williams, & Bevan, 2004; Zehn, Lee, & Bevan, 2009). Several pathogens have been genetically modified to express ovalbumin (Carreño et al., 2007; Pope et al., 2001) and to facilitate the analysis of “pathogen-specific” OT-I and OT-II TCR-transgenic T cells. We prefer the view that such reduced systems do not represent the natural host-pathogen relationship and that important features of T cell responses directed, for example, against a virus may be overlooked. Hence, we have developed a novel genetic tool to allow more comprehensive studies of T cell responses against a natural mouse pathogen.

The use of TCR transgenic mice specific for LCMV (Brändle et al., 1995; Oxenius et al., 1998), MCMV (Torti et al., 2011), Hepatitis B virus (Guidotti et al., 1995) or herpes simplex virus (HSV-1) (Mueller et al., 2003) greatly contributed to our knowledge of antiviral immunity. Application of these virus-specific TCR transgenic cells allowed insight into general mechanisms of antiviral T cell responses such as memory formation (Mueller et al., 2010; Araki et al., 2009; Kaech et al., 2002), T cell exhaustion (Zinselmeyer et al., 2013; Wherry et

## Results

---

al., 2007), effector mechanisms (Schenkel et al., 2013; Roth and Pircher, 2004) and others. More specifically, analysis of virus-specific T cell responses using TCR transgenic T cells reveal the mechanisms utilized by particular viruses or group of viruses contributing to the pool of knowledge necessary to design successful vaccination and adoptive T cell therapy strategies. Therefore, generation of TCR transgenic mice specific for the cytopathic virus capable of establishing the infection in both liver and CNS offers a great tool to dissect the mechanism regulating T cell behavior within these specific anatomic sites. Moreover, as MHV A59 represents the model of cytopathic viral infection that shares molecular characteristics with other coronaviruses capable of infecting humans (SARS-CoV, Mers-CoV), investigation of MHV-specific T cell responses would contribute to a better understanding of mechanisms responsible for the defense against relevant human pathogens.

Initial characterization of the functionality of Spiky transgenic T cells revealed the need for high peptide concentration to elicit proliferative response indicative for low avidity of the MHV-specific transgenic cells. While antiviral CD8<sup>+</sup> T cell are thought to be of rather high avidity revealing functional responses after stimulation with only 10<sup>-9</sup> M of the relevant peptide (Oxenius et al., 1998; Mueller et al., 2002), recent findings indicate important contribution of low avidity CD8<sup>+</sup> T cells during ongoing immune responses (Rosenberg, 2008; Boon et al., 2006; Zehn and Bevan, 2006). However, the lack of tools in the past precluded a thorough analysis of the role of low avidity CD8<sup>+</sup> T cells in immune responses. We believe that newly generated TCR transgenic Spiky mouse will help close this analytical gap and shed light on the role of low avidity T cells during antiviral immune responses.

In conclusion, we have successfully generated a novel TCR transgenic model with specificity for the MHC I-restricted MHV spike protein-derived epitope s598. The cloned Spiky TCR offers the opportunity to systematically examine the natural CD8<sup>+</sup> T cell response triggered by a cytopathic virus infection.

## **5.6 Acknowledgments**

We would like to thank Rita DeGiuli and Fabienne Soppelsa for technical support.

## **5.7 Data contribution**

Jovana Cupovic characterized the s598-specific TCR, generated TCR-S cassette vectors and characterized Spiky transgenic mouse under the supervision of Veronika Nindl and Burkhard Ludewig. Thomas Rüllicke performed DNA microinjection.

## 6 Extra-lymphatic CCR7-ligand expression controls virus-induced CNS inflammation

Jovana Cupovic<sup>1</sup>, Cristina Gil-Cruz<sup>1</sup>, Lucas Onder<sup>1</sup>, Elke Weiler<sup>2</sup>, Ingo Bachmann<sup>2</sup>, Sonja Firner-Caviezel<sup>1</sup>, Christian Perez-Shibayama<sup>1</sup> and Burkhard Ludewig<sup>1</sup>

<sup>1</sup>Institute for Immunobiology, Kanton Hospital St. Gallen, St. Gallen, Switzerland

<sup>2</sup>Institute of Anatomy, University of Leipzig, Germany

### 6.1 Abstract

The constitutive chemokines CCL19 and CCL21, i.e. the ligands of chemokine receptor 7 (CCR7), are critical regulators of immune homeostasis and activation within secondary lymphoid organs. Importantly these chemokines are also expressed in the CNS and their expression is significantly elevated in patients suffering from multiple sclerosis. However, it has remained elusive whether and how these chemokines impinge on virus-driven inflammatory processes in the CNS that precipitate demyelination. Using Ccl19-Cre reporter mice facilitating in vivo tracking of CCL19-producing cells, immunohistochemistry and RT-PCR analysis, we assessed to which extent CCR7 ligands produced in the CNS contribute to the control of coronavirus-mediated CNS inflammation. We found that CCL19 was produced predominantly by endothelial cells of brain microvessels, astrocytes and stromal cells adjacent to the axonal trajectories of infected neurons. Moreover, we identified podoplanin-expressing endothelial cells of blood-brain-barrier microvessels as main producers of CCL21. To assess whether the disruption of the CCR7-CCL19/CCL21 axis in the CNS impacts on virus-induced CNS inflammation, we utilized mice lacking either CCR7 on all cells or CCR7-ligands selectively within secondary lymphoid organs (paucity of lymph node T cell (plt/plt) mice). CCR7-deficient mice rapidly lost weight and were terminally ill at day 10 post infection. In strong contrast, plt/plt mice that have preserved expression of the Ccl21-Lec isoform in the

CNS, completely recovered from the infection. Moreover, antiviral T cell responses in CCR7-deficient mice were more severely affected compared to plt/plt mice resulting in impaired virus control. Importantly, competitive adoptive transfer of CCR7-proficient and CCR7-deficient, virus-specific CD8<sup>+</sup> T cells resulted in preferential recruitment of CCR7-expressing cells to the brains of plt/plt animals further showing that CNS-restricted expression of CCR7 crucially regulates cell recruitment to the brain. Further along the same line, adoptive transfer of CCR7-proficient virus-specific cells rescued CCR7-deficient mice from lethal CNS inflammation. Taken together, these data indicate that expression of CCR7 ligands in the CNS provides a crucial advantage for the host during neurotropic viral infection.

### 6.2 Introduction

Successful adaptive immune responses against pathogens rely on activation of specific lymphocytes within secondary lymphoid organs (Junt et al., 2008) and the recruitment of appropriately activated cells to sites of pathogen replication where the cells can exert their effector functions. Chemokines play a central role in these processes by coordinating the localization of immune cells in defined areas of the body thereby allowing specific interactions to occur (Bromley et al., 2008). CCR7 and its ligands CCL19 and CCL21 represent the core chemokine axis of adaptive immunity responsible for multiple aspects of development, activation and migration of lymphocytes (Comerford et al., 2013). The primary function of CCR7 and its ligands is to establish and propagate anatomical microenvironments that support cognate interactions between antigen-presenting cells (APCs) and antigen-specific lymphocytes. In lymph nodes, this is achieved by constitutive expression of CCL19/CCL21 on stromal cells that organize “molecular highways” for incoming CCR7-expressing lymphocytes. Fibroblastic reticular cells (FRCs) of LNs produce both chemokines, but only CCL21 is secreted by endothelial cells (ECs) of high endothelial venules (HEVs) as well as lymphatic endothelial cells (LECs). Whereas CCL19 is encoded by one gene, gene duplication gave rise to two functional CCL21 variants that differ by only one amino acid and exhibit different expression patterns. While the CCL21a variant bears a serine at position 65 and is expressed in lymphoid organs such as thymus, lymph node and spleen, the CCL21b leucine-isoform is expressed in non-lymphoid organs such as lung, heart, colon, stomach, brain and skin (Chen et al., 2002). Even though both chemokines bind CCR7 with similar affinity, the structures of CCL19 and CCL21 are disparate implying differences in their function as well as regulation. While CCL19 exists only as a locally available, soluble molecule, the extended C-terminal tail of CCL21 enables this chemokine high affinity binding to glycosaminoglycans (GAGs) and other molecules of the extracellular matrix enhancing its presentation on the surface of ECs (Gunn et al., 1998; Rot and von Andrian, 2004).

Furthermore, the proteoglycan podoplanin expressed by stromal cells can specifically present CCL21 and has been shown to regulate the availability of this chemokine (Förster et al., 2008). Nevertheless, the soluble form of CCL21 can also be available upon cleavage of matrix-bound chemokine.

Differences in the availability of the two CCR7 ligands are associated with disparate functions. The matrix bound CCL21 induces both chemotactic migration and cell adhesion (Schumann et al., 2010), which is important for extravasation processes. However, the soluble forms of both chemokines can induce chemotaxis, but not adhesion (Schumann et al., 2010). Additionally, CCL19 has been found to have an additional role by providing non-migratory signals such as promoting cell survival (Link et al., 2007). These functions of CCL19 and CCL21 are exerted following binding to their G protein-coupled receptor, CCR7 that contains seven transmembrane-spanning domains and propagates the signal to a distinct set of intracellular downstream signaling modules including mitogen-activated protein kinase and Rho-cofilin signaling axis (Noor and Wilson, 2012).

CCR7 is expressed by thymocytes during different stages of their development, naïve T and B cells, mature and semi-mature DCs, T regulatory cells as well central memory (CM) T cells (Comerford et al., 2013). Research on CCR7-deficient mice revealed strong dependency of T cells on CCR7 signaling for efficient entry into LNs and PPs (Stein et al., 2000). The inability of CCR7-deficient T cells to receive instructions from CCL19/CCL21-producing FRCs of LNs resulted in their reduced motility (Worbs et al., 2007). Even though migration of both T cells and DCs and their motility within LNs in CCR7-deficient mice is strongly impaired, interactions between T cells and DCs in these mice still do occur but with diminished efficiency and within altered anatomical locations of spleen and LNs (Förster et al., 1999; Gunn et al., 1999). However, numerous studies using infections of CCR7-deficient mice have shown that the effects of CCR7-deficiency on adaptive immune responses strongly relies on the nature of the pathogen (Kursar et al., 2005; Olmos et al., 2010; Noor et al., 2010; Junt et al., 2004).

Importantly, some CCL19 and CCL21 expression can also be found in non-lymphoid, peripheral organs such as skin (Christopherson et al., 2003), lung (Lo et al., 2003) and CNS (Krumbholz et al., 2007; Columba-Cabezas et al., 2003; Pashenkov et al., 2003; Kivisäkk et al., 2004). Moreover, the production of CCR7 ligands can be increased during inflammatory reactions such as in the CNS (Krumbholz et al., 2007; Pashenkov et al., 2003), lung (Rangel-Moreno et al., 2007) or liver (Burke et al., 2010). The finding that ectopic expression of CCL21 is sufficient to allow for the development of tertiary lymphoid organs (Marinkovic et al., 2006) suggests that CCR7 ligands can actively regulate immune cell localization and function at peripheral sites of inflammation.

The central nervous system requires particularly strict entry and functional control of lymphocytes because immunopathological damage of this organ has to be kept at a minimum (Owens et al., 2008). However, the finding that more than 80% of the cells in the cerebro-spinal fluid (CSF) of healthy individuals are CM T cells, expressing high levels of CCR7 (Giunti et al., 2003; Kivisäkk et al., 2004) suggest that entry and maintenance of T cells in the CNS is controlled – at least in part – via this molecule. Moreover, chronic inflammatory diseases of the CNS such as multiple sclerosis (MS) are associated with elevated CCL19 expression in active and inactive lesions (Pashenkov et al., 2003; Krumbholz et al., 2007). In an experimental model of MS, both CCL19 and CCL21 can be detected in inflamed venules and perivascular cuffs (Columba-Cabezas et al., 2003). However, it is not known whether the expression of CCR7 ligands in the CNS is sufficient to protect from severe CNS inflammation.

To address this question, we utilized the intranasal (i.n.) infection with the mouse hepatitis virus (MHV) strain A59 which leads to a transient encephalitis in immunocompetent animals, but causes chronic demyelinating and lethal disease in animals with particular immunodeficiencies (Cervantes-Barragan et al., 2009; Gil-Cruz et al., 2012). Here, we focused on the events that take place early during the establishment of the infection, when MHV causes more than 1,000-fold upregulation of the chemokines in affected regions of the CNS. We found that these chemokines are mainly produced by CNS stromal cells, i.e. ECs



and perivascular fibroblasts, around postcapillary venules. Importantly, ablation of CCR7 was associated with reduced recruitment of antiviral CD8<sup>+</sup> T cells to the CNS and development of lethal CNS disease. However, expression of the CCL21b isoform outside of SLOs secured sufficient CD8<sup>+</sup> T cell recruitment to the CNS and hence provided protection from virus-mediated disease. Taken together, our data revealed that CCR7 ligands expressed in the CNS exert crucial functions for optimal control of neurotropic viral infection.

## 6.3 Materials and Methods

### *Ethical statement*

Experiments were performed in accordance with federal and cantonal guidelines under permission number SG09/87 following review and approval by the Cantonal Veterinary Office (St. Gallen, Switzerland).

### *Mice*

C57BL/6 (B6) mice were purchased from Charles River Laboratories (Sulzfeld, Germany). CCR7-deficient, CXCR3-deficient and plt/plt mice were obtained from the institute für Labortierkunde (University of Zürich). All mice were maintained in individually ventilated cages and were used in the age of 6 to 9 weeks.

### *Virus infection and determination of virus-induced pathology*

Mice were infected intranasally using  $5 \times 10^4$  pfu MHV A59 (Coley et al., 2005) or MHV eGFP (Cervantes-Barragan et al., 2009a). At indicated time points mice were sacrificed, organs were collected, weighed and stored at  $-80^{\circ}\text{C}$  until further analysis. Virus titers were determined from homogenized organs using standard plaque assay on L929 cells (Züst et al., 2007).

### *RNA isolation and quantitative RT-PCR*

Samples from indicated areas of the brains were collected and stored at  $-80^{\circ}\text{C}$  as described above. Brain samples were disrupted in TRIzol and RNA was isolated according to the manufacturer's instructions (Invitrogen). To remove residual DNA, RNA samples were treated with DNasefree (Life technologies) according to the manufacturer's protocol. cDNA was prepared using the High Capacity cDNA Reverse Transcription kit (Applied Biosystems). HotStar Taq DNA polymerase (Qiagen) was used to amplify cDNA by conventional RT-PCR. Quantitative real-time PCR was performed using the LightCycler 1.5 (Roche Diagnostics) and the LightCycler FastStart DNA master SYBR Green I kit (Roche Diagnostics) following the manufacturer's protocol. For LightCycler analysis, expression of TATA-binding protein (TBP) was used for normalization. Relative expression of samples from naive and MHV A59-infected mice was calculated by the comparative cycling threshold method ( $\Delta\Delta\text{-CT}$  method). Amplification program for the LightCycler instrument was  $95^{\circ}\text{C}$  15 min; 50 cycles –  $95^{\circ}\text{C}$  10 sec,  $58^{\circ}\text{C}$  10 sec,  $72^{\circ}\text{C}$  20 sec.

The primer pairs described previously (Scandella et al., 2008) were used for the analyses of

Ccl19:

Forward: 5'-CTGCCTCAGATTATCTGCCAT-3';

reverse: 5'-AGGTAGCGGAAGGCTTTTAC-3'

Ccl21:

Forward: 5'-AAGGCAGTGATGGAGGGG-3';

reverse: 5'-CGGGGTAAGAACAGGATTG-3'

TBP:

Forward: 5'-CCTTCACCAATGACTCCTATGAC-3';

reverse: 5'- CAAGTTTACAGCCAAGATTAC-3'

### *Immunohistochemistry*

Brains were fixed over night in freshly prepared 4% paraformaldehyde (Merck) at 4°C under agitation and subsequently washed in PBS for one additional day. Fixed brains were embedded in 4% low melting agarose (Invitrogen) in PBS and sectioned with a vibratome (VT-1200; Leica). 20–30- $\mu$ m-thick sections were blocked in PBS containing 10% FCS, 1 mg/ml anti-FcR $\gamma$  (BD) and 0.1% Triton X-100 (Sigma-Aldrich). Sections were incubated over night at 4°C with the following antibodies: anti-CCL21 (Abcam), anti-gp38/podoplanin, conjugated anti-CD31 (eBioscience). Unconjugated antibodies were detected using Alexa-fluor labelled secondary antibodies and Alexa-fluor labelled streptavidin (Jackson Immunotools). Microscopic analysis was performed using a confocal microscope (LSM-710; Carl Zeiss) and images were processed with ZEN 2010 software (Carl Zeiss).

### *Cell isolation and adoptive transfer*

Single-cell suspensions from spleens were prepared by mechanical disruption of the organ. For adoptive transfer, splenocytes were depleted of erythrocytes using lysis buffer (0.15 M NH<sub>4</sub>Cl, 1 mM KHCO<sub>3</sub>, 0.1 mM EDTA). For in vivo proliferation and protection studies, splenocytes were labeled using 10  $\mu$ l 5 mM CFSE (Molecular Probes, Leiden, Netherlands) according to the manufacturer's protocol and 10<sup>7</sup> cells (corresponding to 1x10<sup>6</sup> CD8<sup>+</sup> TCR transgenic T cells) were transferred intravenously (i.v) into recipient mice. CD8<sup>+</sup> T cells or CD3<sup>+</sup> cells from spleens were obtained using anti-CD8 or anti-CD3 MACS beads (Miltenyi Biotec). Twelve hours post adoptive transfer of sorted cells, the indicated recipient mice were infected with MHV A59.

### *Flow cytometry*

Mice were sacrificed at the indicated time points and immediately perfused with PBS. Single-cell suspensions from spleens were obtained as described above. To obtain stromal cells from the brains, the indicated areas were dissected into small pieces, transferred into a 24-

## Results

---

well dish filled with RPMI 1640 medium containing 2% FCS, 20 mM Hepes (all from Lonza), 1 mg/ml Collagenase Type IV (Sigma-Aldrich), and 25 µg/ml DNaseI (AppliChem), and incubated at 37°C for 30 min. After enzymatic digestion, cell suspensions were washed with PBS containing 0.5% FCS and 10 mM EDTA (MACS buffer). CNS-infiltrating lymphocytes were isolated using mechanical disruption of the organ followed by enrichment based on 70–30% Percoll gradients (GE Healthcare) and centrifugation for 25 min at 800×g. Characterization of the cells was performed using surface staining with antibodies against gp38/podoplanin (BD), CD31, CD8-FITC, Thy1.1-APC or PerCP (eBioscience), CCR7-PeCy7, CXCR3-APC (BioLegend) and PE-conjugated MHV S598/H-2Kb tetramers (Sanquin, Amsterdam, The Netherlands). 7-amino-actinomycin D (7AAD; Calbiochem) was used to discriminate dead cells in flow cytometric analyses. For peptide-specific cytokine production, 10<sup>6</sup> splenocytes or CNS-derived lymphocytes were restimulated with s598 peptide ((RCQIFANI) or M133 (TVYVRPIIEDYHTLT), Neosystem (Strasbourg, France)) in the presence of brefeldin A (5 µg/ml) and anti-Lamp 1-AlexaFluor 647 (BioLegend) for 5 h at 37°C. Cells were stimulated with PMA (50 ng/ml) and ionomycin (500 ng/ml; both purchased from Sigma-Aldrich) as positive control or left untreated as a negative control. For intracellular staining, restimulated cells were surface stained and fixed with Cytofix-Cytoperm (BD Biosciences) for 20 min. Fixed cells were incubated at 4°C for 40 min in the presence of anti-CCL21 (Abcam), anti-IFN-γ and anti-TNFα (eBiosciences) mAb diluted in permeabilization buffer (2% FCS/0.5% saponin/PBS). Samples were analyzed by flow cytometry using a FACSCanto flow cytometer (BD Biosciences); data were analyzed using FlowJo software (Tree Star).

### *Statistical analyses*

All statistical analyses were performed with Prism 4.0 (GraphPad). Data were analyzed with the unpaired Student's t test. A p-value of <0.05 was considered significant.

## 6.4 Results

### 6.4.1 CNS-restricted MHV infection drives strong induction of CCR7 ligands within CNS tissue

Following i.n. infection with MHV, active viral replication is detectable within the CNS for up to two weeks post infection (Matthews et al., 2001). To determine the precise distribution of the virus during the first 10 days, we assessed viral titers in draining lymph nodes (cervical lymph nodes – cLNs) and different areas of the CNS, namely the olfactory bulb, mid brain, brain stem and spinal cord (Fig. 10a). Infectious viral particles were first detectable within olfactory bulbs and cLNs at day 2. By day 4, viral titers had reached peak values in olfactory bulbs and the virus had spread to all other CNS areas, including the spinal cord. At day 6, virus had been cleared from draining cLNs while clearance from the CNS tissues had not been achieved by day 10 (Fig. 10a). Using GFP-labeled virus to track infected cells at day 6, we found that viral spread followed olfactory projections from the olfactory bulb (Fig. 10b(i)) to the thalamus (Fig. 10b(ii)) and pons (Fig. 10 b(iii)). Interestingly, neurons and glial cells were infected supporting the notion that the virus utilizes both axonal transport (Perlman et al., 1990) and cell-to-cell spread (Gallagher and Buchmeier, 2001). To assess whether viral infection correlates with the expression of CCR7 ligands, we performed quantitative RT-PCR analysis using samples from the major infected areas. We found that both CCL19 and CCL21 expression was profoundly elevated and that the pattern of upregulation reflected the kinetics of viral replication (Fig. 10c and d). Hence, the presence of actively replicating virus within the CNS tissue, particularly in the olfactory bulbs as virus entry points, drives a rapid and vigorous transcriptional activity of the genes encoding for CCR7 ligands.

## Results

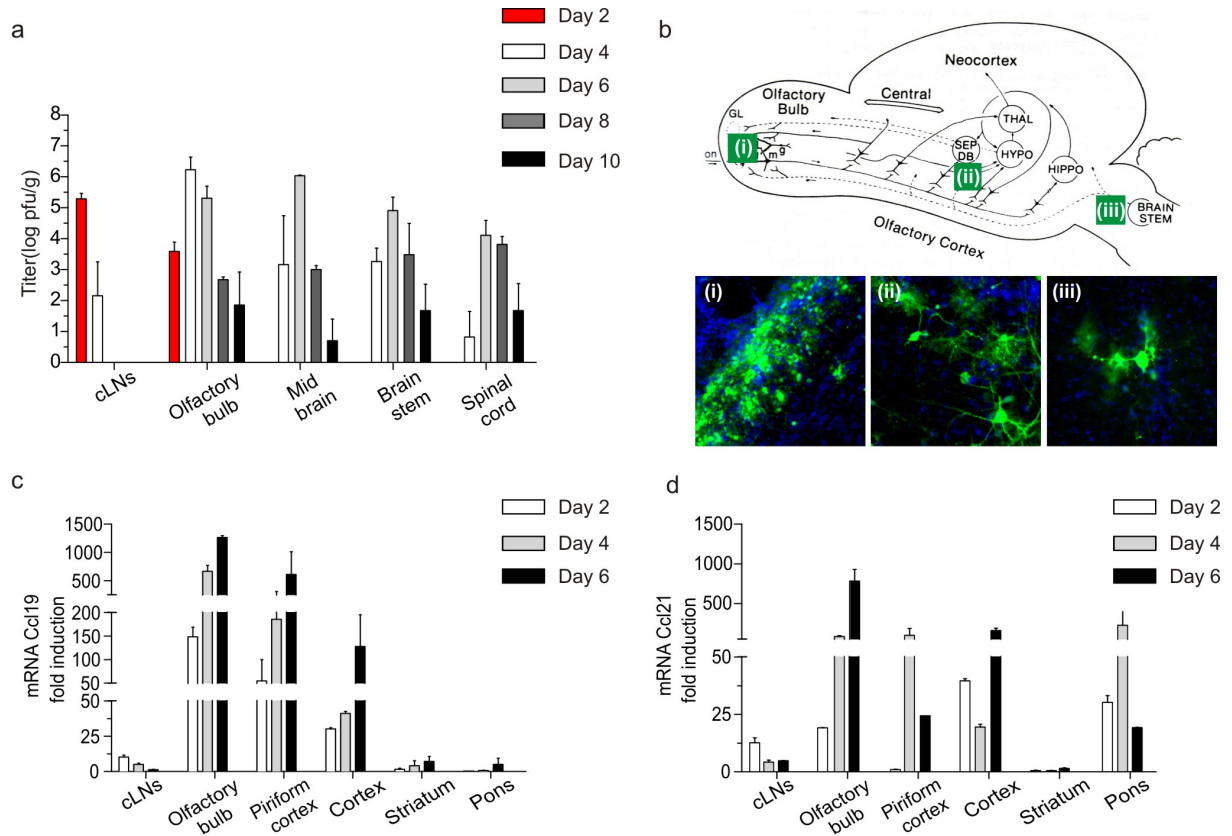


**Figure 10. Distribution of MHV in the CNS and concomitant upregulation of CCR7 ligands.**

a) C57BL/6 mice were infected i.n. with  $5 \times 10^4$  pfu MHV A59. Viral titers in cervical lymph nodes (cLN) and the indicated CNS regions were determined at different days post infection (mean $\pm$ SEM, n=4 mice per time point). (b) Distribution of MHV infected cells visualized by the expression of fluorescent protein (GFP), as surrogate viral antigen, was determined 6 days after i.n. infection with GFP-recombinant MHV. mRNA expression of the CCR7 ligands c) Ccl19 and d) Ccl21 was determined by quantitative RT-PCR at the indicated time points (mean $\pm$ SEM, n=4 mice per time point).

#### 6.4.2 Mapping of CCL19 and CCL21 producing cells in the MHV-infected CNS

To define the cellular source of CCL19 and CCL21, we took advantage of Ccl19-Cre/EYFP reporter mouse (Chai et al., 2013) and combined this detection method with anti-CCL21 staining. Since the olfactory bulb represents the major source of both virus and CCR7 ligand transcripts, we focused our in situ analysis on this area. Confocal microscopy revealed very low Ccl19 promoter activity and hence almost no EYFP in naïve mice (Fig. 11a). At the peak of viral replication on day 6, Ccl19 promoter-driven EYFP expression could be detected mainly in sub-meningeal areas (Fig. 11b arrows), whereas both CCL21 and Podoplanin (PDPN) were produced in a more scattered fashion (Fig. 11b). High resolution analysis of these sections showed that both CD31<sup>+</sup> endothelial cells (ECs) of blood microvessels (Fig. 11c, asterisk) and PDPN<sup>+</sup> fibroblastic cells surrounding the blood vessels (Fig. 11c, arrow) expressed the EYFP marker. Interestingly, the phenotype and shape of these Ccl19-Cre<sup>+</sup> fibroblastic cells with ERTR7 and PDPN expression (Fig. 11d, arrow) resemble fibroblastic reticular cells (FRCs) of secondary lymphoid organs (Chai et al., 2013). Moreover, it appears that these PDPN<sup>+</sup> cells support CCL21 deposition in the perimeter of postcapillary venules (Fig. 11e). Using flow cytometric analyses to detect intracellular CCL21, we found that CD31<sup>+</sup> blood endothelial cells are a major source of CCL21 (Fig. 11f, left panel) and that PDPN<sup>+</sup> cells not only deposit CCL21 on their surface, but also contribute to its production (Fig. 11f, right panel). Additionally, immunohistological analysis on day 12, i.e. after the resolution of the infection, showed that astrocytes represent another cellular source of CCL19 (Fig. 11g). Taken together, high-level production of CCR7 ligands was linked to areas of active viral replication and focused to ECs and FRC-like cells in and around postcapillary venules that support leukocyte recruitment, activation and survival. Hence, it is possible that CCR7 ligands contribute to the creation of a perivascular microenvironment that supports and controls the action of antiviral lymphocytes.

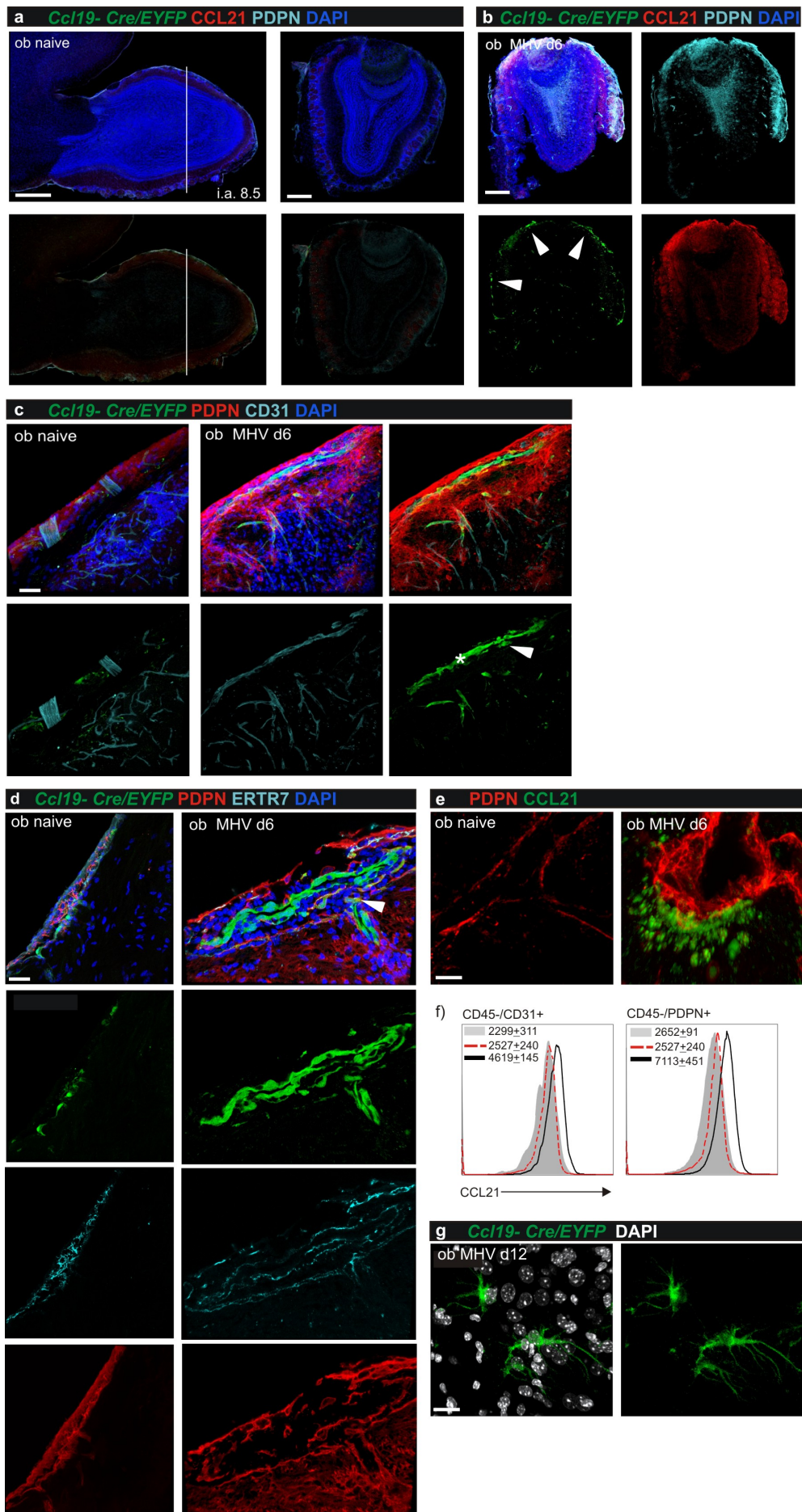




**Figure 11. CNS-resident cellular components involved in the production of CCR7 ligands.**

Histological analyses of the *Ccl19* gene expression and CCL21 production in naïve and MHV infected olfactory bulbs. Data are representative of at least two independent experiments. a) Olfactory bulbs of naïve *Ccl19-cre/EYFP* mice stained with indicated antibodies. Left-side panels show the longitudinal overview of the olfactory bulb with indicated level of the perpendicular cuts. Right-side panels show the perpendicular overview. Scale bar=200µm. b) Expression of EYFP in the olfactory bulbs of *Ccl19-cre/EYFP* MHV infected mice, day 6 p.i. Sections were stained with antibodies against PDPN and CCL21 and counterstained with DAPI, merged channels in the upper right plot, scale bar=200µm. c) High magnification of meningeal areas of olfactory bulbs of naïve (right-side panels) and day 6 MHV infected *Ccl19-cre/EYFP* mice. The samples were stained with antibodies against CD31 and PDPN and counterstained with DAPI, merged channels in the first two upper right plot, scale bar=30µm. d) High magnification of olfactory bulb postcapillary venules of *Ccl19-cre/EYFP* naïve (left-side panels) or day 6 MHV infected (right-side panels) mice. The samples were stained with antibodies against PDPN and ERTR7 and counterstained with DAPI. Merged channels in the upper plot scale, scale bar=30µm. e) High magnification of postcapillary vessels in the olfactory bulbs of naïve and day 6 MHV infected mice. The samples are stained with antibodies against CCL21 and CD31, scale bar=10µm. g) EYFP expression in astrocytes of day 12 MHV infected *Ccl19-cre/EYFP* mice, scale bar =10µm. Production of CCL21 in the olfactory bulbs of day 6 MHV infected mice was determined by intracellular staining using flow cytometric analyses. f) CCL21 production by CD45<sup>-</sup>/CD31<sup>+</sup> positive cells (left-side plot-black lines), CD45<sup>-</sup>/PDPN<sup>+</sup> cells (right-side plot-black lines) and CD45<sup>+</sup> cells – red-dotted lines. Gray-shaded plots represent staining with isotype control antibody. The values in the histograms represent the mean MFI value±SEM. The data are pooled from 3 independent experiments, n=6.

#### 6.4.3 CCR7 expression is essential for successful control of neurotropic MHV infection

Next, we assessed whether and to which extent CCR7 and its ligands contribute to control of MHV CNS infection. To this end, we used the intranasal route of infection in mice lacking either *Ccr7* (Förster et al., 1999) or *Ccl19* and *Ccl21a* in SLOs (Gunn et al., 1999). The latter

mouse strain, known as *plt/plt* (paucity of lymph node T cells) still shows expression of the *Ccl21b* isoform in extra-lymphatic tissue (Nakano and Gunn, 2001). Both mouse strains exhibit impaired T cell zone development in SLOs due to the migration defects of DCs and lymphocytes (Gunn et al., 1999; Förster et al., 1999) and hence show a comparable loss of immunocompetence (Junt et al., 2004; Kursar et al., 2005). While B6 mice successfully controlled the infection, experiencing transient weight loss during first two weeks, CCR7-deficient mice demonstrated a strong drop in weight early upon the infection and were finally unable to control viral replication succumbing to infection by day 10 (Fig. 12a). In sharp contrast, *plt/plt* mice recovered from the initial weight loss and were able to successfully control the infection as shown by weight gain during the recovery phase (Fig. 12a). Determining viral titers in the brains of infected animals at day 10, confirmed that *plt/plt* mice better controlled the virus compared to CCR7-deficient mice (Fig. 12b). The lack of efficient viral control in both *plt/plt* and CCR7-deficient mice was associated with a pronounced reduction of antiviral CD8<sup>+</sup> T cell numbers (Fig. 12c) and function (Fig. 12d), as well as a reduction of antiviral CD4<sup>+</sup> T cell function (Fig. 12e). Importantly, CCR7-deficient mice demonstrated a more pronounced reduction in antiviral CD8<sup>+</sup> T cell responses compared to *plt/plt* mice (Fig. 12c and d), whereas the antiviral CD4<sup>+</sup> T cell response was not different the two strains. It is noteworthy that lack of CXCR3, a chemokine receptor that can function as alternative, low affinity receptor for CCL21 that regulates T cell migration to the CNS via inflammatory cytokines (Stiles et al., 2006; Liu et al., 2001) did not affect survival following intranasal MHV infection (Supplementary Fig. S16). Hence, the presence of CCR7 appears to be essential for the rapid control of CNS infection with a neurotropic coronavirus. The finding that *plt/plt* mice have a decisive advantage in coping with this viral infection suggests that the *CCL21b* isoform may preserve a critical level of *Ccr7* signaling within the CNS thereby supporting successful antiviral CD8<sup>+</sup> T cell responses in this vulnerable organ.

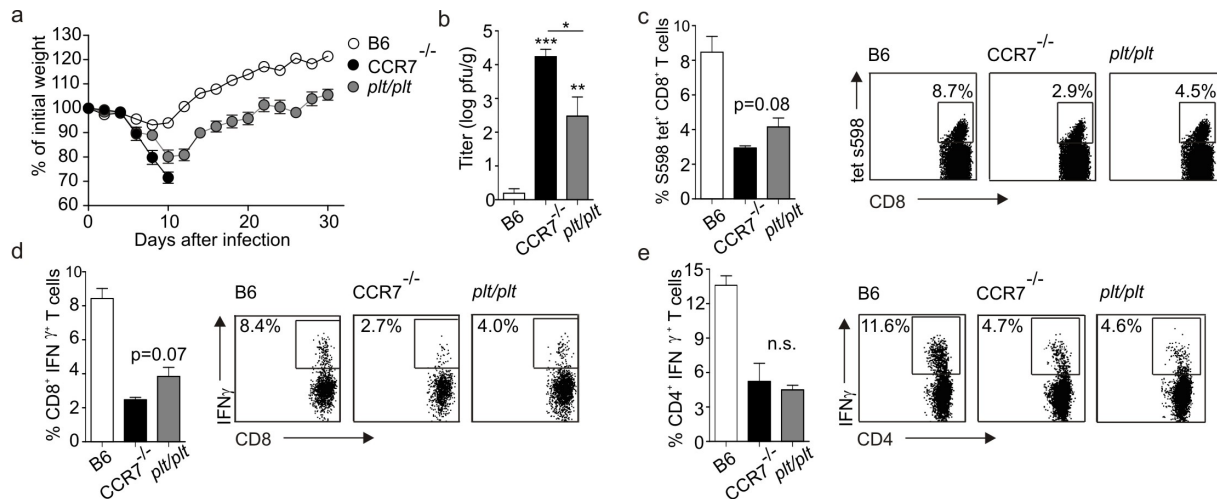


**Figure 12. CCR7 ligands control MHV CNS infection and prevent severe disease.**

C57BL/6 (B6) control mice, CCR7-deficient or plt/plt mice were i.n. infected with  $5 \times 10^4$  pfu of MHV A59. a) Weight loss of CCR7-deficient and B6 mice was recorded at the indicated time points following infection. Values indicate mean percentage of the initial weight  $\pm$  SEM ( $n=6-7$  mice per group). b) Viral titers in CNS were determined at day 10 after infection. Data indicate means of log transformed values  $\pm$  SEM ( $n=5$  mice per group). c) Tetramer-binding and IFN- $\gamma$  production by CNS-infiltrating d) CD8<sup>+</sup> and e) CD4<sup>+</sup> T cells was evaluated by flow cytometry on day 10 after infection. Values of the bar graphs indicate mean  $\pm$  SEM of the respective virus-specific T cell population ( $n=3$  mice per group). Plots show representative dot plot analysis with percentage of the specific T cell population indicated.

#### 6.4.4 CCR7-proficiency of CD8<sup>+</sup> T cells protects against viral CNS infection

Next, we assessed the activation and migration of MHV-specific CD8<sup>+</sup> T cells in the presence or absence of the CCR7. To track antiviral CD8<sup>+</sup> T cells in vivo and to ablate CCR7 on a specific population, we made use of a MHV spike protein-specific TCR transgenic mouse (Spiky). Adoptive transfer of congenic CFSE-labeled Spiky cells into MHV-infected B6 mice showed detectable activation at 74 h post infection (Fig. 13a). After this delay of approximately 3 days, transgenic cells vigorously proliferated in cLNs shown by the loss of CFSE (Fig. 13a). As expected, activation of Spiky cells in cLNs resulted in down-regulation of CCR7 (Fig. 13b). Intriguingly, accumulation of activated, i.e. CFSE<sup>low</sup> Spiky cells in the

infected CNS could only be detected after day 4 (Fig. 13c), suggesting that the cells undergo at least 8 rounds of proliferation within cLNs before they gain the ability to migrate to the CNS. Importantly, CNS-infiltrating Spiky cells had maintained CCR7 expression (Fig. 13d) suggesting that the highly abundant CCR7 ligands in the inflamed regions could affect MHV-specific CD8<sup>+</sup> T cells.

Distribution of activated Spiky cells at day 6 within the brain revealed that the majority of cells resided within olfactory bulbs (Fig. 13e) further supporting the notion that the antiviral immune responses in the CNS are highly focused to infected areas hence sparing non-infected regions from potential immunopathological damage.

Next, we assessed whether restoration of CCR7 expression specifically on Spiky CD8<sup>+</sup> T cells facilitates control over CNS-restricted MHV infection. Therefore, we adoptively transferred 10<sup>6</sup> CCR7-proficient Spiky T cells into CCR7-deficient mice and infected the recipients with MHV. Controls included adoptive transfer of polyclonal CD3<sup>+</sup> cells from B6 or CCR7-deficient mice. As expected CCR7-deficient mice that had received CCR7-deficient CD3<sup>+</sup> cells were not protected from MHV CNS infection, whereas CCR7-proficient CD3<sup>+</sup> T cells from B6 mice provided protection (Fig. 14a, b). Importantly, CCR7-deficient mice that had received CCR7-proficient Spiky CD8<sup>+</sup> T cells survived the infection (Fig. 14a, b) indicating that protection against this neurotropic viral infection critically depends on CCR7 signaling in antiviral CD8<sup>+</sup> T cells.

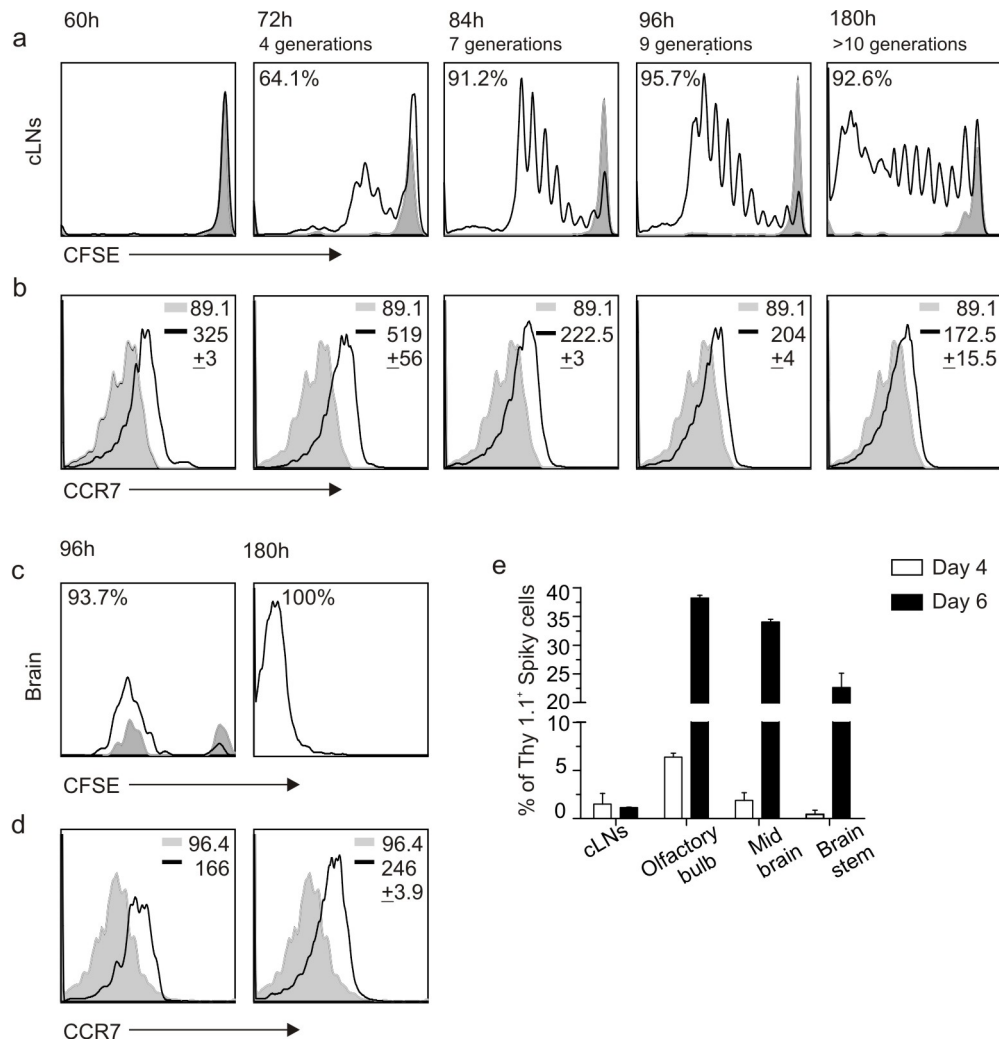


**Figure 13. Activation and recruitment of MHV-specific CD8<sup>+</sup> T cells to the infected CNS.**

A total of  $10^7$  of transgenic Thy 1.1<sup>+</sup> Spiky cells (corresponding to  $10^6$  of transgenic CD8<sup>+</sup> T cells) labeled with the intracellular dye carboxy-fluorescein succinimidyl ester (CFSE) were adoptively transferred into Thy1.2<sup>+</sup> B6 mice. 12 h later the mice were i.n. infected with  $5 \times 10^4$  pfu of MHV A59 and a) CFSE dilution and b) CCR7 expression of Thy1.1<sup>+</sup>CD8<sup>+</sup> T cells from the cLN were determined by flow cytometry at the indicated time points. Values in the histograms indicate percentage of proliferated cells (black line) compared to naïve controls (grey shadowed line). The data are representative of 2 independent experiments with 3 mice per group. (c, b) Flow cytometric analysis of c) CFSE dilution and d) CCR7 expression of Thy1.1<sup>+</sup>CD8<sup>+</sup> T in the brain was performed at 96 h and 180 h p.i. The values in the histograms represent the mean of MFI $\pm$ SEM of the total Thy1.1<sup>+</sup>CD8<sup>+</sup> T population (black lines) compared to isotype control (gray shaded lines). The data are representative of 2 independent experiments with 3 mice per group. e) Frequencies of Thy1.1<sup>+</sup>CD8<sup>+</sup> T cells in

## Results

the cLNs and indicated areas of the brain obtained day 4 and 6 p.i. Data represent mean value $\pm$ SEM of two independent experiments, n=4 mice.

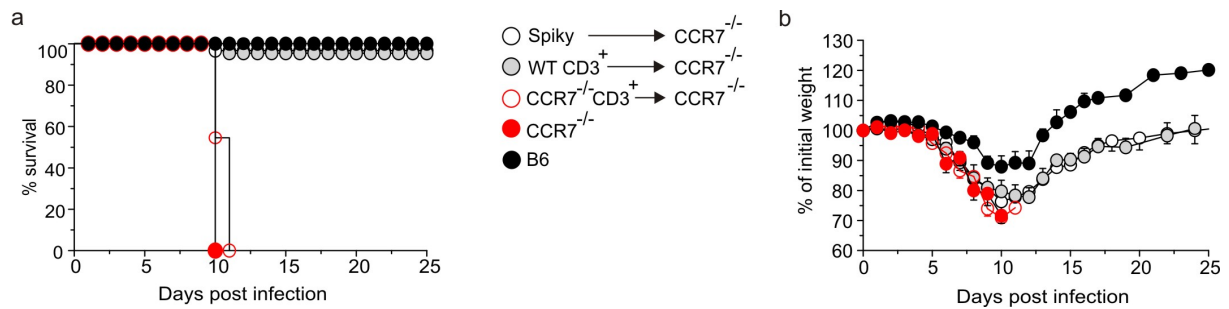


**Figure 14. CCR7-proficient T cells protect against MHV induced neuroinflammation.**

A total of  $10^7$  of CD3<sup>+</sup> CCR7-proficient, CD3<sup>+</sup> CCR7-deficient or  $10^6$  of transgenic Spiky cells were adoptively transferred to CCR7-deficient mice. 12 h after the transfer, recipient mice and control groups of CCR7-deficient and B6 mice were infected i.n. with  $5 \times 10^4$  pfu of MHV A59. a) Survival and b) weight loss of the mice were followed over the indicated period of time. Values indicate mean percentage of the initial weight $\pm$ SEM (n=10 mice per group).

### 6.4.5 CNS-restricted expression of CCR7 ligands is sufficient to provide CD8<sup>+</sup> T cell-mediated immunity

Phenotypical characterization of adoptively transferred TCR transgenic Spiky cells revealed that these cells were highly active and performed the major antiviral functions, namely degranulation and production of antiviral cytokines such as IFN- $\gamma$  and TNF $\alpha$  (Supplementary Fig. S17). Since CCR7 ligands expressed within SLOs not only support T cell migration, but also support T cell function, it is likely that antiviral CD8<sup>+</sup> T cells are not only recruited more efficiently to inflamed areas of the CNS by locally produced CCR7 ligands, but can also perform decisively better if they receive stimuli via CCR7. To test this hypothesis, we used competitive co-transfer of CCR7-proficient and -deficient CD8<sup>+</sup> Spiky T cells into plt/plt mice which produce CCR7 ligands only in peripheral, non-lymphoid organs. This analysis revealed substantially better recruitment of CCR7-proficient (Ly 5.1<sup>+</sup>) cells compared to CCR7-

deficient (Thy1.1) antiviral CD8<sup>+</sup> T cells to the CNS of MHV-infected plt/plt mice (Fig. 15a and b). Importantly, during the critical phase of the infection, i.e. at day 6, frequencies of both cell types were comparable in draining cLNs (Fig. 15b), indicating that the absence CCR7 ligands did not affect priming. Moreover, we found that CCR7-deficiency of Spiky cells significantly affected their functionality, i.e. the ability to produce IFN- $\gamma$  in the CNS (Fig. 15c). Overall, these competitive transfer experiments have shown that CCR7 ligand expression in the CNS not only supports recruitment of virus-specific CD8<sup>+</sup> T cells to the CNS, but is also required for the execution of antiviral functions.

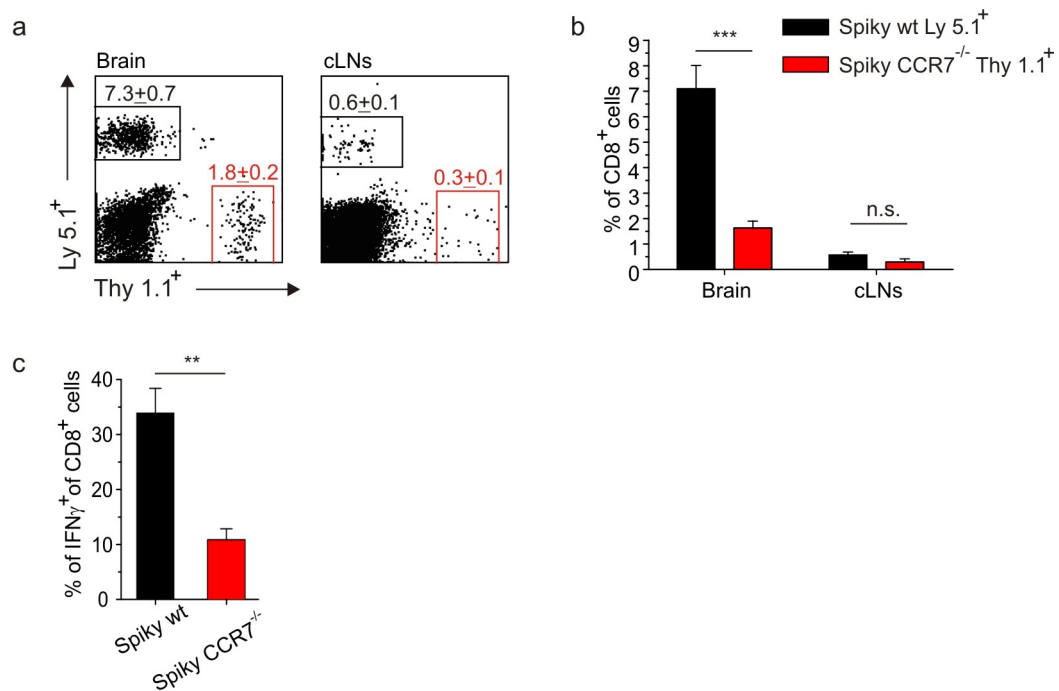


**Figure 15. Expression of CCR7 ligands in the CNS controls CD8<sup>+</sup> T cell recruitment and function.**

10<sup>4</sup> of Ly5.1<sup>+</sup> CCR7-proficient Spiky transgenic CD8<sup>+</sup> T cells were co-transferred with 10<sup>4</sup> of Thy1.1<sup>+</sup> CCR7-deficient Spiky transgenic CD8<sup>+</sup> T cells into plt/plt mice. 12 h after the transfer mice were infected i.n. with 5x10<sup>4</sup> MHV A59. Flow cytometric analysis of the frequencies and functionality of CCR7-proficient or -deficient Spiky cells in the brain and cLNs was performed 6 days after the infection. a) Representative dot plots of the accumulation of CCR7-proficient or CCR7-deficient Spiky CD8<sup>+</sup> T cells. The values in the plots indicate the mean percentage $\pm$ SEM of CCR7-proficient or -deficient Spiky cells of CD8<sup>+</sup>T cell population.

b) Frequencies of CCR7-proficient and CCR7-deficient transgenic CD8<sup>+</sup> T cells in the brain and cLNs. c) Frequencies of IFN- $\gamma$  producing CCR7-proficient or -deficient Spiky transgenic

CD8<sup>+</sup>T cells in the brain and cLNs. Data represent mean value±SEM (n=4 mice). Statistical analyses was performed using the Student's t test (\*,p<0.05;\*\*p,0.01;\*\*\*,p<0.001; n.s. not significant).

## 6.5 Discussion

Recruitment of cytotoxic T cells to the CNS and regulation of their function during neurotropic viral infections are critical for the delicate balance between antiviral immunity and immunopathology. The CNS is considered an immunologically privileged site and some of the immunological pathways used in peripheral organs should be particularly well controlled within this vital organ (Engelhardt and Ransohoff, 2005). Hence, potent immune effectors such as antiviral CD8<sup>+</sup> T cells should be directed specifically to sites of viral replication. Our work indicates that CCR7 ligands produced in the CNS during viral infection function as part of a multi-layered control network that secures spatio-temporal focusing of the immune responses to the areas of viral infection. It appears that CCL19 and CCL21 not only guide cytotoxic CD8<sup>+</sup> T cells to the CNS, but also support execution of their full antiviral function. These conclusions are supported by the finding that infection with neurotropic virus MHV A59 leads to substantial increase in transcript levels of *Ccl19* and *Ccl21* and enhanced production of the chemokines in the perivascular space of postcapillary venules. The inability of antiviral CD8<sup>+</sup> T cells to respond to CCL19/CCL21 resulted in a fatal outcome of the infection. Importantly, CCL21b expression outside of secondary lymphoid organs provided sufficient stimulation of virus-specific CD8<sup>+</sup> T cells to control the neurotropic viral infection. Taken together, we demonstrate that T cell-restricted expression of CCR7 is necessary and sufficient to allow recruitment and guarantee optimal functionality of antiviral CD8<sup>+</sup> T cells during neurotropic viral infection.

Delayed and impaired immune responses detected in CCR7-deficient and *plt/plt* mice, particularly in the situation of limiting amount of antigen, have been explained by inefficient recruitment of T cells and DCs to the local lymph nodes (Förster et al., 1999; Gunn et al.,



1999). Nevertheless, it has been reported that under the conditions of strong inflammatory responses with abundant antigen, the need for CCR7 signaling can be bypassed, ensuring successful pathogen clearance albeit the lack of optimal interactions between T cells and DCs within LNs (Junt et al., 2004; Scandella et al., 2007). Although intranasal infection with MHV leads to high levels of viral replication, our experiments show that abrogation of CCR7 signaling results in fatal consequences. Similar results have been obtained in a study using *Toxoplasma gondii* infection that leads to rapid replication of tachyzoites and dissemination to the brain (Noor et al., 2010). Although high levels of parasites are reached shortly after infection, CCR7-deficient mice were unable to raise sufficiently strong immune responses against the pathogen (Noor et al., 2010). Therefore, previous findings support our interpretation that CCR7 is not only an important driver of adaptive immune responses within SLOs, but also exerts important functions in non-lymphoid tissues such as the CNS.

Reduced numbers of CCR7-deficient virus-specific CD8<sup>+</sup> T cells compared to CCR7-proficient ones in the brains of MHV infected plt/plt animals in our co-transfer study pointed towards an important role of CCR7 ligands in the recruitment of T cells to the CNS. It is possible that CCR7 ligands control T cell recruitment to the LNs via HEVs and through brain vessel epithelium to the CNS by similar mechanisms. Indeed, inflamed brain vessels express increased levels of selectins and integrins (Steffen et al., 1994) which reduce the rolling velocity of lymphocytes and permit prolonged interactions with the endothelial wall (Engelhardt, 2006). Moreover, CCL19 and CCL21 expression by brain blood vessels further enhances T cell interaction with endothelial cells facilitating diapedesis. Importantly, the lack of L-selectin ligands expression by brain blood endothelium prevents naïve T cells from slowing down at the level of postcapillary venules, thus precluding them from sensing CCL19 and CCL21 via CCR7 (Alt et al., 2002). In the same line, the lack of CD62L expression of activated CCR7-expressing T cells seems to prevent their recirculation through local LNs and leads to preferential migration towards CCL19/CCL21 expressing inflamed brain endothelium. Interestingly, enhanced CCL19/CCL21 production of brain endothelial cells and perivascular cells detected in our study suggest that inflamed brain vessels of blood brain

barrier could acquire some of the properties of HEVs as suggested by previous studies (Alt et al., 2002; Columba-Cabezas et al., 2003).

Crossing the endothelial barrier is just the first step in T cell migration to the parenchyma. Crossing over a second barrier composed of astrocyte endfeet is most relevant for activated T cells to finally reach neuronal tissue (Owens et al., 2008). While the processes regulating the first step are well understood, the second step requires further analysis. We found that at later stages of the infection, astrocytes had become Ccl19-Cre/EYFP positive indicating that these cells contribute to perivascular CCL19 expression at some stage of the infection. It will be interesting to further delineate the timing and magnitude of astrocyte-derived CCR7 ligand production and to dissect whether this activity is connected to persisting viral replication.

As T cells travel from blood through the walls and membranes of postcapillary venules, they make additional contacts with antigen presenting cells in the perivascular space and collect further information that can influence their functionality once they have reached brain parenchyma (Greter et al., 2005; Kang et al., 2011). Interestingly, podoplanin-expressing cells of brain meninges can serve as antigen presenting cells (Kang et al., 2011). Hence, it is possible that prolonged expression of CCL21 by these cells, as shown in our experiments, could serve to attract and engage CD8<sup>+</sup> T cells in additional contacts with local APCs. Therefore, stromal cells of the brain may provide further instructions to transmigrating cells and tune their functionality within neuronal tissues. Additionally, CCL19 provided by astrocytes at the level of the glia limitans could also serve to instruct T cell behavior and function. This notion is further supported by our finding that virus-specific CD8<sup>+</sup> T cells, both the ones retrieved from the brains of plt/plt mice following adoptive co-transfer and the ones obtained from CCR7-deficient mice, showed markedly decreased effector function as measured by IFN- $\gamma$  production. The fact that CCR7-deficient virus-specific CD8<sup>+</sup> T cells did not show impaired IFN- $\gamma$  production during systemic viral infection (Junt et al., 2004), further supports the conclusion that CCR7 and its ligands provide important stimuli to T cells during CNS infection.

In conclusion, our study shows that CCR7 and the expression of its ligands outside of lymphoid organs are critical for the containment of neurotropic virus infection. The understanding of the cellular basis and molecular mechanism involved in regulation of T cell recruitment to the CNS and their function within may guide establishment of improved therapeutic approaches to manage T cell-mediated inflammatory conditions that affect the brain.

#### 6.5.1.1 Supplementary material

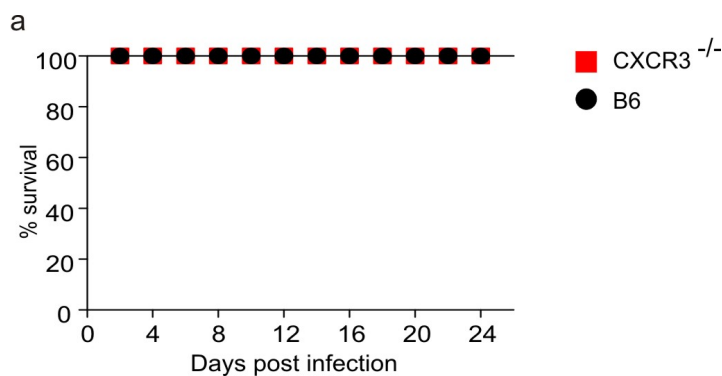


**Figure S16. Chemokine CXCR3 is not necessary for the control of MHV induced inflammation.**

a) Survival curves of CXCR3-deficient mice and control B6 mice infected i.n. with MHV A59. (n=5 mice per group).

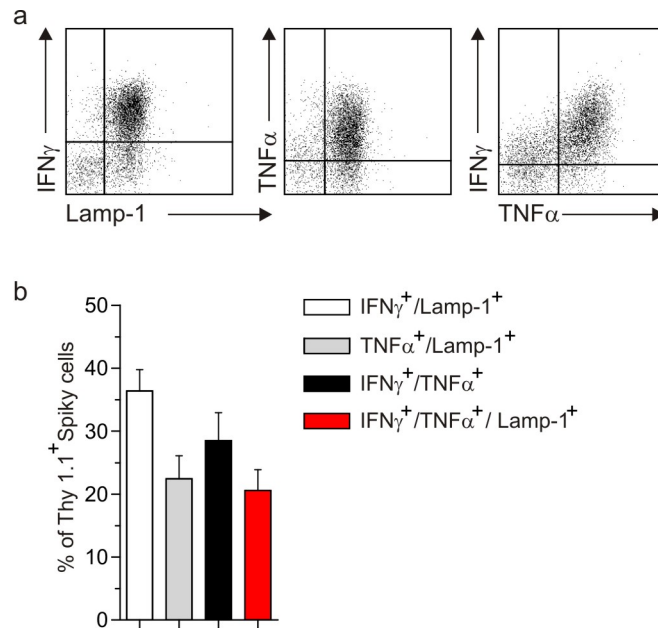


**Figure S17. Functionality of CNS-infiltrating Spiky transgenic CD8<sup>+</sup> T cells.**

A total of  $10^7$  splenocytes of transgenic Thy 1.1<sup>+</sup> Spiky cells (corresponding to  $10^6$  of transgenic CD8<sup>+</sup>T cells) were adoptively transferred to B6 mice and 12h later mice were infected i.n. with MHV A59. Functionality of CNS-infiltrating Spiky cells on day 6 p.i. was determined by intracellular staining for the production of cytokines TNF $\alpha$ , IFN- $\gamma$  and/or expression of the degranulation marker Lamp-1. a) Representative plots of cytokine production/degranulation profile of transgenic Spiky CD8<sup>+</sup> T cells, b) frequencies of cytokine producing and/or degranulating transgenic Spiky CD8<sup>+</sup> T cells. Data represent the mean percentage $\pm$ SEM, (n=3).

## 6.6 Acknowledgments

We would like to thank Rita DeGiuli and Fabienne Soppelsa for technical support.

## 6.7 Data contribution

Jovana Cupovic generated Spiky transgenic mouse, performed experiments (Figure 10a, b; Figure 11f; Figure 13a-e; Figure 14a, b; Figure 15a-c; Figure S17a, b) and wrote the paper. Lucas Onder performed confocal microscopy analysis (Figure 11a-e, g). Cristina Gil-Cruz and Christian Perez-Shibayama performed MHV infection assay with CCR7-deficient and *plt/plt* mice (Figure 12a-e; Figure S16). Sonja Firner-Caviezel performed the analysis of MHV distribution in CNS (Figure 10a). Elke Weiler performed the analysis of MHV distribution in CNS using GFP-labeled MHV virus (Figure 10b). Ingo Bechmann discussed data. Burkhard Ludewig designed the study.

## 7 Tuning the functional avidity of virus-specific CD8<sup>+</sup> T cells

Jovana Cupovic<sup>1</sup>, Lilian Staerck<sup>2</sup>, Tatyana Luzyanina<sup>3</sup>, Wolfgang Uckert<sup>2</sup>, Gennady Bocharov<sup>4</sup> and Burkhard Ludewig<sup>1</sup>

<sup>1</sup>Institute of Immunobiology, Kanton Hospital St. Gallen, Switzerland

<sup>2</sup>Max Delbrück Center for Molecular Medicine Berlin, Campus Buch, Germany

<sup>3</sup>Institute of Numerical Mathematical Problems in Biology of the Russian Academy of Sciences, Pushchino, Russia

<sup>4</sup>Institute of Numerical Mathematics of the Russian Academy of Sciences Moscow, Russia

### 7.1 Abstract

Adoptive T cell therapy has become a promising approach for treatment of cancer and persistent virus infections. Importantly, it is mainly the functional avidity of the engineered T cells that determines the success of the treatment. As a measurement of their biological performance, functional avidity of T cells combines different factors such as co-receptor expression, T cell receptor (TCR) affinity and density. To assess the contribution of TCR density on the performance of CD8<sup>+</sup> T cells recognizing the spike protein of a cytopathic mouse coronavirus, we have used TCR retrogenic (Rg) mice engineered to express variable numbers of TCRs on the surface of their T cells. Based on TCR numbers, Rg T cells were classified as low, intermediate, high and xhigh TCR density groups. Activation of antiviral Rg CD8<sup>+</sup> T cells was assessed by CFSE dilution assay and further analyzed using a mathematical model that describes the essential performance parameters of T cells. We found that increasing TCR density led to increased commitment rates, reduced death rate and shortened doubling times. Surprisingly, TCR expression above physiological levels, i.e.

xhigh TCR density, resulted in very fast commitment to initial proliferation and cycling arrest after the second round of proliferation. Moreover, xhigh TCR density cells showed drastically reduced apoptosis indicating that supraphysiological levels of TCR expression significantly alter T cell behavior. Importantly, adoptive transfer of antiviral TCR Rg CD8<sup>+</sup> T cells into coronavirus-infected mice revealed that both high and intermediate TCR Rg CD8<sup>+</sup> T cells provide optimal control of the viral infection and hence reduce infection-associated tissue damage. Taken together, our results indicate that engineered, low avidity CD8<sup>+</sup> T cell exhibit optimal performance within a broad range of TCR densities.

### 7.2 Introduction

CD8<sup>+</sup> T cells are important for the successful defense against viruses and tumors (Alexander-Miller, 2005; Zhang and Bevan, 2011). The high specificity of CD8<sup>+</sup> T cell-mediated target cell destruction is therefore utilized in adoptive T cell therapy (ATT) approaches. Indeed, ATT with transfer of antigen-specific CD8<sup>+</sup> T cells has shown to be a promising treatment for malignancies and viral infections, particularly in the context of bone marrow transplantation (Walter et al., 1995; Leen et al., 2006; Kennedy-Nasser et al., 2009; Feuchtinger et al., 2006). Although initial application of ex vivo expanded, autologous lymphocytes showed success in treating patients with metastatic melanoma (Dudley et al., 2010, 2008) and immunodeficient bone marrow transplant recipients (Dobrovina et al., 2012; Leen et al., 2013), isolation, expansion and maintenance of antigen-specific CD8<sup>+</sup> T cells has been a major hurdle in translation to broad clinical application.

The demonstration that specificity of a T cell is solely determined by the T cell receptor (TCR)  $\alpha\beta$  genes and therefore can be redirected by antigen-specific TCR gene transfer (Dembic et al., 1986) has opened new opportunities for ATT. Successful gene-mediated redirection of T cells using TCRs with specificity for melanoma (Clay et al., 1999) or influenza virus (Kessels et al., 2001) has demonstrated the applicability of genetically engineered T cell adoptive therapy in the human system. Moreover, a successful phase I clinical trial treating patients with metastatic melanoma with autologous T cells genetically modified to express a MART-1 specific TCR (Morgan et al., 2006), has proven clinical feasibility. Nevertheless, these pioneering studies have identified several technical problems that have to be solved to establish ATT as a safe and highly effective treatment option. An important element that determines the success of ATT is the functional avidity of the TCR of choice (Stone et al., 2009). Functional avidity is defined by functional measures such as half-maximal cytokine production or target cell lysis following exposure to the cognate peptide in graded concentrations (Nauerth et al., 2013). Hence, functional avidity determines the true



biological potential of a T cell population, but incorporates several independent factors that mutually influence T cell performance. The major component determining T cell function is the structural affinity of the TCR (L. a. Johnson et al., 2006). Additionally, factors such as CD8 or CD4 co-receptor expression levels, adhesion molecules or changes in the molecules of the signaling cascade significantly affect magnitude and quality of the T cell response (Stone et al., 2009). Moreover, the TCR surface expression levels crucially influence T cell functional avidity because it determines the overall signal strength received by the T cell during the activation phase. Unlike the structural affinity of the TCR to its cognate peptide/MHC complex that is a hardwired characteristic, TCR surface levels represent an adjustable property that allows modulation of the signal strength (Valitutti et al., 1997; San José et al., 2000; Finkel et al., 1989). Moreover, TCR density impinges on the optimal performance of genetically engineered T cells because the lack of stable and high level TCR expression results in functional impairment of such engineered T cells (Fujio et al., 2000; Cooper et al., 2000). Thus, for ATT, it is important to define the optimal range of TCR density and determine the functional consequences of different TCR expression levels.

Previous studies have established that a particular threshold of TCR surface expression is required to ensure full activation of polyclonal T cell populations (Valitutti et al., 1995; Viola and Lanzavecchia, 1996; Blichfeldt et al., 1996). However, quantitative estimation of T cell functional performance parameters is not possible using polyclonal T cells because diverse TCRs may exhibit different properties. To overcome these limitations, we have used retrogenic mouse technology (Bettini et al., 2012) that allowed us to create T cells differing solely in the numbers of surface expressed TCRs. By introducing a mouse hepatitis virus (MHV)-specific TCR with low functional avidity into the genome of RAG1-deficient stem cells, we ensured development of mice harboring only one monoclonal CD8<sup>+</sup> T cell population. Combining CFSE-based in vitro proliferation assay with mathematical modeling, we have assessed the performance of T cells expressing different levels of TCRs. We found a biphasic TCR density-dependent behavior of these T cells: (i) no or very low activation and in vivo protection against viral challenge at <5,000 TCRs per cell, (ii) efficient activation,

differentiation and high protective capacity at TCR levels between 5,000 and <17,000 per cell, and (iii) swift activation, proliferative arrest and loss of in vivo protective capacity at TCR levels above 17,000 per cell. These findings indicate that engineering of low avidity TCRs for ATT can rely on a rather broad TCR surface density window to secure optimal T cells performance.

### 7.3 Material and Methods

#### *Ethical statement*

Experiments were performed in accordance with federal and cantonal guidelines under permission numbers SG08/11, SG03/14 and SG11/03 following review and approval by the Cantonal Veterinary Office (St. Gallen, Switzerland).

#### *Mice*

C57BL/6 (B6) mice were purchased from Charles River Laboratories (Sulzfeld, Germany). RAG1-deficient mice and  $\beta 2m$ -deficient mice were obtained from the Institut für Labortierkunde (University of Zürich). All mice were maintained in individually ventilated cages and were used at the age of 6 to 9 weeks.

#### *Cells lines*

L929 were purchased from the European Collection of Cell Cultures. Plat-E packaging cells were described previously (Klump et al., 2001). Plat E cells were cultured in Dulbecco's modified Eagle's medium supplemented with 10% heat-inactivated fetal calf serum (FCS)(Sigma-Aldrich) and 100 IU/ml penicillin, streptomycin. The selective culture medium of Plat-E cells contained 10  $\mu$ g/ml blasticidin and 1  $\mu$ g/ml puromycin (antibiotics: Sigma-Aldrich, Switzerland). During the transduction process, cells were left without antibiotics. The murine cell line 58 cells (M58) (Letourneur and Malissen, 1989) were grown in RPMI 1640 medium

supplemented with 10% FCS (Lonza), 1 mM sodium pyruvate, 2 mM glutamine (Gibco, Invitrogen) 50  $\mu$ M 2-mercaptoethanol (Sigma-Aldrich), 100 IU/ml penicillin, streptomycin, and 1 mM HEPES.

### *Generation of BM-derived DCs*

Bone marrow was flushed from femurs and tibias of C57BL/6 mice and erythrocytes were lysed by osmotic shock with 1 ml lysis buffer (0.15 M NH<sub>4</sub>Cl, 1 mM KHCO<sub>3</sub>, 0.1 mM EDTA) for 1 min at room temperature. Cells were washed twice with BSS and cultured in 5% RPMI 1640 (Sigma-Aldrich) supplemented with 5% FCS (Lonza), 100 U penicillin-streptomycin (Lonza) and 5% GM-CSF (supernatant of X63 GM-CSF cells). Medium was replenished on days 2 and 4 of culture. Non-adherent cells were harvested on day 6.

### *Construction of retroviral vectors*

Characterization of the MHV spike protein-specific TCR has been described in Chapter 2. Sequences of  $\alpha$  and  $\beta$  TCR genes on the cDNA level were linked using a P2A sequence (de Felipe et al., 1999). Briefly, two successive PCR steps were performed: (a) TCR sequences were amplified using a set of gene-specific primers (GSPs) with overlapping P2A-encoding regions (75-90 amino acids in length). The 5' genes were amplified excluding the stop codon. (b) P2A-appended TCR chain genes were combined by annealing of complementary P2A sequences and subsequently amplified using GSPs harboring NotI and EcoRI restriction sites. Finally, the generated TCR cassette for MHV-specific TCR ( $\beta\alpha$ :  $\nu\beta 16$ -P2A- $\nu\alpha 2$ ) was integrated into the MP71-PRE vector (Engels et al., 2003) using ligation via NotI and EcoRI restriction sites. A second MHV-specific TCR ( $\beta\alpha$ :  $\nu\beta 16$ -P2A- $\nu\alpha 2$ ) construct with codon-optimized sequences and two additional cysteine residues within the constant regions of  $\alpha$  and  $\beta$  chains was generated by GENEART (Regensburg, Germany). The optimized s598-specific TCR construct was incorporated into MP71-PRE using ligation via NotI and EcoRI restriction sites as above.

### *Production of s598-specific TCR-encoding retroviral particles*

Retrovirus-containing supernatants were produced by transient calcium phosphate transfection (Soneoka et al., 1995) of the packaging cell line Plat-E using 18 µg of TCR-S expression vectors. DMEM supplemented with 10% FCS (Sigma-Aldrich) and 100 U/ml penicillin/streptomycin was used for virus production. After 48 and 72 h, supernatants were harvested, filtered through a 0.45-µm pore filter, and stored at -80°C for subsequent use. Quality of the virus supernatant was assessed by transduction of the TCR-deficient murine cell line M58 (seeded into 24-well plates at density of 10<sup>5</sup>/ml) with 1 ml of retroviral supernatants at 37°C for 48 h. Percentage of M58 cells expressing the introduced TCR was measured using surface staining for the transgenic Vα2 TCR chain. For generation of low TCR expressing retrogenic mice, supernatants were diluted up to 5-fold, while non-diluted supernatants were used for generation of intermediate TCR expressing group. Mice with high and xhigh TCR expression were generated using retroviral supernatants obtained with expression vectors containing codon-optimized TCR constructs. Virus particle concentration was further increased using Amicon Ultra Centrifugal Filters (Millipore, Ireland) according to the manufacturer's instructions. Supernatants (500 µl per well) were loaded onto RetroNectin-coated (12.5 µg/ml, TaKaRa, Saint-Germain-en-Laye, France) 24-well non-tissue culture plates (Becton Dickinson, Switzerland) which were then centrifuged for 90 min at 2500×g and 4°C.

### *Generation of TCR-engineered retrogenic mice*

Bone marrow (BM) cell suspensions were prepared from hind leg tibias and femurs of B6 or RAG1-deficient mice. BM cells were enriched for (hematopoietic stem cells) HSCs using the EasySep mouse SCA1 positive selection kit (StemCell Technologies, Grenoble, France) following to the manufacturer's protocol. Cells were prestimulated at a density of 10<sup>6</sup>/ml for 3 days in StemPro-34 medium supplemented with 5% FCS (Sigma-Aldrich), 100 U/ml penicillin/streptomycin, 2 mM L-glutamine, 10 ng/ml murine IL-3, 50 ng/ml murine IL-6, and

50 ng/ml murine stem cell factor (PeproTech, Hamburg, Germany). On day 3, cell numbers were adjusted to  $4 \times 10^5$ /ml in freshly supplemented media and cultured overnight in RetroNectin/virus-coated 24-well plates. Transduction was repeated on day 4. For generation of xhigh TCR expressing mice, numbers of stem cells per well were reduced by a factor of 2 at the second transduction. One day later, stem cells were harvested and  $5 \times 10^5$  to  $10^6$  cells were i.v. injected into RAG1-deficient mice, which previously received 5.5 Gy total body irradiation from a linear accelerator (Clinic of Radio-Oncology, Kanton Hospital, St. Gallen). Recipient mice received drinking water supplemented with sulfadoxin and trimethoprim (Borgal; Veterinaria) for 6 wk.

#### *Virus infection and determination of virus-induced pathology*

Mice were infected intraperitoneally (i.p.) using 50 or 500 pfu MHV A59 (Coley et al., 2005). Mice were sacrificed at the indicated time points and blood samples and organs were collected. Serum was obtained by centrifugation of blood samples and stored at  $-80^\circ\text{C}$  until determination of alanine aminotransferase (ALT) levels with a Hitachi 747 auto-analyzer (Tokyo, Japan). Organs were weighed and stored at  $-80^\circ\text{C}$  until virus titer determination by standard plaque assay on L929 cells (Züst et al., 2007).

#### *Cell isolation and adoptive transfer*

Single-cell suspensions from spleens were prepared by mechanical disruption of the organ. For adoptive transfer, splenocytes were depleted of erythrocytes using lysis buffer (0.15 M  $\text{NH}_4\text{Cl}$ , 1 mM  $\text{KHCO}_3$ , 0.1 mM EDTA). For in vivo proliferation studies, splenocytes were labeled using 10  $\mu\text{l}$  5mM CFSE (Molecular Probes, Leiden, Netherlands) according to the manufacturer's protocol and  $10^6$  cells (corresponding to  $2 \times 10^5$   $\text{CD}8^+$  Rg T cells) were transferred intravenously (i.v) into recipient mice. One day after transfer, mice were infected with MHV A59. For in vivo protection studies,  $10^6$  splenocytes (corresponding to  $2 \times 10^5$   $\text{CD}8^+$

## Results

---

Rg T cells) were i.v. transferred into recipient B6 mice. One day after the transfer, recipient mice were infected using 50 pfu MHV A59 as described above.

### *Flow cytometry*

Blood samples were collected in 3 ml FACS buffer to prevent coagulation and subsequently treated with BD FACS Lysing Solution (BD Bioscience). Blood cells and single-cell suspensions from spleens were characterized using surface staining with antibodies against CD4-PerCP, CD8-APC (BioLegend), CD3-PE (eBioscience) and PE-conjugated MHV S598/H-2Kb tetramers (Sanquin, Amsterdam, The Netherlands). For the analysis of Rg cells after adoptive transfer, mice were sacrificed 8 days post infection and immediately perfused with PBS. Single-cell suspensions from spleen and liver lymphocytes (enriched on 70–30% Percoll gradients (GE Healthcare)) were characterized using surface staining with antibodies against CD8-PeCy7, Ly5.1-APC (eBioscience) and PE-conjugated MHV S598/H-2Kb tetramers (Sanquin, Amsterdam, The Netherlands). 7-amino-actinomycin D (7AAD; Calbiochem) was used to discriminate dead cells in flow cytometric analysis. For peptide-specific cytokine production,  $10^6$  splenocytes or liver lymphocytes were restimulated with s598 peptide ((RCQIFANI), Neosystem (Strasbourg, France)) in the presence of brefeldin A (5 µg/ml) and anti-Lamp 1-AlexaFlour 647 (BioLegend) for 5 h at 37°C. Cells were stimulated with PMA (50 ng/ml) and ionomycin (500 ng/ml; both purchased from Sigma-Aldrich) as positive control or left untreated as a negative control. For intracellular staining, restimulated cells were surface stained and fixed with Cytofix-Cytoperm (BD Biosciences) for 20 min. Fixed cells were incubated at 4°C for 40 min in the presence of anti-IFN $\gamma$  and anti-TNF $\alpha$  (eBiosciences) mAb diluted in permeabilization buffer (2% FCS/0.5% saponin/PBS). For determination of IFN- $\gamma$ -EC50, restimulation of the cells was performed using graded concentrations of s598 peptide as indicated. Samples were analyzed by flow cytometry using a FACSCanto flow cytometer (BD Biosciences); data were analyzed using FlowJo software (Tree Star).

*In Vitro CFSE-based proliferation assay*

Single-cell suspensions obtained from spleens were subjected to erythrocyte lysis by osmotic shock. Cells were labeled using 10  $\mu$ l 5 mM CFSE (Molecular Probes, Leiden, Netherlands) according to the manufacturer's protocol.  $10^5$  splenocytes and  $2 \times 10^4$  bone marrow derived DCs were seeded in 96-well round-bottom plates and s598 peptide was added at the indicated concentrations. Cells were analyzed by flow cytometry at 12, 36, 48, 60, 72, 84, and 96 h. Surface staining was performed using anti-CD8-PeCy7 and 7-amino-actinomycin D was used for discrimination of dead cells. At each measuring time point total, cell numbers were determined prior to the staining procedure using trypan blue (Sigma-Aldrich, Switzerland) dye exclusion and a Neubauer improved haemocytometer. CFSE dilution was determined on a FACSCanto flow cytometer (BD Biosciences); data were analyzed using FlowJo software (Tree Star).

*TCR density determination*

Number of TCRs expressed on the surface of Rg cells was determined using Quantum PE MESF kit (Bangs laboratories, Fishers, USA) according to the manufacturer's instructions. Briefly, T cells were incubated with PE-labeled anti-V $\alpha$ 2 Ab and analyzed by flow cytometry together with standard calibration beads. Based on the mean fluorescence values of the calibration beads, a calibration curve was generated using QuickCal v2.3 provided by the manufacturer. TCR density was determined as Molecules of Equivalent Soluble Fluorochrome (MESF) indicative for fluorescence intensity of a given number of fluorochrome molecules present on the cell surface. Antibody density-dependent fluorochrome intensity, i.e. the exact numbers of antibodies bound per cell was determined using Simply Cellular anti-mouse IgG (Bangs laboratories, Fishers, USA) according to the manufacturer's instructions.

### *Mathematical model describing T cell performance parameters*

This section is a summary of work described in detail in our previous work in (Bocharov et al., 2013; Luzyanina et al., 2013). In brief, division of CFSE-labeled T cells as determined by flow cytometry leads to CFSE histograms which are characterized by broadly varying patterns from highly distinct generational peaks to poorly resolved peaks. The poor resolution of the generational clusters in CFSE histograms is a consequence of an overlap of the successive generations in terms of CFSE heterogeneity due to an asymmetric partition of labeled proteins between the daughter cells. For a quantitative analysis of the corresponding CFSE histograms a novel approach is needed.

We performed the analysis of proliferative performance of Rg T cells from the CFSE dilution time series data generated here. The model considers the clonal population dynamics of T cells as a superposition of the subpopulations of cells which differ in terms of (1) completed rounds of division, (2) position with respect to the cell cycle (resting and proliferating subsets), and (3) CFSE content (UI, unit of intensity). In contrast to all existing models developed for the analysis of CFSE-based lymphocyte proliferation assay thus far, the division-cycle-label structured model considers an asymmetric mitosis which leads to an unequal distribution of CFSE-labeled proteins between sister cell pairs upon division and, in addition, explicitly accounts for the duration of the cell cycle.

*Model variables, parameters and equations.* The division-structured model considers the populations dynamics of the cohorts of resting and cycling T cells differing in terms of the number of completed divisions (generation-structure):  $N_i^R(t)$ ,  $N_i^C(t)$ , where  $t$  stands for time and  $i$  refers to the generation number, which is equal to the division age of the cells since activation. In our analysis the number of successive generations was below 8. The rates of change of the resting- and cycling cell populations was modeled by the following set of delay-differential equations:



$$\begin{aligned}\frac{d}{dt}N_0^R(t) &= -(\alpha_0 + \beta_0)N_0^R(t), \\ \frac{d}{dt}N_i^R(t) &= -(\alpha_i + \beta_i)N_i^R(t) + 2\alpha_{i-1}N_{i-1}^R(t - \tau_{i-1}), \quad i = 1, 2, \dots, I, \\ \frac{d}{dt}N_i^C(t) &= \alpha_i(N_i^R(t) - N_i^R(t - \tau_i)), \quad i = 0, 1, 2, \dots, I - 1,\end{aligned}$$

with the information about the starting cell number  $N^0$  and CFSE distribution of the naïve population entering the model solution via the so-called initial conditions:

$$\begin{aligned}N_0^R(s) &= 0, \quad s \in [-\tau_0, 0), \quad N_0^R(0) = N^0; \\ N_i^R(s) &= 0, \quad s \in [-\tau_i, 0], \quad i = 1, 2, \dots, I, \\ N_i^C(s) &= 0, \quad s \in [-\tau_i, 0], \quad i = 0, 1, 2, \dots, I - 1.\end{aligned}$$

The model depends on parameters that characterize the generation-specific activation- (transition from  $G_0$  to  $G_1$ ) and death rates  $(\alpha_i, \beta_i)$ , the duration of the progression from  $G_1$ - to M-phase  $(\tau_i)$ . The above model refers to the total number of cells in each generation that is sometimes difficult to assess, e.g., in the asymmetric division case. To this end, the above model is converted into a distributed parameter version that allows a direct reference to the CFSE histogram data. The label-structured mathematical model for asymmetric T cell division describes the evolution of the distribution density function of cells in successive generations (representing a CFSE histogram)  $n_i(t, x)$ , where  $t$  stands for time and  $x$  for the CFSE fluorescence intensity. The two models are related via following equality: total number of cells in generation “ $i$ ” is equal to the integral under the distribution density function

$$N_i(t) = \int_0^t n_i(s, x) ds. \quad \text{As in the division-structured model each generation of cells is}$$

subdivided into the resting- and cycling subsets:

$$n_i(t, x) = n_i^R(t, x) + n_i^C(t, x), \quad i = 0, 1, \dots, I - 1, \quad n_I(t, x) = n_I^R(t, x).$$

The temporal evolution of the cell distribution functions are modeled by the following label-structured cell population balance partial differential equations:

$$\begin{aligned}
\frac{\partial}{\partial t} n_0^R(t, x) - k \frac{\partial}{\partial x} (x n_0^R(t, x)) &= -(\alpha_0 + \beta_0) n_0^R(t, x), \\
\frac{\partial}{\partial t} n_i^R(t, x) - k \frac{\partial}{\partial x} (x n_i^R(t, x)) &= -(\alpha_i + \beta_i) n_i^R(t, x) + \dots \\
&+ \alpha_{i-1} e^{k\tau_{i-1}} \left( \frac{1}{m_1} n_{i-1}^R(t - \tau_{i-1}, e^{k\tau_{i-1}} \frac{x}{m_1}) + \frac{1}{1 - m_1} n_{i-1}^R(t - \tau_{i-1}, e^{k\tau_{i-1}} \frac{x}{1 - m_1}) \right), \quad i = 1, 2, \dots, I, \\
\frac{\partial}{\partial t} n_i^C(t, x) - k \frac{\partial}{\partial x} (x n_i^C(t, x)) &= \alpha_i (n_i^R(t, x) - e^{k\tau_i} n_i^R(t - \tau_i, e^{k\tau_i} x)), \quad i = 0, 1, \dots, I - 1,
\end{aligned}$$

With the initial conditions  $n_0^R(s, x) = 0$ ,  $s \in [-\tau_0, 0)$  and  $n_0^R(0, x)$  being the initial cell density function determined by the experimental CFSE histogram at the start of experiment. In addition, as only the initial cell generation is present we have the following initial data for the other cell generations:

$$n_i^R(s, x) = 0, \quad s \in [-\tau_i, 0], \quad i = 1, 2, \dots, I; \quad n_i^C(s, x) = 0, \quad s \in [-\tau_i, 0], \quad i = 0, 1, \dots, I - 1.$$

*Data fitting and parameter estimation.* The solution of the label- and division-structured model can be expressed in terms of the solution of division-structured model as described elsewhere (Luzyanina et al., 2013). Both models have common parameters characterizing the proliferative performance of T cells, however the more complex model also characterizes the degree of asymmetry of lymphocyte division via the parameter  $m_1$  and the label loss rate parameter  $k$ . The model is fitted to the time-series of the CFSE histograms to estimate the parameters of cell proliferation.

The fitting of the mathematical model to the CFSE histograms provides estimates of the following parameters: a): generation-specific activation- (transition from  $G_0$  to  $G_1$ ) and death rates  $(\alpha_i, \beta_i)$ , duration of the progression from  $G_1$ - to M-phase ( $\tau_i$ ), the asymmetry factor ( $m_{1i}$ ), the natural decay rate of CFSE fluorescence intensity of the labeled cells ( $k$ ). The model is fitted to the CFSE histogram data directly, i.e. without need to identify distinct generations, being a problem for standard software in case of asymmetrically dividing cells.

In fact, the model enables prediction of the generation's structure of a clonally expanding population as a function of time. The number of time series data available for analysis allows one to reliably estimate key integrative parameters of the T cell performance – the generation dependent population doubling time  $(\tau_i + \frac{1}{\alpha_i})$ , and the number of dead cells in every

generation normalized by the initial size of the population in the assay  $\frac{\int_0^{84} \beta_i N_i^R(t) dt}{N^0}$ , where

$N_i^R(t)$  is the function describing the size of the T cell population of the  $i$ -th generations subject to death. The total number of generations over 84 hours does not exceed 7 ( $I=7$ ). It should be noted that the in vitro conditions pose a limit on the possibility to observe the turnover of successive generations of T cells in a setting resembling physiological conditions. Firstly, the earlier and massive division of cells results in an exhaustion of the growth factors available for later generations. Therefore, further divisions are likely to take place in a biased milieu conditions. Secondly, as the observation time window for higher generations gets shorter, the uncertainty in the parameter estimates increases for later divisions starting from the third one. The above arguments suggest that for a physiologically consistent and mathematically robust characterization of the T cell performance parameters, only the first three generations of clonally dividing Rg CD8<sup>+</sup> T cells should be considered.

The parameters of the model were estimated using maximum likelihood approach as described elsewhere (Luzyanina et al., 2013). We further used Monte Carlo Markov Chain method (Haario et al., 2006) implemented as MCMC toolbox for MATLAB to quantify the probability densities, the posterior means and standard deviations of the estimated doubling times. Overall, the mathematical model was a key tool for characterizing the proliferative performance of T cells in relation to the number of the surface TCRs.

### *Statistical analyses*

All statistical analyses were performed with Prism 4.0 (GraphPad). Data were analyzed with the unpaired Student's t test. A p value of <0.05 was considered significant.

## **7.4 Results**

### **7.4.1 Polyclonal low avidity CD8<sup>+</sup> T cell responses during MHV infection**

Following systemic infection with MHV A59 virus, viral replication is largely restricted to spleen and liver. Although early viral replication is controlled through hematopoietic cell-derived type I IFN (Cervantes-Barragan et al., 2009), elevated serum alanine aminotransferase (ALT) levels, which reflect the degree of virus-induced hepatitis, become evident at day 3 post infection and reach maximal levels at day 5 (Eriksson et al., 2008). CD8<sup>+</sup> T cells are indispensable for elimination of the virus and hence secure survival of the host as shown by the fact that mice lacking CD8<sup>+</sup> T cells succumb to MHV infection (Fig. 18a). Maximal expansion of CD8<sup>+</sup> T cells directed against the immunodominant s598 epitope is reached at day 8 post infection with approximately 7% of tetramer H2-K<sup>d</sup>/s598-binding cells (Fig. 18b). Following ex vivo stimulation, s598-specific cells produced IFN- $\gamma$  (Fig. 18c) and had upregulated the degranulation marker Lamp-1 (not shown). To determine the functional avidity of the s598-specific CD8<sup>+</sup> T cell population, IFN- $\gamma$  production in response to graded s598 concentrations was examined. As shown in Fig. 18d, half-maximal IFN- $\gamma$  production (EC<sub>50</sub>, 50% effective concentration) was at  $7.8 \times 10^{-6}$  M (Fig. 18e), indicating that endogenous polyclonal CD8<sup>+</sup> T cells directed against the MHV spike protein exhibit a rather low functional avidity.

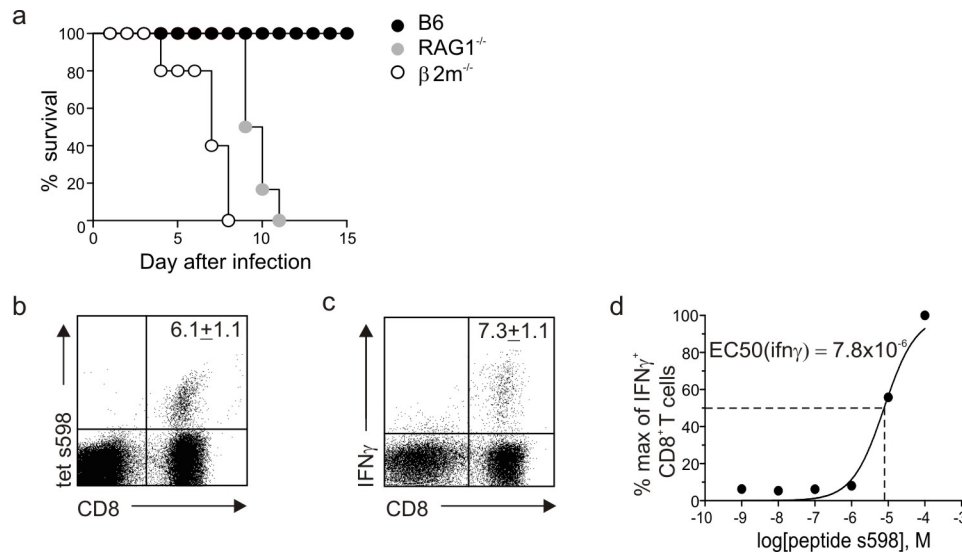


**Figure 18. Endogenous CD8<sup>+</sup> T cell responses during MHV infection.**

a) Survival rates of B6, RAG1-deficient and  $\beta 2m$ -deficient mice intraperitoneally infected with MHV A59 (n=5 mice per group). b)-c) Antiviral B6 CD8<sup>+</sup> T response in liver at day 8 post infection as determined by b) H2-K<sup>d</sup>/s598 tetramer analyzes and c) intracellular staining (ICS) for s598 responsive IFN- $\gamma$  producing CD8<sup>+</sup> T cells. Values in the upper right quadrant indicate mean percentage  $\pm$  SEM of CD8<sup>+</sup> T cell population derived from 2 independent experiments n=6 mice.

d) Half-maximal IFN- $\gamma$  production (EC50) of s598-specific CD8<sup>+</sup> T cells from liver at day 8 post infection. Pooled data from two independent experiments, n=6 mice.

#### 7.4.2 Generation of s598-specific TCR retrogenic CD8<sup>+</sup> T cells

To assess whether and to which extent TCR expression levels affect T cell behavior, we utilized retrogenic (Rg) TCR technology (Bettini et al., 2012). Starting from the sequence information obtained from the monoclonal hybridoma population expressing the rearranged s598 epitope-specific V $\alpha 2J\alpha 7/V\beta 16J\beta 2-1$  TCR (nomenclature according to Wilson et al.), a suitable construct for retroviral expression was designed. A P2A linker (de Felipe et al., 1999) was utilized to secure equimolar expression of the  $\beta$  and  $\alpha$  TCR chains in a myeloproliferative sarcoma virus (MPSV)-based vector (Engels et al., 2003). Retrogenic T cells showed stable expression of the TCR with up to 99% of CD8<sup>+</sup> T cells being V $\alpha 2$ <sup>+</sup> (Fig.

## Results

---

19a), CD3<sup>+</sup> (Fig. 19b) and CD4<sup>-</sup> (Fig. 19c). Importantly, TCR retrogenic CD8<sup>+</sup> T cells bound the H2-K<sup>d</sup>/s598 tetramer (Fig. 19d) and showed rapid proliferation in response to s598 peptide-presenting DCs (Fig. 19e). Likewise, the engineered CD8<sup>+</sup> T cells proliferated vigorously following adoptive transfer into virus-infected mice (Fig. 17f and g). Importantly, TCR retrogenic cells differentiated into IFN- $\gamma$ -producing effector T cells in vivo (Fig. 19h), exhibiting low functional avidity with an EC50 of  $4.4 \times 10^{-6}$  M (Fig. 19i). Despite their low functional avidity, the adoptively transferred cells displayed the profile of highly active effector T cells with simultaneous production of IFN- $\gamma$  and the expression of the degranulation marker Lamp-1 (Fig. 19j). Taken together, s598-specific Rg CD8<sup>+</sup> T cells show almost identical functional avidity and poly-functionality pattern as the polyclonal s598-specific CD8<sup>+</sup> T cell population that arises during MHV infection.

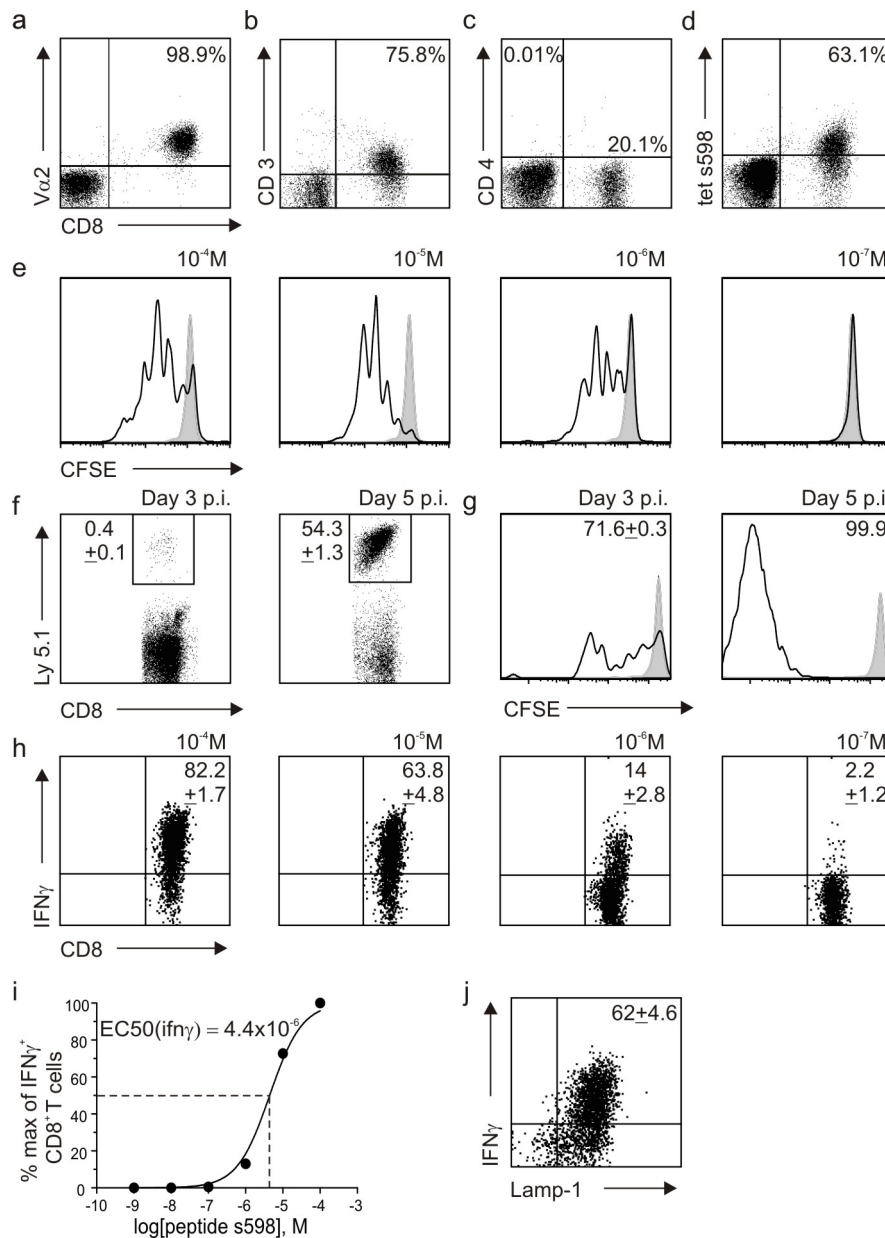


**Figure 19. Characteristics of retrogenic s598-specific CD8<sup>+</sup> T cells.**

a) Expression of Vα2 chain of the specific TCR, b) expression of CD3, c) lack of CD4<sup>+</sup> T cells in retrogenic mice d) tetramer H2-K<sup>d</sup>/s598 binding profile of CD8<sup>+</sup> T cells. The values in the upper right quadrants indicate the percentage of CD8<sup>+</sup> T cells with the respective markers. (n=10 mice). e) CFSE-labeled retrogenic splenocytes were incubated with DCs loaded with indicated concentrations of s598 peptide (black lines) or left untreated (gray shaded lines) and proliferative response was determined by CFSE dilution at 72 h of incubation. f) and g) CFSE-labeled, Ly5.1<sup>+</sup> s598-specific retrogenic cells were adoptively transferred into B6 mice. One day after the transfer the recipient mice were i.p. infected with MHV A59 or left untreated. At indicated time points post infection livers of recipient mice were analyzed to determine the f) accumulation and g) CFSE dilution profile of the adoptively transferred s598-

specific retrogenic cells (black lines - infected mice, gray shaded lines - uninfected controls). The values in plots represent the mean percentage $\pm$ SEM of f) CD8<sup>+</sup> T cells or g) Ly 5.1<sup>+</sup>CD8<sup>+</sup> T cell, n=3 mice. h)-j) Ly5.1<sup>+</sup> retrogenic cells were adoptively transferred into B6 mice subsequently infected with MHV. 8 days upon the infection h) IFN- $\gamma$  production of adoptively transferred retrogenic cells retrieved from livers was estimated upon stimulation with indicated amounts of s598 peptide. The values indicate the mean percentage $\pm$ SEM of Ly5.1<sup>+</sup> CD8<sup>+</sup> T cells. Data are pooled from two independent experiments, n=6. i) Half-maximal IFN- $\gamma$  production (EC50) of Ly5.1<sup>+</sup> CD8<sup>+</sup> T cells from liver at day 8 post infection e) Simultaneous production of INF- $\gamma$  and expression of degranulation marker by in vitro restimulated Ly5.1<sup>+</sup> CD8<sup>+</sup> T cells from liver day 8 post infection. The values in the upper right quadrant indicate the mean percentage $\pm$ SEM, n=3 mice.

### 7.4.3 Tunable expression of the s598-specific TCR

To modulate TCR signal strength, we created Rg mice with T cells expressing different number of TCRs varying the concentration of retroviral supernatant during stem cell transduction with both the natural V $\alpha$ 2J $\alpha$ 7/V $\beta$ 16J $\beta$ 2-1 TCR and the codon-optimized variant (Scholten et al., 2006). Through this approach, we could obtain four distinct expression densities termed low (Fig. 20a) and intermediate (Fig. 20b) for the natural TCR and high (Fig. 20c) and xhigh (Fig. 20d) for the codon-optimized version. It is interesting to note that the optimized retrogenic TCR generated at standard conditions resembled the expression pattern observed with the transgenic TCR suggesting that the TCR density of the “high” TCR density group (Fig. 20c) represent a physiological optimum. Importantly, molecular optimization of the TCR together with high-efficacy stem cell transduction could further increase the TCR density (Fig. 20d) with more than 20,000 TCR molecules per cell (Fig. 20e). Noteworthy, xhigh TCR density cells showed substantially higher V $\alpha$ 2 expression and H2-Kd/s598 tetramer binding compared to the high TCR density group (Fig. 20d). Moreover, quantification of TCR density by enumeration of surface-expressed V $\alpha$ 2 molecules revealed a strong correlation of these values with H2-Kd/s598 tetramer binding (Fig. 20e) and clearly



distinct TCR expression pattern of the four groups. Thus, the Rg system facilitated tunable expression of the TCR on the surface of CD8<sup>+</sup> T cells.

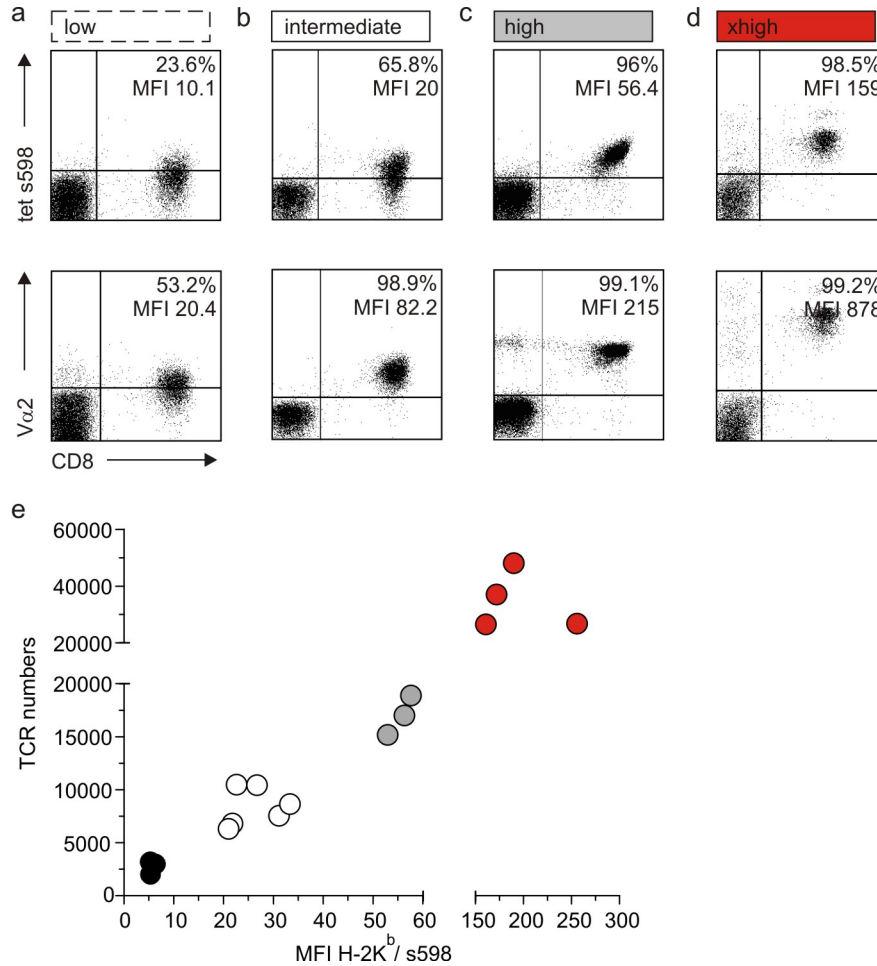


**Figure 20. Tunable expression of s598-specific TCR.**

Groups of retrogenic mice expressing different levels of s598-specific TCR were generated using a), b) natural sequence of s598 epitope-specific Vα2Jα7/Vβ16Jβ2-1 TCR; or c), d) codon-optimized sequence. Variations in the concentration of viral particles applied during the transduction process was used to obtain CD8<sup>+</sup> T cell with a) low, b) intermediate, c) high and d) xhigh levels of Vα2 chain expression (upper plots) and tetramer H2-K<sup>d</sup>/s598 binding profile (lower plots), assessed from the blood. The upper numbers in the upper right quadrant indicate percentage of H2-K<sup>d</sup>/s598 binding of CD8<sup>+</sup> T cells (upper plots) and percentage of Vα2<sup>+</sup> of CD8<sup>+</sup> T cells (lower plots). The lower numbers in the upper right quadrant indicate median fluorescence intensity of H2-K<sup>d</sup>/s598 binding (upper plots) and the mean fluorescence intensity of Vα2<sup>+</sup> on CD8<sup>+</sup> T cells. The plots are representative of at least 3 independent experiments. The absolute numbers of TCRs expressed on the surface of retrogenic T cells

and H2-K<sup>d</sup>/s598 binding profile were determined from splenocytes of all four groups. e) Correlation between the numbers of expressed TCRs and H2-K<sup>d</sup>/s598 binding profile (black dots-low, white dots-intermediate, gray dots-high and red dots xhigh TCR density group).

### 7.4.4 TCR density determines T cell activation threshold

To assess how tuned TCR expression on virus-specific T cells affects their activation, we performed in vitro proliferation assays using CFSE-labeled splenic Rg CD8<sup>+</sup> T cells stimulated with peptide-loaded DCs. The peptide dose of 10<sup>-5</sup> M was used to pulse DCs because this concentration is almost exactly equal to the EC50 (IFN- $\gamma$ ) of both endogenous and retrogenic s598-specific T cells (Fig. 18d and 19i). As expected “low” TCR Rg T cells failed to respond and did not show dilution of the dye (Fig. 21a). Both “intermediate” (Fig. 21b) and TCR optimized “high” (Fig. 21c) Rg T cells had initiated proliferation after 36 h and showed a regular division pattern. Interestingly, Rg cells in the “xhigh” group showed a highly synchronized CFSE dilution pattern within the first 48 h, i.e. with a single division of all cells (Fig. 21d). Moreover, within the next 48 h “xhigh” T cells underwent only one more round of division (Fig. 21d) suggesting that a shift of TCR density above a second threshold of ~ 20,000 molecules per cell profoundly alters their response pattern. Indeed, whereas death of “intermediate” and “high” TCR Rg T cells could be observed in the cultures, lymphocyte death in the cultures with “xhigh” T cells was not detectable (not shown). These data suggest that the effect of TCR density on T cell performance follows a strictly biphasic function with lack of responsiveness below a certain threshold of TCR expression, full activation in a certain range of TCR density and an altered functional mode above a second threshold.

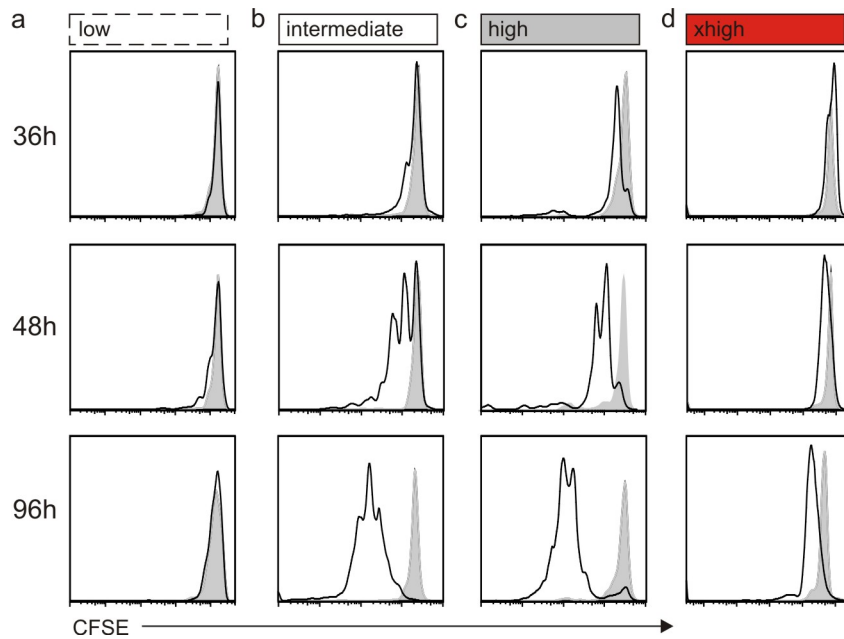


**Figure 21. TCR expression levels critically determine CD8<sup>+</sup> T cell activation threshold and intensity of the proliferative response.**

The influence of the tuned s598-specific TCR expression on the behavior of retrogenic CD8<sup>+</sup> T cells was determined using in vitro proliferation assay. CFSE-labeled splenocytes derived from spleens of retrogenic mice from each of four TCR density groups were incubated with DCs loaded with  $10^{-5}$  M of s598 peptide or left untreated. Proliferative response of retrogenic cells was determined by CFSE dilution. Representative plots show CFSE dilution prolife of a) low, b) intermediate, c) high and d) xhigh cells determined after indicated times of incubation with DCs loaded with peptide (black lines) or left untreated (gray shaded lines). The results are representative of at least three independent experiments.

#### 7.4.5 Modeling TCR density-dependent CD8<sup>+</sup> T cell behavior

The processes involved in T cell activation, differentiation and decay are highly complex and involve a plethora of molecules on the surface and within the T cell (Chen and Flies, 2013; Brownlie and Zamoyska, 2013; Acuto et al., 2008; Smith-Garvin et al., 2009). To further analyze the behavior of Rg T cells in dependence of their surface TCR density, we resorted to a recently developed mathematical model that facilitates the extraction of essential T cell performance parameters from CFSE dilution data (Luzyanina et al., 2013; Bocharov et al.,

2013). The model permits resolution of T cell performance in terms of the population doubling time, death intensity and asymmetry of cell division (Fig. 22a). The model correctly describes the behavior “low” TCR Rg T cells as a lack of proliferation and constant decay of cell number (Fig. 22b). The predicted generation structure of both “intermediate” (Fig. 22c) and “high” TCR density Rg T cells (Fig. 22d) reveals the balance of proliferation, loss of cells in one generation due to transition into the next generation and loss of cells due to cell death. Moreover, the model correctly reflects the slower onset of proliferation of “intermediate” (Fig. 22c) compared to “high” TCR density cells (Fig. 22d). Likewise, “xhigh” cells showed a fast onset of proliferation (Fig. 22e) which is reflected in a lower doubling time of the first round of division (Fig. 22f). Interestingly, “xhigh” cells maintained a rather slow doubling time whereas both “intermediate” and “high” cells showed fast proliferation cycles after the first division (Fig. 22f). Moreover, the model predicts increasing death rates for both “intermediate” and “high” TCR density cells after the second division, i.e. in the 3<sup>rd</sup> and 4<sup>th</sup> generation (Fig. 22f). The steady accumulation of the slowly proliferating “xhigh” cells (data points in Fig. 22f) is explained by the very low death rates during the observation period (Fig. 22g). Thus, the mathematical model confirms the biphasic response pattern of retrogenic CD8<sup>+</sup> T cells with a lower activation threshold for full activation and differentiation and an upper threshold that results in an altered proliferation and decay pattern.

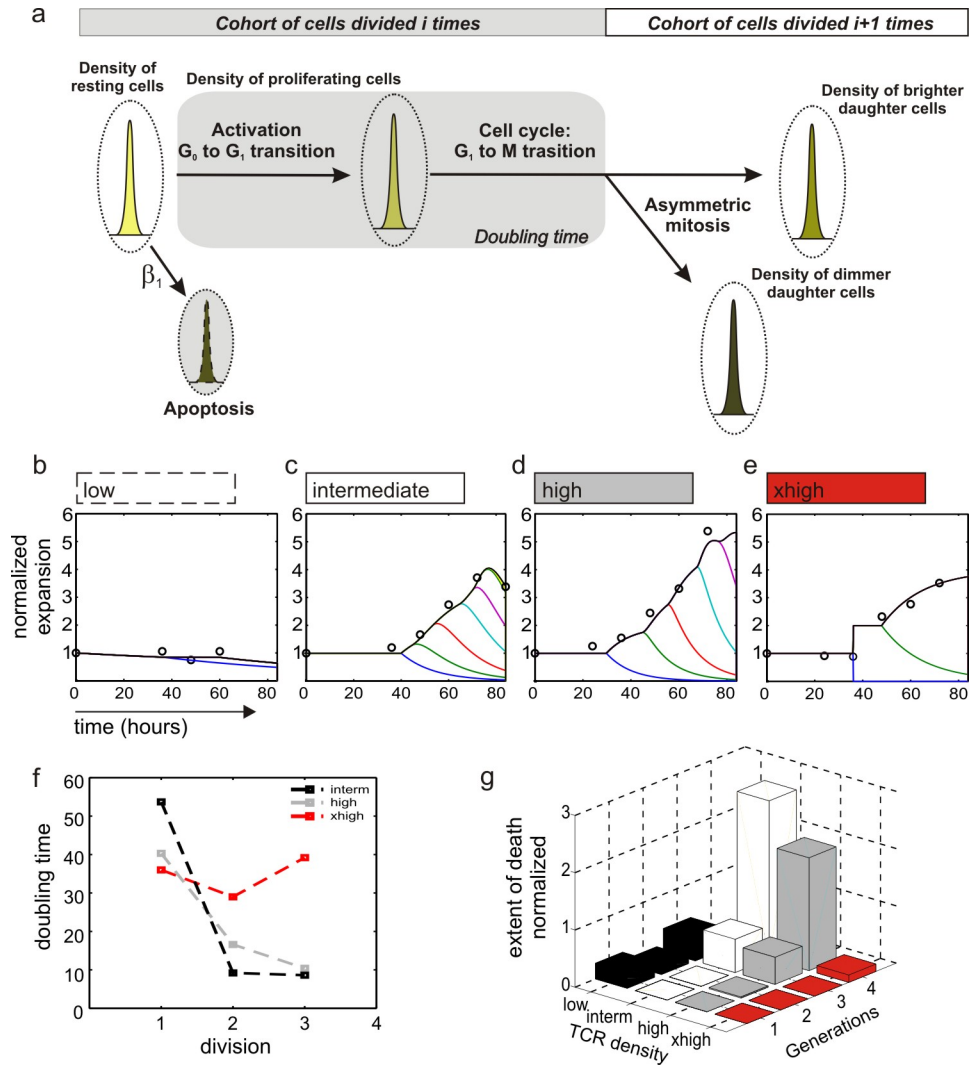


**Figure 22. Model-based analysis of TCR-density-dependent CD8<sup>+</sup> T cell performance.**

a) Schematic representation of the biological processes considered in the model. The model discriminates cells by the number of completed divisions and the CFSE fluorescence intensity. Shown are the cell distributions in generations “ $i$ ” and “ $i+1$ ” that completed “ $i-1$ ” and “ $i$ ” division cycles, respectively. Cells are considered to be either in a resting state ( $G_0$ -phase), or progressing through the cell cycle ( $G_1$ -S- $G_2$ -M phases). Activated cells from the generation “ $i$ ” will start the division and make the transition from  $G_0$  to  $G_1$  with the activation rate and cell cycle duration as generation-specific parameters. Upon finalization of the  $G_2$  phase the cells will divide by an asymmetric division resulting in the generation of two daughter cells that contain different amount of CFSE-labeled proteins. The model considers that cells undergo apoptosis at generation-dependent death rate ( $\beta_1$ ). The natural degradation of CFSE is taken into account and is characterized by the decay rate constant ( $k$ ). b) - e) Kinetics of the generation structure of proliferating b) low, c) intermediate, d) high and e) xhigh TCR density groups of s598-specific retrogenic CD8<sup>+</sup> T cells. Open symbols

represent the experimental results of the clonal expansion of proliferating retrogenic CD8<sup>+</sup> T cells determined at the indicated time points. Solid black lines indicate the best-fit solution of the mathematical model. The cell cohorts belonging to different generations are shown by color lines (blue – naïve, green – divided once, red – divided twice, light blue – divided three times, violet – four times, yellow – five times, respectively). The clonal expansion of cells is characterized by the expansion factor obtained by dividing the population size determined at the given time points by the numbers of cells determined at the start of the assay. f) Doubling times (duration of the cell cycle, from activation until cell division) calculated for the first three generations of intermediate (black dashed lines), high (gray dashed line) and xhigh (red dashed line) TCR density groups of retrogenic cells. The doubling time of the cells with a low TCR density is beyond the observation window and is, therefore, not shown.

g) The extent of death calculated for the first four generations of proliferating retrogenic cells with low (black bars), intermediate (white bars), high (gray bars) and xhigh (black bars) TCR densities. The bars characterize the number of cells that died during 84 hours of the assay in the respective generation divided by the initial T cell population size.

### 7.4.6 In vivo protective capacity TCR retrogenic CD8<sup>+</sup> T cells

To assess the antiviral potential of s598-specific CD8<sup>+</sup> T cells, we adoptively transferred Rg CD8<sup>+</sup> T cells into B6 mice and subsequently infected the mice with MHV A59. Viral replication and distribution and virus-induced liver pathology was determined on days 3 and 5 post infection. As expected, mice that had received “low” TCR cells showed ALT values comparable to control animals (Fig. 23a and b) and had failed to reduce viral titers (Fig. 23c and d). Antiviral CD8<sup>+</sup> T cells equipped with TCRs at “intermediate” or “high” levels significantly reduced liver pathology (Fig. 23a and b) and fostered faster clearance of the virus (Fig. 23c and d). Strikingly, “xhigh” CD8<sup>+</sup> T cells not only failed to reduce viral titers (Fig. 23c and d), but even exacerbated liver inflammation on day 3 post infection (Fig. 23a). These findings confirm the notion that the expression of the TCRs above a certain threshold ensures full functionality of CD8<sup>+</sup> T cells, even in vivo. Moreover, these data reveal that supra-physiological levels of TCR expression profoundly alters T cell function and can even

lead to adverse consequences for the host if such engineered cells are utilized in an adoptive transfer setting.

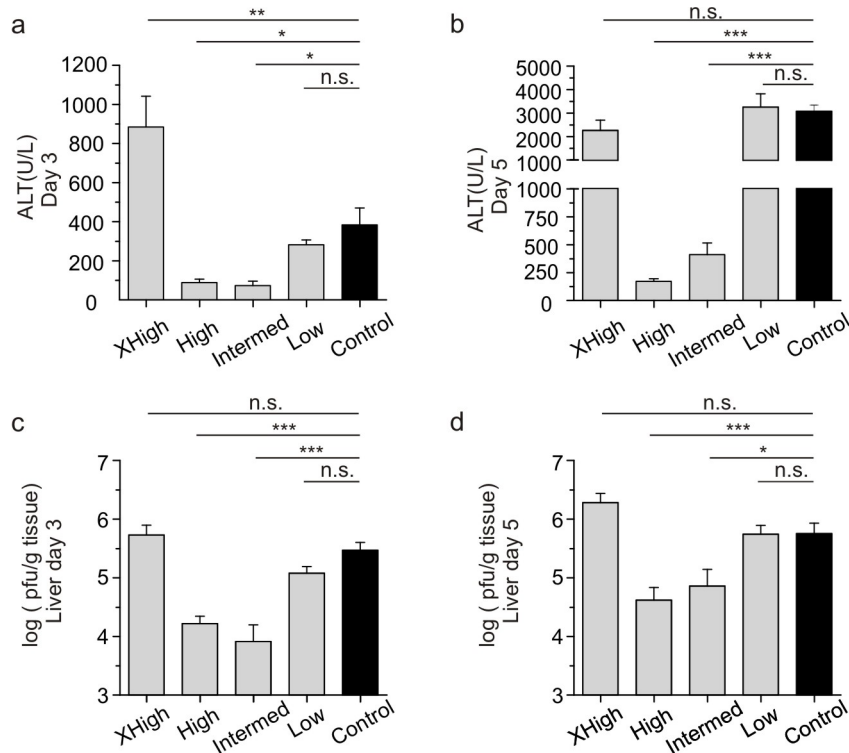


**Figure 23. In vivo protective capacity of TCR retrogenic CD8<sup>+</sup> T cells.**

Protective capacity of four groups of retrogenic cells with different TCR expression levels was estimated in the settings of adoptive transfer. Each of four TCR density groups of retrogenic splenocytes was transferred into separate group of B6 mice, while one group of B6 mice was left untreated. One day after the transfer all five groups of B6 mice were infected intraperitoneally with MHV A59. Serum levels of alanine aminotransferase (ALTs) were determined on a) day 3 and b) day 5 post infection. The data represent the mean values $\pm$ SEM obtained from at least two independent experiments. Adoptively transferred groups n=6, control group n=12. Viral titers in liver were determined on c) day 3 and d) day 5 post infection. Data indicate mean of log transformed values $\pm$ SEM from at least two independent experiments. Day 3- high, xhigh and control group n=6, low and intermediate groups, n=4. Day 5 – adoptively transferred groups n=6, control group n=12. Statistical analysis was performed using Student's t test (\*, p<0.05, \*\*, p<0.01, \*\*\*, p<0.001; n.s., not significant).

### 7.5 Discussion

Timely activation and optimal maintenance of antiviral and antitumor CD8<sup>+</sup> T cells are crucial elements to ensure successful eradication of infected or altered cells. While redirecting T cell specificity by TCR gene transfer usually guarantees that redirected cell will inherit both specificity (Clay et al., 1999; Morgan et al., 2003; Zhao et al., 2005) and functional avidity (Wilde et al., 2009; Johnson et al., 2006) determined by the TCR structure, other factors influencing T cell avidity may come into play and affect the performance of engineered T cells. One of the most frequent problems in ATT that has constrained its fast progression and introduction into routine clinical procedures is the stable expression of the TCR on the surface of T cells (Uckert and Schumacher, 2009; Kieback and Uckert, 2010; Thomas et al., 2010). To better understand the consequences of different TCR expression levels on the activation and in vivo function of CD8<sup>+</sup> T cells, we have cloned a TCR specific for the mouse coronavirus MHV and expressed the heterodimer as retrogenic TCR at different densities. This novel approach provides a constant structural affinity of the TCR, but permits tunable avidity of CD8<sup>+</sup> T cells.

The complex data sets generated with CD8<sup>+</sup> T cells expressing the Rg TCR at four different levels were analyzed using a novel mathematical model of CFSE dilution (Luzyanina et al., 2013; Bocharov et al., 2013). The model predicts that both early activation and survival of antiviral CD8<sup>+</sup> T cells rely on the signaling strength received through the TCRs. Furthermore, adoptive transfer experiments demonstrated a clear dependence of the in vivo protective capacity of antiviral CD8<sup>+</sup> T cells on TCR numbers. While transfer of cells expressing TCR numbers at physiological levels provided best protection against virus-induced pathology, further increase in TCR expression levels had the opposite effect leading to uncontrolled viral replication in the liver and elevated liver disease.

It has been suggested that only high avidity CD8<sup>+</sup> T cell can efficiently contribute to control of tumors and viruses (Alexander-Miller et al., 1996; Stone et al., 2009). The ability of these



cells to sense low levels of pMHC complexes on the surface of APCs allows for earlier activation during immune response which together with the rapid kinetics of target cell lysis (Derby et al., 2001) allows high avidity T cells swift and successful eradication of infected or altered cells. Additionally, high avidity CD8<sup>+</sup> T cells exhibit a broader cytokine profile (La Gruta et al., 2004) which correlates with a higher potency to eradicate infected cells. Interestingly, the functional avidity of s598-specific CD8<sup>+</sup> T cells, a value that is often taken as a proxy for the overall avidity of T cells, is rather low. Nevertheless, these cells respond fast and efficiently following encounter with their cognate peptide presented by DCs, both in vitro and in vivo. Moreover, the ability of adoptively transferred Rg CD8<sup>+</sup> T cells to produce several cytokines simultaneously most likely contributed to the capacity to dramatically reduce viral titers and virus-induced pathology. Hence, in contrast to the frequently assumed need for high avidity T cells in the defense against viruses, also low avidity T cells can efficiently contain a viral infection. It would be interesting to perform more comprehensive analysis to assess to which extent low avidity T cells participate in the defense against murine coronavirus and other natural mouse pathogens. Such studies would have important consequences for the design of vaccination and ATT approaches.

Clinical application of TCR gene-modified hematopoietic stem cells (HSC)-derived T cells still awaits safety approval (Hacein-Bey-Abina et al., 2003; Ott et al., 2006). However, retrogenic or TCR-engineered HSC-transplanted mice already provided not only important insight into T cell biology (Day et al., 2011; Bartok et al., 2010; Alli et al., 2008), but facilitated proof-of-principle studies in valuable pre-clinical models (Stärck et al., 2014; Spranger et al., 2012). Moreover, combining molecular strategies to improve TCR expression such as TCR sequence optimization and disulfide bond addition (Cohen et al., 2007) were introduced as technologies to further optimize TCR expression. Here, we utilized these latter methods together with well-adjusted variations in the transduction of HSC to achieve defined levels in TCR surface expression, i.e. covering the range from sub-optimal to supra-physiological TCR levels. We found that the combination of the tetramer-binding profile with TCR numbers provided the basis of a clear distinction of four different groups. Since tetramer-binding is

## Results

---

primarily dependent on the TCR-pMHC affinity and CD8 co-receptor expression (Stone et al., 2009), the observed differences in the percentage and MFI of cells binding H2-K<sup>d</sup>/s598 tetramer are clearly the result of different TCR expression levels. Hence, our finding that enhanced TCR expression results in faster activation of virus-specific CD8<sup>+</sup> T cells, is very well in line with the previous reports trying to correlate TCR expression levels with changes in T cell responsiveness (Schodin et al., 1996; Labrecque et al., 2001; Blichfeldt et al., 1996). Indeed, it has been described that particular thresholds of TCR expression have to be reached to facilitate T cell activation. Nevertheless, different experimental approaches revealed different TCR threshold levels, e.g. 6000 TCRs were required for activation of T cell clones (Viola and Lanzavecchia, 1996) while only 1000 TCRs per cell appeared to be required in an in vivo model of T cell activation (Labrecque et al., 2001). It might well be that the variation in this lower TCR threshold is due to the fact that T cells expressing different TCRs have been analyzed in these studies. Indeed, the affinity of the TCR for pMHC determines how many TCR molecules have to be expressed by a T cell to reach the activation threshold (Schodin et al., 1996). The threshold number of TCRs needed for T cell activation in our experimental system is ~5000 TCRs, i.e. a value that falls within the previously described range of TCR expression levels required for activation (Viola and Lanzavecchia, 1996; Labrecque et al., 2001; Schodin et al., 1996).

Importantly, tuning of T cell performance by up-scaling TCR numbers from intermediate to high led to faster activation and moderately higher overall expansion. However, such tuned TCR levels did not provide a significantly improved in vivo protection, at least in the chosen test. It would be worth to assess the protective function of TCR tuned T cells under more demanding assay conditions. Nevertheless, the experiments presented here revealed a certain higher threshold level of TCR expression that precipitates profoundly altered T cell behavior.

Supra-physiological levels of TCRs on the surface of T cells (xhigh) mediated highly synchronized proliferation during the interaction with DCs, reduced cell death and constant expansion of the cell population in vivo. Importantly, xhigh cells failed to protect mice from

viral challenge. It is possible that too high TCR expression results in altered cell cycle regulation. Indeed, Yoon et al. (Yoon et al., 2010) have showed that T cells receiving strong stimuli can significantly shorten cell cycle times by reducing the time cells spends in G<sub>1</sub> phase. Moreover, faster progression through cell cycle may restrict the time needed for the cells to undergo DNA repair and therefore result in clonal progeny with higher incidence of mutations and chromosomal instabilities (Aoki et al., 2003). In addition, dysregulation of cell cycle progression may be coupled with altered apoptosis as predicted by our mathematical model. Future work will show whether cell cycle dysregulation and/or changes in cellular death pathways are involved in the altered T cell behavior observed in xhigh cells.

A second possible scenario for the lack of protection by xhigh cells is the rapid emergence of escape variants in the presence of these cells. Indeed, the genomic region coding for the spike protein has previously been described as prone to deletions and single-base mutations (Banner et al., 1990; Castro and Perlman, 1995; Rowe et al., 1997). Other MHV strains such as JHM have been shown to escape from CD8<sup>+</sup> T cell recognition under high selection pressure on an immunodominant epitope (Pewe et al., 1997, 1996).

In conclusion, the rheostat function of the TCR for T cell activation is – in part – determined by two distinct density thresholds. While the first threshold defines the lowest signal strength needed for activation of T cells to occur, the second threshold defines an upper limit of efficient T cell activation and function. Importantly, it appears that the range of TCR densities that permit efficient activation is rather broad and that TCR optimization should avoid overtuning which might result in aberrant T cell behavior.

### **7.6 Acknowledgments**

We thank Marcus Arn and the Department of Radiation Oncology, Cantonal Hospital St. Gallen for the irradiation of mice; Rita DeGiuli and Fabienne Soppelsa for technical support.

### **7.7 Data contribution**

Burkhard Ludewig designed the study. Jovana Cupovic performed research and wrote the paper. Lilian Stärck supported the establishment of retrogenic mice. Tatyana Luzyanina and Gennady Bocharov developed the mathematical model and discussed data.

## 8 Discussion

### 8.1 Selecting an appropriate system to study T cell biology

Characterization and usage of clonotypic TCRs facilitate high-resolution studies of pathogen-specific T cell responses. In this work, a MHC I-restricted TCR specific for mouse hepatitis virus (MHV) has been characterized. The cloned TCR has been analyzed in two alternative experimental systems, thereby providing the opportunity to study different aspects of T cell biology. Different TCR expression systems were selected according to the needs of the respective experimental questions. Stable incorporation of the TCR into the genome of transgenic mice provided a source of identical cells that were used to study the migratory and functional properties of virus-specific T cells during virus-induced neuroinflammation. Pathogen-specific, TCR transgenic T cells have been widely used to assess the role of T cells in various infection models (Oxenius et al., 1998; Torti et al., 2011; Roth and Pircher, 2004; Mueller et al., 2003). However, the laborious and time-consuming procedure of TCR transgenesis is not well suited, for example, to investigate the elements that determine TCR signaling. Retrogenic mice represent a more flexible system that allows rapid introduction of defined alterations and hence fast analysis of multiple variables in TCR behavior (Bettini et al., 2012; Liu et al., 2009; Day et al., 2011; Arnold et al., 2004). Utilizing retrovirus-mediated gene transfer and combining this approach with genetic TCR optimization, we created a system with tunable TCR expression covering a broad range from suboptimal to supraphysiological TCR signaling. Application of this system allowed for comprehensive analyzes of the functional consequences of graded TCR expression on in vitro and in vivo performance of MHV-specific CD8<sup>+</sup> T cells.

## 8.2 Underestimated efficacy of low avidity CD8<sup>+</sup> T cells

The sequence of the TCR dictates the affinity of this molecule for the peptide-MHC complex and in large determines the responsiveness of the T cell bearing the particular TCR (Wilde et al., 2009; Johnson et al., 2006). However, the performance of the T cell can be strongly influenced by other elements involved in T cell signaling such as expression levels of co-receptors, co-stimulatory and co-inhibitory molecules and as shown here, the level of TCR expression. The functional analysis of s598-specific CD8<sup>+</sup> T cells, either polyclonal, TCR transgenic or retrogenic, revealed that a rather high concentration (at least  $10^{-6}$  M) of peptide is needed to activate the cells. Since this threshold has been confirmed using different functional readouts such as *vitro* proliferation and *ex vivo* cytokine secretion assays, it is reasonable to conclude that the cloned s598-specific TCR exhibits a low functional avidity when the TCR is expressed at physiological levels.

It is noteworthy that we have not performed any of the measurements that would determine the true affinity of the TCR for the pMHC complex (e.g. dissociation constant  $K_D$  measurements, tetramer dissociation rate -  $K_{off}$ , or surface plasmon resonance). Hence, we cannot definitely conclude that the TCR is of low affinity, although the functional analysis performed here strongly suggests that. The fact that the affinity of peptide binding to MHC complex significantly influences the strength of TCR binding to the peptide-MHC complex (Stone et al., 2009) indicates that the high peptide concentration needed for s598-specific cells activation is the consequence of the low-affinity binding of the peptide to MHC complex. Clearly, it will be interesting to further explore the basic properties of the TCR-S-s598/H2-Kb interactions.

Although, it is broadly accepted in the field that immune responses against pathogens are dominated by high avidity T cells (Alexander-Miller et al., 1996), recent findings have revealed a previously unappreciated role of low avidity CD8<sup>+</sup> T cells in pathogen elimination (Zehn and Bevan, 2006; Zehn et al., 2009). One reason for the “ignorance” of low avidity T

cell responses is the fact that these cells can be outnumbered by high avidity T cell clones in particular experimental systems (Kunert et al., 2013) and therefore hidden from detection. Therefore, higher magnification analysis, i.e. utilizing higher numbers of TCR transgenic or retrogenic T cells, can permit assessment of low avidity T cell function during antiviral immune responses. Our observation that low avidity CD8<sup>+</sup> T cells can efficiently migrate to the infected tissue at early time points after infection and produce wide range of antiviral effector molecules indicates that low avidity CD8<sup>+</sup> T cells actively contribute to the elimination of viruses from tissues. Moreover, recent findings indicate that low avidity CD8<sup>+</sup> T cells specific for tumor-derived epitopes are capable of destroying cancer cells in vivo (Boon et al., 2006; Rosenberg et al, 2008). Thus, if both low avidity and high avidity T cells are able to protect the host from viral infection and eliminate tumor cells, the question arises which factors determine whether low or high avidity T cells will be recruited into a particular immune response.

Here, we demonstrate that during virus-induced neuroinflammation, low avidity CD8<sup>+</sup> T cells can exhibit a crucial function in controlling viral replication within the CNS. The high frequency of Spiky cells within the CNS during MHV infection suggests that the overall efficacy of low avidity CD8<sup>+</sup> T cells is regulated through their abundance in the tissues. Highly abundant CD8<sup>+</sup> effector T cells that recognize their target cells only when high amounts of peptide is presented can guarantee coverage of large areas of infected tissue and a rather high specificity. The ability to destroy only those cells that express the viral peptide at high concentrations may facilitate the distinction of infected cells from non-infected cells that had acquired peptides through cross-presentation (Kurts et al., 2001) or cross-dressing (Wakim and Bevan, 2011). In sum, we believe that low avidity CD8<sup>+</sup> effector T cells permit viral clearance from infected tissues and help to reduce immunopathological damage of fragile tissues such as the CNS.

### **8.3 CCR7 ligands control CD8<sup>+</sup> T cells during CNS inflammation**

Immune homeostasis, i.e. the balance between effective surveillance and minimal immune damage, is prerequisite for proper functioning of the neuronal system. Maintenance of this homeostasis is achieved through distinct barriers in the CNS vascular tree that control trafficking of molecules and cells in and out of the brain (Owens et al., 2008; Galea et al., 2007). Immune cells can only transit into the CNS when specific molecular keys are presented. Hence, cytotoxic T cells as mediators of antiviral immunity in the brain should follow particular rules to allow eradication of infected cells, while avoiding damage of neuronal tissue (Moseman and McGavern, 2013). Indeed, the failure to control CD8<sup>+</sup> T cell influx into and their function within the CNS can cause serious diseases as shown for CNS infection with Borna disease virus and LCMV (Bizler and Stitz, 1994; Kim et al., 2009). Moreover, autoreactive CD8<sup>+</sup> T cells which may be involved in CNS diseases such as multiple sclerosis (MS) (Skulina et al., 2004; Huseby et al., 2001; Killestein et al., 2003) might have escaped from thorough control. Hence, it is important to understand the mechanisms that regulate the recruitment of CD8<sup>+</sup> T cells to CNS tissue and to assess their function.

In order to investigate recruitment of cytotoxic T cells to virus-infected tissues, we used the transgenic Spiky cells. Following intranasal inoculation, MHV infects olfactory cells in the nasal mucosa and migrates along olfactory neurons to reach the brain (Barnett and Perlman, 1993). Infection with GFP-labeled MHV virus allowed us to identify neurons and glial cells as the major cellular targets of viral replication. Eradication of MHV-infected cells is predominantly achieved through the action of cytotoxic T cells (Bergmann et al., 2003). The activation of virus specific CD8<sup>+</sup> T cell takes place in cervical lymph nodes (cLNs) that receive CNS-derived antigens through CSF and CNS-derived interstitial fluid. We found that transgenic Spiky cells were activated in the cLNs only after a lag phase of approximately 3 days. Importantly, only 24 h later, the first activated Spiky cells had immigrated to the MHV-infected brain. While the mediators of initial interactions between activated T cells and the



inflamed CNS endothelium such as PSGL-1 and P-selectin have been described extensively (Kerfoot and Kubes, 2002; Piccio et al., 2002; Battistini et al., 2003) the impact of G-protein coupled receptor and constitutive chemokines involved in the activation of integrin molecules had not been fully clarified.

First indications of the involvement of the constitutive chemokines CCL19 and CCL21 in the regulation of T cell trafficking to the brain came from several studies demonstrating the presence of these chemokines in and around inflamed blood vessels (Krumbholz et al., 2007; Pashenkov et al., 2003). Moreover, abrogation of CCR7 axis during infection with the brain-invading parasite *Toxoplasma gondii* exacerbated CNS inflammation (Noor et al., 2010). Importantly, the finding of Buonamici and colleagues that T-cell acute lymphoblastic leukemia cells are highly dependent on the CCR7 axis for their entry to the CNS (Buonamici et al., 2009) suggests that CCR7-dependent entry to the CNS is broad pathway exploited by different cells.

Our study shows that CCR7 and its ligands critically regulate activation and recruitment of CD8<sup>+</sup> T cell to the virus-infected CNS. Importantly, our experiments comparing the immune responses of MHV-infected CCR7 and plt/plt mice revealed that expression of a CCR7 ligand within the CNS is sufficient to secure protection against otherwise lethal CNS infection. It appears that extra-lymphatic CCL21b not only promotes CD8<sup>+</sup> T cell recruitment to the infected CNS areas, but also fosters T cell function. It would be of interest, to delineate whether and to which extent CCR7 ligands promote local antigen presentation. It is possible that the constitutive chemokines contribute to the generation of tertiary lymphoid tissues in the CNS (Comerford et al., 2013) which can be observed during chronic CNS inflammation (Kuersten et al., 2012).

From the above, we can conclude that the localization of the cellular sources of CCR7 ligands within the CNS most likely bears important consequences for T cell behavior. Usage of a novel mouse model that targets CCL19-producing cells (Chai et al., 2013) allowed for a precise identification of these cells in the MHV infected brains. Our analysis indicated that both endothelial cells and perivascular cells are involved in the production of CCL19.

However, CCL21 appears to be more dispersed on the surface of cells in the perimeter of the inflamed blood vessel and produced by a broader range of cells including microglia. Phenotypic characterization of the fibroblastic cells involved in production of CCR7 ligands revealed that these cells show features of fibroblastic reticular cells (FRC) of secondary lymphoid organs. Indeed, the appearance of ERTR7<sup>+</sup> stromal cells in the brains of infected animals has been previously described in the cases of CNS restricted infections with LCMV (Kim et al., 2009) and *Toxoplasma gondii* (Wilson et al., 2009). Importantly, distribution of ERTR7<sup>+</sup> cells reported by these two studies is comparable to the cellular location observed in our study. Interestingly, parasite- or virus-specific CD8<sup>+</sup> T cells are frequently found in close vicinity to activated fibroblastic stromal cells in the brain (Kim et al., 2009; Wilson et al., 2009). These findings suggest that activated fibroblastic stromal cells in the brain could be responsible for generating chemokine coated reticular networks that provide a physical scaffold and motogenic signals for T cells migration (Worbs et al., 2007). This notion is strongly supported by our finding that ERTR7<sup>+</sup>/podoplanin<sup>+</sup> cells are indeed coated with CCL21 and - at the same time - are involved in the production of this chemokine. Collectively, these studies reveal that under pathogenic conditions, reticular stromal cells of the brain start to produce CCR7 ligands and actively participate in the recruitment of T cells to the endangered tissue. The finding that CCL19 and, to the lesser extent, CCL21 are upregulated in patients suffering from MS (Krumbholz et al., 2007) opens the possibility that a similar stromal cell network could be established in the course of this disease, fostering the accumulation of autoimmune T cells in the affected CNS. Targeting these structures might open new options for the more successful treatment of such autoimmune disorders.

Finally, our observation that activated astrocytes produce CCL19 later during the course of the infection indicates possible function of these cells in guiding T cells into the CNS parenchyma. Since astrocytes build the glia limitans, expression of CCL19 by these cells might promote CD8<sup>+</sup> T cells recruitment to the neuronal tissue. Furthermore, by regulating the dwelling time of CD8<sup>+</sup> T cells in the perivascular spaces astrocytes might influence the overall signal CD8<sup>+</sup> T cells receive during multiple contacts with antigen presenting cells

residing within perivascular spaces (Pesic et al., 2013), thereby adjusting their functionality. Additionally, CCL19 expression by astrocytes within the parenchyma could be involved in positioning of antiviral T cells within virus-infected regions thereby fostering faster eradication of the virus.

Overall, inflammatory stimuli within the immunologically specialized CNS tissue seem to utilize similar molecular pathways that operate in the periphery to recruit immune cells to the highly vulnerable neuronal tissue. Importantly, accumulating experimental evidence indicates a critical role for stromal cells in regulating T cell recruitment and function within the CNS.

#### **8.4 Varying the strength of TCR engagement – implications for adoptive T cell therapy**

The major aim of adoptive T cells therapy (ATT) is to achieve highly efficient and specific destruction of infected or altered cells (June, 2007). Achieving this aim relies on the ability of CD8<sup>+</sup> T cells to recognize altered or infected cells with high specificity, reach high numbers of effector cells through extensive proliferations and persist in the organism for sufficiently long time to allow full eradication of target cells. Extensive work has been invested over the years to fulfill the safety and efficacy preconditions for successful application of ATT in the clinic. One important prerequisite for successful ATT relies in large on the selection of optimal TCRs to direct the specificity of the cells to carefully selected epitopes (Linnemann et al., 2011). Results from preclinical tests and clinical trials clearly show that the successful eradication of the target cells depends on the use of TCRs that recognize peptide-MHC with high affinity (Morgan et al., 2006; Zeh et al., 1999; Yee et al., 1999). As CD8<sup>+</sup> T cells bearing high affinity TCRs are able to recognize target cells expressing low numbers of pMHC complexes they allow more potent eradication of tumor and virus-infected cells (Stone et al., 2009). However, tumor antigens are to large extent true self-antigens, therefore mechanism

of central tolerance may delete T cells bearing high affinity TCR precluding their identification and usage in clinical settings. Hence, affinity maturation of patient-derived TCRs specific for tumor-derived epitopes has been employed to improve tumor cell eradication (Stone et al., 2009). However, while a few studies have shown a benefit for affinity matured TCRs (Robbins et al., 2008; Bowerman et al., 2009; Johnson et al., 2009), other indicate decreased function (Zhong et al., 2013; Schmid et al., 2010; Hebeisen et al., 2013). Moreover, application of T cells equipped with affinity matured TCRs may results in off-target destruction leading to fatal consequences (Johnson et al., 2009; Linette et al., 2013; Therapy et al., 2013).

However, affinity of the TCR for the pMHC complex is just one of the determinants dictating T cell performance. Our study demonstrates that the overall avidity of T cell interaction with APCs critically influences T cell functionality and protective capacity. Importantly, we have demonstrated that tuning the overall strength of T cell engagement can enhance T cell proliferation and allow accumulation of higher numbers of effector T cells. Additionally, by setting the optimal level of signaling, we have achieved prolonged survival of effector CD8<sup>+</sup> T cells. Thus, we have demonstrated that reaching the optimal signal strength has beneficial effect on two important factors of protective CD8<sup>+</sup> T cell responses – high numbers and longevity of effector cells. Combined effect of these two elements finally resulted in highest level of protection, indicating the necessity for finely balanced level of signaling to obtain the maximal effects. Importantly, in strong agreement with the reports of adverse effects resulting from application of extremely high affinity TCRs, we have shown that over-expression of TCRs leads to aberrant T cell behavior and loss of protective function. While the mechanistic basis of T cell dysfunction in these two examples is most likely different, both findings indicate that subtle differences in signal strength can turn protective into destructive T cell responses.

Over the past decade great success has been made in the clinical application of TCR redirected ATT. Significant clinical responses have been reported for patients suffering of colorectal carcinoma (Parkhurst et al., 2011), metastatic melanoma and synovial sarcoma (Robbins et al., 2011). In patients with congenital and acquired immunodeficiency, genetically modified T cells have been shown to persist for years in humans following adoptive transfer (Blaese et al., 1995; Mitsuyasu et al., 2000). As more and more technical problems are been solved, TCR redirected ATT becomes a relevant clinical treatment option (Kunert et al., 2013). However, reports of adverse events indicate that our understanding of T cell biology is not complete and needs to be frequently reexamined to allow further improvement in safety and efficacy of current T cell-based treatment approaches.

## 9 Appendix

### 9.1 Literature

- Acuto, O., V. Di Bartolo, and F. Michel. 2008. Tailoring T-cell receptor signals by proximal negative feedback mechanisms. *Nat. Rev. Immunol.* 8:699–712..
- Acuto, O., and D. Cantrell. 2000. T cell activation and the cytoskeleton. *Annu. Rev. Immunol.* 18:165–84.
- Agrawal, S., P. Anderson, M. Durbeej, N. van Rooijen, F. Ivars, G. Opdenakker, and L.M. Sorokin. 2006. Dystroglycan is selectively cleaved at the parenchymal basement membrane at sites of leukocyte extravasation in experimental autoimmune encephalomyelitis. *J. Exp. Med.* 203:1007–19.
- Aivazian, D., and L.J. Stern. 2000. Phosphorylation of T cell receptor zeta is regulated by a lipid dependent folding transition. *Nat. Struct. Biol.* 7:1023–6.
- Alexaki, A., and B. Wigdahl. 2008. HIV-1 infection of bone marrow hematopoietic progenitor cells and their role in trafficking and viral dissemination. *PLoS Pathog.* 4:e1000215.
- Alexander-Miller, M. a, G.R. Leggatt, and J. a Berzofsky. 1996. Selective expansion of high- or low-avidity cytotoxic T lymphocytes and efficacy for adoptive immunotherapy. *Proc. Natl. Acad. Sci. U. S. A.* 93:4102–7.
- Alexander-Miller, M.A. 2005. High-avidity CD8+ T cells: optimal soldiers in the war against viruses and tumors. *Immunol. Res.* 31:13–24.
- Alli, R., P. Nguyen, and T.L. Geiger. 2008. Retrogenic Modeling of Experimental Allergic Encephalomyelitis Associates T Cell Frequency but Not TCR Functional Affinity with Pathogenicity. *J. Immunol.* 181:136–145.
- Alt, C., M. Laschinger, and B. Engelhardt. 2002. Functional expression of the lymphoid chemokines CCL19 ( ELC ) and CCL 21 ( SLC ) at the blood-brain barrier suggests their involvement in G-protein- dependent lymphocyte recruitment into the central nervous system during experimental autoimmune encephalo. 19:2133–2144.
- Aoki, K., Y. Tamai, S. Horiike, M. Oshima, and M.M. Taketo. 2003. Colonic polyposis caused by mTOR-mediated chromosomal instability in Apc+/Delta716 Cdx2+/- compound mutant mice. *Nat. Genet.* 35:323–30.
- Ara, T., M. Itoi, K. Kawabata, T. Egawa, K. Tokoyoda, T. Sugiyama, N. Fujii, T. Amagai, and T. Nagasawa. 2003. A Role of CXC Chemokine Ligand 12/Stromal Cell-Derived Factor-1/Pre-B Cell Growth Stimulating Factor and Its Receptor CXCR4 in Fetal and Adult T Cell Development in Vivo. *J. Immunol.* 170:4649–4655.
- Araki, K., A.P. Turner, V.O. Shaffer, S. Gangappa, S. a Keller, M.F. Bachmann, C.P. Larsen, and R. Ahmed. 2009. mTOR regulates memory CD8 T-cell differentiation. *Nature.* 460:108–12.
- Arnold, P.Y., A.R. Burton, and D.A.A. Vignali. 2004a. Diabetes incidence is unaltered in glutamate decarboxylase 65-specific TCR retrogenic nonobese diabetic mice: generation by retroviral-mediated stem cell gene transfer. *J. Immunol.* 173:3103–11.
- Badovinac, V.P., J.S. Haring, and J.T. Harty. 2007. Initial T cell receptor transgenic cell precursor frequency dictates critical aspects of the CD8(+) T cell response to infection. *Immunity.* 26:827–41.
- Banchereau, J., and R.M. Steinman. 1998. Dendritic cells and the control of immunity. *Nature.* 392:245–52.
- Banner, L.R., J.G. Keck, and M.M. Lai. 1990. A clustering of RNA recombination sites adjacent to a hypervariable region of the peplomer gene of murine coronavirus. *Virology.* 175:548–55.

- Bao, X., E.A. Moseman, H. Saito, B. Petryniak, B. Petryniak, A. Thiriot, S. Hatakeyama, Y. Ito, H. Kawashima, Y. Yamaguchi, J.B. Lowe, U.H. von Andrian, and M. Fukuda. 2010. Endothelial heparan sulfate controls chemokine presentation in recruitment of lymphocytes and dendritic cells to lymph nodes. *Immunity*. 33:817–29.
- Barnett and Perlman, 1993. 1993. The olfactory Nerve and Not the Trigeminal Nerve Is the Major Site of CNS Entry for Mouse Hepatitis Virus, Strain JHM. 185–191. doi:8386871.
- Barry, M., and R.C. Bleackley. 2002. Cytotoxic T lymphocytes: all roads lead to death. *Nat. Rev. Immunol.* 2:401–9.
- Bartok, I., S.J. Holland, H.W. Kessels, J.D. Silk, M. Alkhinji, and J. Dyson. 2010. T cell receptor CDR3 loops influence alphabeta pairing. *Mol. Immunol.* 47:1613–8.
- Di Bartolo, V., B. Montagne, M. Salek, B. Jungwirth, F. Carrette, J. Fournane, N. Sol-Foulon, F. Michel, O. Schwartz, W.D. Lehmann, and O. Acuto. 2007. A novel pathway down-modulating T cell activation involves HPK-1-dependent recruitment of 14-3-3 proteins on SLP-76. *J. Exp. Med.* 204:681–91.
- Battegay, M., D. Moskophidis, a Rahemtulla, H. Hengartner, T.W. Mak, and R.M. Zinkernagel. 1994. Enhanced establishment of a virus carrier state in adult CD4+ T-cell-deficient mice. *J. Virol.* 68:4700–4.
- Battistini, L., L. Piccio, B. Rossi, S. Bach, S. Galgani, C. Gasperini, L. Ottoboni, D. Ciabini, M.D. Caramia, G. Bernardi, C. Laudanna, E. Scarpini, R.P. McEver, E.C. Butcher, G. Borsellino, and G. Constantin. 2003. CD8<sup>+</sup> T cells from patients with acute multiple sclerosis display selective increase of adhesiveness in brain venules: a critical role for P-selectin glycoprotein ligand-1. 101:4775–4782. doi:10.1182/blood-2002-10-3309.Supported.
- Bechmann, I., I. Galea, and V.H. Perry. 2007. What is the blood-brain barrier (not)? *Trends Immunol.* 28:5–11.
- Bedoui, S., and T. Gebhardt. 2011. Interaction between dendritic cells and T cells during peripheral virus infections: a role for antigen presentation beyond lymphoid organs? *Curr. Opin. Immunol.* 23:124–30.
- Bender, S.J., and S.R. Weiss. 2010. Pathogenesis of murine coronavirus in the central nervous system. *J. Neuroimmune Pharmacol.* 5:336–54.
- Bennett, S.R., F.R. Carbone, F. Karamalis, J.F. Miller, and W.R. Heath. 1997. Induction of a CD8+ cytotoxic T lymphocyte response by cross-priming requires cognate CD4+ T cell help. *J. Exp. Med.* 186:65–70.
- Berg, L.J., B. Fazekas de St Groth, A.M. Pullen, and M.M. Davis. 1989. Phenotypic differences between alpha beta versus beta T-cell receptor transgenic mice undergoing negative selection. *Nature*. 340:559–62.
- Bergmann, C.C., J.D. Altman, D. Hinton, and S. a Stohlman. 1999. Inverted immunodominance and impaired cytolytic function of CD8+ T cells during viral persistence in the central nervous system. *J. Immunol.* 163:3379–87.
- Bergmann, C.C., T.E. Lane, and S. a Stohlman. 2006. Coronavirus infection of the central nervous system: host-virus stand-off. *Nat. Rev. Microbiol.* 4:121–32.
- Bergmann, C.C., B. Parra, D.R. Hinton, R. Chandran, M. Morrison, and S. a Stohlman. 2003. Perforin-Mediated Effector Function Within the Central Nervous System Requires IFN- $\gamma$ -Mediated MHC Up-Regulation. *J. Immunol.* 170:3204–3213.
- Bettini, M.L., M. Bettini, and D. a Vignali. 2012. T-cell receptor retrogenic mice: a rapid, flexible alternative to T-cell receptor transgenic mice. *Immunology*. 136:265–72.
- Bevan, M.J. 2004. Helping the CD8(+) T-cell response. *Nat. Rev. Immunol.* 4:595–602.
- Bevan, M.J. and Z.D. 2006. Avidity and the art of self non-self discrimination. *Immunity*. 25:191–3.
- Bilzer, T., and L. Stitz. 1994. Immune-mediated brain atrophy. CD8+ T cells contribute to tissue destruction during borna disease. *J. Immunol.* 153:818–23.

- Blaese, R.M., K.W. Culver, a D. Miller, C.S. Carter, T. Fleisher, M. Clerici, G. Shearer, L. Chang, Y. Chiang, P. Tolstoshev, J.J. Greenblatt, S. a Rosenberg, H. Klein, M. Berger, C. a Mullen, W.J. Ramsey, L. Muul, R. a Morgan, and W.F. Anderson. 1995. T lymphocyte-directed gene therapy for ADA- SCID: initial trial results after 4 years. *Science*. 270:475–80.
- Blattman, J.N., R. Antia, D.J.D. Sourdive, X. Wang, S.M. Kaech, K. Murali-Krishna, J.D. Altman, and R. Ahmed. 2002. Estimating the precursor frequency of naive antigen-specific CD8 T cells. *J. Exp. Med.* 195:657–64.
- Blichfeldt, E., L.A. Munthe, J.S. Røtnes, and B. Bogen. 1996. Dual T cell receptor T cells have a decreased sensitivity to physiological ligands due to reduced density of each T cell receptor. *Eur. J. Immunol.* 26:2876–84.
- Bocharov, G., T. Luzyanina, J. Cupovic, and B. Ludewig. 2013. Asymmetry of Cell Division in CFSE-Based Lymphocyte Proliferation Analysis. *Front. Immunol.* 4:264.
- Bonilla, W. V, A. Fröhlich, K. Senn, S. Kallert, M. Fernandez, S. Johnson, M. Kreutzfeldt, A.N. Hegazy, C. Schrick, P.G. Fallon, R. Klemenz, S. Nakae, H. Adler, D. Merkler, M. Löhning, and D.D. Pinschewer. 2012. The alarmin interleukin-33 drives protective antiviral CD8<sup>+</sup> T cell responses. *Science*. 335:984–9.
- Boon, T., P.G. Coulie, B.J. Van den Eynde, and P. van der Bruggen. 2006. Human T cell responses against melanoma. *Annu. Rev. Immunol.* 24:175–208.
- Bosc, N., and M.P. Lefranc. 2000. The mouse (*Mus musculus*) T cell receptor beta variable (TRBV), diversity (TRBD) and joining (TRBJ) genes. *Exp. Clin. Immunogenet.* 17:216–28.
- Bousso, P., N.R. Bhakta, R.S. Lewis, and E. Robey. 2002. Dynamics of thymocyte-stromal cell interactions visualized by two-photon microscopy. *Science*. 296:1876–80.
- Bowerman, N. a, T.S. Crofts, L. Chlewicki, P. Do, B.M. Baker, K. Christopher Garcia, and D.M. Kranz. 2009. Engineering the binding properties of the T cell receptor:peptide:MHC ternary complex that governs T cell activity. *Mol. Immunol.* 46:3000–8.
- Brändle, D., K. Brduscha-Riem, a C. Hayday, M.J. Owen, H. Hengartner, and H. Pircher. 1995. T cell development and repertoire of mice expressing a single T cell receptor alpha chain. *Eur. J. Immunol.* 25:2650–5.
- Bromley, S.K., T.R. Mempel, and A.D. Luster. 2008. Orchestrating the orchestrators: chemokines in control of T cell traffic. *Nat. Immunol.* 9:970–80.
- Brownlie, R.J., and R. Zamoyska. 2013. T cell receptor signalling networks: branched, diversified and bounded. *Nat. Rev. Immunol.* 13:257–69.
- Brugnera, E., a Bhandoola, R. Cibotti, Q. Yu, T.I. Ginter, Y. Yamashita, S.O. Sharrow, and a Singer. 2000. Coreceptor reversal in the thymus: signaled CD4+8+ thymocytes initially terminate CD8 transcription even when differentiating into CD8+ T cells. *Immunity*. 13:59–71.
- Buller, R.M., K.L. Holmes, A. Hügin, T.N. Frederickson, and H.C. Morse. 1987. Induction of cytotoxic T-cell responses in vivo in the absence of CD4 helper cells. *Nature*. 328:77–9.
- Bumann, D. 2003. T cell receptor-transgenic mouse models for studying cellular immune responses to Salmonella in vivo. *FEMS Immunol. Med. Microbiol.* 37:105–109.
- Buonamici, S., T. Trimarchi, M.G. Ruocco, L. Reavie, S. Cathelin, B.G. Mar, A. Klinakis, Y. Lukyanov, J.-C. Tseng, F. Sen, E. Gehrie, M. Li, E. Newcomb, J. Zavadil, D. Meruelo, M. Lipp, S. Ibrahim, A. Efstratiadis, D. Zagzag, J.S. Bromberg, M.L. Dustin, and I. Aifantis. 2009. CCR7 signalling as an essential regulator of CNS infiltration in T-cell leukaemia. *Nature*. 459:1000–4.
- Burke, M.L., D.P. McManus, G. a Ramm, M. Duke, Y. Li, M.K. Jones, and G.N. Gobert. 2010. Co-ordinated gene expression in the liver and spleen during *Schistosoma japonicum* infection regulates cell migration. *PLoS Negl. Trop. Dis.* 4:e686. Butz, E. a, and M.J. Bevan. 1998. Massive expansion of antigen-specific CD8+ T cells during an acute virus infection. *Immunity*. 8:167–75.



- Call, M.E., and K.W. Wucherpfennig. 2004. Molecular mechanisms for the assembly of the T cell receptor-CD3 complex. *Mol. Immunol.* 40:1295–305.
- Carreño, L.J., S.M. Bueno, P. Bull, S.G. Nathenson, and A.M. Kalergis. 2007. The half-life of the T-cell receptor/peptide-major histocompatibility complex interaction can modulate T-cell activation in response to bacterial challenge. *Immunology.* 121:227–37.
- Casrouge, a., E. Beaudoin, S. Dalle, C. Pannetier, J. Kanellopoulos, and P. Kourilsky. 2000. Size Estimate of the TCR Repertoire of Naive Mouse Splenocytes. *J. Immunol.* 164:5782–5787.
- Cassell, D., and J. Forman. 1988. Linked recognition of helper and cytotoxic antigenic determinants for the generation of cytotoxic T lymphocytes. *Ann. N. Y. Acad. Sci.* 532:51–60.
- Castellino, F., and R.N. Germain. 2006. Cooperation between CD4+ and CD8+ T cells: when, where, and how. *Annu. Rev. Immunol.* 24:519–40..
- Castro, R.F., and S. Perlman. 1995. CD8+ T-cell epitopes within the surface glycoprotein of a neurotropic coronavirus and correlation with pathogenicity. *J. Virol.* 69:8127–31.
- Cemerski, S., J. Das, E. Giurisato, M. a Markiewicz, P.M. Allen, A.K. Chakraborty, and A.S. Shaw. 2008. The balance between T cell receptor signaling and degradation at the center of the immunological synapse is determined by antigen quality. *Immunity.* 29:414–22.
- C.F. Barker, R.E. Billingham Immunologically privileged sites. *Adv. Immunol.*, 25 (1977), pp. 1–54
- Cervantes-Barragan, L., U. Kalinke, R. Zust, M. Konig, B. Reizis, C. Lopez-Macias, V. Thiel, and B. Ludewig. 2009. Type I IFN-Mediated Protection of Macrophages and Dendritic Cells Secures Control of Murine Coronavirus Infection. *J. Immunol.* 182:1099–1106.
- Cervantes-Barragan, L., R. Züst, F. Weber, M. Spiegel, K.S. Lang, S. Akira, V. Thiel, and B. Ludewig. 2007. Control of coronavirus infection through plasmacytoid dendritic-cell-derived type I interferon. *Blood.* 109:1131–7.
- Chai, Q., L. Onder, E. Scandella, C. Gil-Cruz, C. Perez-Shibayama, J. Cupovic, R. Danuser, T. Sparwasser, S. a Luther, V. Thiel, T. Rülcke, J. V Stein, T. Hehlhans, and B. Ludewig. 2013. Maturation of lymph node fibroblastic reticular cells from myofibroblastic precursors is critical for antiviral immunity. *Immunity.* 38:1013–24.
- Chen, L., and D.B. Flies. 2013. Molecular mechanisms of T cell co-stimulation and co-inhibition. *Nat. Rev. Immunol.* 13:227–42.
- Chen, S.-C., G. Vassileva, D. Kinsley, S. Holzmann, D. Manfra, M.T. Wiekowski, N. Romani, and S. a. Lira. 2002. Ectopic Expression of the Murine Chemokines CCL21a and CCL21b Induces the Formation of Lymph Node-Like Structures in Pancreas, But Not Skin, of Transgenic Mice. *J. Immunol.* 168:1001–1008.
- Choudhuri, K., and P.A. van der Merwe. 2007. Molecular mechanisms involved in T cell receptor triggering. *Semin. Immunol.* 19:255–61.
- Christopherson, K.W., A.F. Hood, J.B. Travers, H. Ramsey, and R.A. Hromas. 2003. Endothelial induction of the T-cell chemokine CCL21 in T-cell autoimmune diseases. *Blood.* 101:801–6.
- Clay, T.M., M.C. Custer, J. Sachs, P. Hwu, S. a Rosenberg, and M.I. Nishimura. 1999. Efficient transfer of a tumor antigen-reactive TCR to human peripheral blood lymphocytes confers anti-tumor reactivity. *J. Immunol.* 163:507–13.
- Cohen, C.J., Y.F. Li, M. El-Gamil, P.F. Robbins, S. a Rosenberg, and R. a Morgan. 2007. Enhanced antitumor activity of T cells engineered to express T-cell receptors with a second disulfide bond. *Cancer Res.* 67:3898–903.
- Coley, S.E., E. Lavi, S.G. Sawicki, L. Fu, B. Schelle, N. Karl, S.G. Siddell, and V. Thiel. 2005. Recombinant mouse hepatitis virus strain A59 from cloned, full-length cDNA replicates to high titers in vitro and is fully pathogenic in vivo. *J. Virol.* 79:3097–106.
- Columba-Cabezas, S., B. Serafini, E. Ambrosini, and F. Aloisi. 2003. Lymphoid chemokines CCL19 and CCL21 are expressed in the central nervous system during experimental

- autoimmune encephalomyelitis: implications for the maintenance of chronic neuroinflammation. *Brain Pathol.* 13:38–51.
- Comerford, I., Y. Harata-Lee, M.D. Bunting, C. Gregor, E.E. Kara, and S.R. McColl. 2013. A myriad of functions and complex regulation of the CCR7/CCL19/CCL21 chemokine axis in the adaptive immune system. *Cytokine Growth Factor Rev.* 24:269–83.
- Constantinescu, C.S., M. Tani, R.M. Ransohoff, M. Wysocka, B. Hilliard, T. Fujioka, S. Murphy, P.J. Tighe, J. Das Sarma, G. Trinchieri, and A. Rostami. 2005. Astrocytes as antigen-presenting cells: expression of IL-12/IL-23. *J. Neurochem.* 95:331–40.
- Cooper, L.J., M. Kalos, D.A. Lewinsohn, S.R. Riddell, and P.D. Greenberg. 2000. Transfer of specificity for human immunodeficiency virus type 1 into primary human T lymphocytes by introduction of T-cell receptor genes. *J. Virol.* 74:8207–12.
- Crotty, S. 2011. Follicular helper CD4 T cells (TFH). *Annu. Rev. Immunol.* 29:621–63.
- Curtsinger, J.M., J.O. Valenzuela, P. Agarwal, D. Lins, and M.F. Mescher. 2005. Cutting Edge: Type I IFNs Provide a Third Signal to CD8 T Cells to Stimulate Clonal Expansion and Differentiation. *J. Immunol.* 174:4465–4469.
- Davis, C.B., N. Killeen, M.E. Crooks, D. Raulet, and D.R. Littman. 1993. Evidence for a stochastic mechanism in the differentiation of mature subsets of T lymphocytes. *Cell.* 73:237–47.
- Davis, M.M. 2002. A new trigger for T cells. *Cell.* 110:285–7.
- Davis, M.M., and P.J. Bjorkman. 1988. T-cell antigen receptor genes and T-cell recognition. *Nature.* 334:395–402.
- Day, E.B., C. Guillonneau, S. Gras, N.L. La, D.A.A. Vignali, P.C. Doherty, A.W. Purcell, J. Rossjohn, and S.J. Turner. 2011. Structural basis for enabling T-cell receptor diversity within biased virus-specific CD8 + T-cell responses.
- Deindl, S., T. a Kadlec, T. Brdicka, X. Cao, A. Weiss, and J. Kuriyan. 2007. Structural basis for the inhibition of tyrosine kinase activity of ZAP-70. *Cell.* 129:735–46.
- Dembic, Z., W. Haas, S. Weiss, J. McCubrey, H. Kiefer, H. von Boehmer, and M. Steinmetz. 1986. Transfer of specificity by murine alpha and beta T-cell receptor genes. *Nature.* 320:232–8.
- Derby, M. a., M. a. Alexander-Miller, R. Tse, and J. a. Berzofsky. 2001. High-Avidity CTL Exploit Two Complementary Mechanisms to Provide Better Protection Against Viral Infection Than Low-Avidity CTL. *J. Immunol.* 166:1690–1697.
- Dieu, M.C., B. Vanbervliet, a Vicari, J.M. Bridon, E. Oldham, S. Ait-Yahia, F. Brière, a Zlotnik, S. Lebecque, and C. Caux. 1998. Selective recruitment of immature and mature dendritic cells by distinct chemokines expressed in different anatomic sites. *J. Exp. Med.* 188:373–86.
- Dössinger, G., M. Bunse, J. Bet, J. Albrecht, P.J. Paszkiewicz, B. Weißbrich, I. Schiedewitz, L. Henkel, M. Schiemann, M. Neuenhahn, W. Uckert, and D.H. Busch. 2013. MHC multimer-guided and cell culture-independent isolation of functional T cell receptors from single cells facilitates TCR identification for immunotherapy. *PLoS One.* 8:e61384.
- Dobrovina, E., B. Oflaz-Sozmen, S.E. Prockop, N. a Kernan, S. Abramson, J. Teruya-Feldstein, C. Hedvat, J.F. Chou, G. Heller, J.N. Barker, F. Boulad, H. Castro-Malaspina, D. George, A. Jakubowski, G. Koehne, E.B. Papadopoulos, A. Scaradavou, T.N. Small, R. Khalaf, J.W. Young, and R.J. O'Reilly. 2012. Adoptive immunotherapy with unselected or EBV-specific T cells for biopsy-proven EBV+ lymphomas after allogeneic hematopoietic cell transplantation. *Blood.* 119:2644–56.
- Drevot, P., C. Langlet, X.-J. Guo, A.-M. Bernard, O. Colard, J.-P. Chauvin, R. Lasserre, and H.-T. He. 2002. TCR signal initiation machinery is pre-assembled and activated in a subset of membrane rafts. *EMBO J.* 21:1899–908.
- Dudley, M.E., C. a Gross, M.M. Langan, M.R. Garcia, R.M. Sherry, J.C. Yang, G.Q. Phan, U.S. Kammula, M.S. Hughes, D.E. Citrin, N.P. Restifo, J.R. Wunderlich, P. a Prieto, J.J. Hong, R.C. Langan, D. a Zlott, K.E. Morton, D.E. White, C.M. Laurencot, and S. a Rosenberg. 2010. CD8+ enriched “young” tumor infiltrating lymphocytes can mediate regression of metastatic melanoma. *Clin. Cancer Res.* 16:6122–31.

- Dudley, M.E., J.C. Yang, R. Sherry, M.S. Hughes, R. Royal, U. Kammula, P.F. Robbins, J. Huang, D.E. Citrin, S.F. Leitman, J. Wunderlich, N.P. Restifo, A. Thomasian, S.G. Downey, F.O. Smith, J. Klapper, K. Morton, C. Laurencot, D.E. White, and S. a Rosenberg. 2008. Adoptive cell therapy for patients with metastatic melanoma: evaluation of intensive myeloablative chemoradiation preparative regimens. *J. Clin. Oncol.* 26:5233–9.
- Dziegielewska, K.M., J. Ek, M.D. Habgood, and N.R. Saunders. 2001. Development of the choroid plexus. *Microsc. Res. Tech.* 52:5–20.
- Egerton, M., R. Scollay, and K. Shortman. 1990. Kinetics of mature T-cell development in the thymus. *Proc. Natl. Acad. Sci. U. S. A.* 87:2579–82.
- Engelhardt, B. 2006. Molecular mechanisms involved in T cell migration across the blood-brain barrier. *J. Neural Transm.* 113:477–85.
- Engelhardt, B. 2008. Immune cell entry into the central nervous system: involvement of adhesion molecules and chemokines. *J. Neurol. Sci.* 274:23–6.
- Engelhardt, B., and R.M. Ransohoff. 2005. The ins and outs of T-lymphocyte trafficking to the CNS: anatomical sites and molecular mechanisms. *Trends Immunol.* 26:485–95.
- Engels, B., H. Cam, T. Schüler, S. Indraccolo, M. Gladow, C. Baum, T. Blankenstein, and W. Uckert. 2003. Retroviral vectors for high-level transgene expression in T lymphocytes. *Hum. Gene Ther.* 14:1155–68.
- Erich, P. 1885. Das Sauerstoff-Bedürfniss des Organismus : eine farbenanalytische Studie. *Verlag von August Hirschwald.*
- Eriksson, K.K., L. Cervantes-Barragán, B. Ludewig, and V. Thiel. 2008. Mouse hepatitis virus liver pathology is dependent on ADP-ribose-1"-phosphatase, a viral function conserved in the alpha-like supergroup. *J. Virol.* 82:12325–34.
- Farina, C., F. Aloisi, and E. Meinl. 2007. Astrocytes are active players in cerebral innate immunity. *Trends Immunol.* 28:138–45.
- Faure, S., L.I. Salazar-Fontana, M. Semichon, V.L.J. Tybulewicz, G. Bismuth, A. Trautmann, R.N. Germain, and J. Delon. 2004. ERM proteins regulate cytoskeleton relaxation promoting T cell-APC conjugation. *Nat. Immunol.* 5:272–9..
- De Felipe, P., V. Martín, M.L. Cortés, M. Ryan, and M. Izquierdo. 1999. Use of the 2A sequence from foot-and-mouth disease virus in the generation of retroviral vectors for gene therapy. *Gene Ther.* 6:198–208.
- Feuchtinger, T., S. Matthes-Martin, C. Richard, T. Lion, M. Fuhrer, K. Hamprecht, R. Handgretinger, C. Peters, F.R. Schuster, R. Beck, M. Schumm, R. Lotfi, G. Jahn, and P. Lang. 2006. Safe adoptive transfer of virus-specific T-cell immunity for the treatment of systemic adenovirus infection after allogeneic stem cell transplantation. *Br. J. Haematol.* 134:64–76.
- Finkel, T.H., P. Marrack, J.W. Kappler, R.T. Kubo, and J.C. Cambier. 1989. Alpha beta T cell receptor and CD3 transduce different signals in immature T cells. Implications for selection and tolerance. *J. Immunol.* 142:3006–12.
- Flicek, P., M.R. Amodé, D. Barrell, K. Beal, K. Billis, S. Brent, D. Carvalho-Silva, P. Clapham, G. Coates, S. Fitzgerald, L. Gil, C.G. Girón, L. Gordon, T. Hourlier, S. Hunt, N. Johnson, T. Juettemann, A.K. Kähäri, S. Keenan, E. Kulesha, F.J. Martin, T. Maurel, W.M. McLaren, D.N. Murphy, R. Nag, B. Overduin, M. Pignatelli, B. Pritchard, E. Pritchard, H.S. Riat, M. Ruffier, D. Sheppard, K. Taylor, A. Thormann, S.J. Trevanion, A. Vullo, S.P. Wilder, M. Wilson, A. Zadissa, B.L. Aken, E. Birney, F. Cunningham, J. Harrow, J. Herrero, T.J.P. Hubbard, R. Kinsella, M. Muffato, A. Parker, G. Spudich, A. Yates, D.R. Zerbino, and S.M.J. Searle. 2014. Ensembl 2014. *Nucleic Acids Res.* 42:D749–55.
- Förster, R., A.C. Davalos-Misslitz, and A. Rot. 2008. CCR7 and its ligands: balancing immunity and tolerance. *Nat. Rev. Immunol.* 8:362–71.
- Förster, R., a Schubel, D. Breitfeld, E. Kremmer, I. Renner-Müller, E. Wolf, and M. Lipp. 1999. CCR7 coordinates the primary immune response by establishing functional microenvironments in secondary lymphoid organs. *Cell.* 99:23–33.

- Fröhlich, A., J. Kisielow, I. Schmitz, S. Freigang, A.T. Shamshiev, J. Weber, B.J. Marsland, A. Oxenius, and M. Kopf. 2009. IL-21R on T cells is critical for sustained functionality and control of chronic viral infection. *Science*. 324:1576–80.
- Fugmann, S.D., a I. Lee, P.E. Shockett, I.J. Villey, and D.G. Schatz. 2000. The RAG proteins and V(D)J recombination: complexes, ends, and transposition. *Annu. Rev. Immunol.* 18:495–527.
- Fujio, K., Y. Misaki, K. Setoguchi, S. Morita, K. Kawahata, I. Kato, T. Nosaka, K. Yamamoto, and T. Kitamura. 2000. Functional Reconstitution of Class II MHC-Restricted T Cell Immunity Mediated by Retroviral Transfer of the TCR Complex. *J. Immunol.* 165:528–532.
- Galea, I., I. Bechmann, and V.H. Perry. 2007. What is immune privilege (not)? *Trends Immunol.* 28:12–8.
- Gallagher, T.M., and M.J. Buchmeier. 2001. Coronavirus spike proteins in viral entry and pathogenesis. *Virology*. 279:371–4.
- Ge, S., L. Song, and J.S. Pachter. 2005. Where is the blood-brain barrier ... really? *J. Neurosci. Res.* 79:421–7.
- Gerlach, C., J.W.J. van Heijst, E. Swart, D. Sie, N. Armstrong, R.M. Kerkhoven, D. Zehn, M.J. Bevan, K. Schepers, and T.N.M. Schumacher. 2010. One naive T cell, multiple fates in CD8+ T cell differentiation. *J. Exp. Med.* 207:1235–46.
- Gil-Cruz, C., C. Perez-Shibayama, S. Firner, A. Waisman, I. Bechmann, V. Thiel, L. Cervantes-Barragan, and B. Ludewig. 2012. T helper cell- and CD40-dependent germline IgM prevents chronic virus-induced demyelinating disease. *Proc. Natl. Acad. Sci. U. S. A.* 109:1233–8.
- Giunti, D., G. Borsellino, R. Benelli, M. Marchese, E. Capello, M.T. Valle, E. Pedemonte, D. Noonan, A. Albin, G. Bernardi, G.L. Mancardi, L. Battistini, and A. Uccelli. 2003. Phenotypic and functional analysis of T cells homing into the CSF of subjects with inflammatory diseases of the CNS. *J. Leukoc. Biol.* 73:584–90.
- Goldrath, a W., and M.J. Bevan. 1999. Selecting and maintaining a diverse T-cell repertoire. *Nature*. 402:255–62.
- González, J.M., C.C. Bergmann, C. Ramakrishna, D.R. Hinton, R. Atkinson, J. Hoskin, W.B. Macklin, and S. a. Stohlman. 2006. Inhibition of Interferon- $\gamma$  Signaling in Oligodendroglia Delays Coronavirus Clearance without Altering Demyelination. *Am. J. Pathol.* 168:796–804.
- Goverman, J., a Woods, L. Larson, L.P. Weiner, L. Hood, and D.M. Zaller. 1993. Transgenic mice that express a myelin basic protein-specific T cell receptor develop spontaneous autoimmunity. *Cell*. 72:551–60.
- Grakoui, a. 1999. The Immunological Synapse: A Molecular Machine Controlling T Cell Activation. *Science (80- )*. 285:221–227.
- Greter, M., F.L. Heppner, M.P. Lemos, B.M. Odermatt, N. Goebels, T. Laufer, R.J. Noelle, and B. Becher. 2005. Dendritic cells permit immune invasion of the CNS in an animal model of multiple sclerosis. *Nat. Med.* 11:328–34.
- Grueter, B., M. Petter, T. Egawa, K. Laule-Kilian, C.J. Aldrian, a. Wuerch, Y. Ludwig, H. Fukuyama, H. Wardemann, R. Waldschuetz, T. Moroy, I. Taniuchi, V. Steimle, D.R. Littman, and M. Ehlers. 2005. Runx3 Regulates Integrin E/CD103 and CD4 Expression during Development of CD4-/CD8+ T Cells. *J. Immunol.* 175:1694–1705.
- La Gruta, N.L., S.J. Turner, and P.C. Doherty. 2004. Hierarchies in Cytokine Expression Profiles for Acute and Resolving Influenza Virus-Specific CD8+ T Cell Responses: Correlation of Cytokine Profile and TCR Avidity. *J. Immunol.* 172:5553–5560.
- Lewandowski, M. Zur Lehre von der Cerebrospinalflüssigkeit. [On the cerebrospinal fluid.], Z. Klein Forsch., 40 (1900), pp. 480–494
- Goldmann, E. Vitalfärbungen am Zentralnervensystem. Beitrag zur Physio-Pathologie des Plexus Choroideus und der Hirnhäute. [Intravital labelling of the central nervous system. A study on the pathophysiology of the choroid plexus and the

- meninges.] Abhandlungen der königlich preußischen Akademie der Wissenschaften Physikalisch-Mathematische Classe, (1913)
- Guidotti, L.G., B. Matzke, H. Schaller, and F. V Chisari. 1995. High-level hepatitis B virus replication in transgenic mice. *J. Virol.* 69:6158–69.
- Gunn, M.D., S. Kyuwa, C. Tam, T. Kakiuchi, A. Matsuzawa, L.T. Williams, and H. Nakano. 1999. Mice lacking expression of secondary lymphoid organ chemokine have defects in lymphocyte homing and dendritic cell localization. *J. Exp. Med.* 189:451–60.
- Gunn, M.D., K. Tangemann, C. Tam, J.G. Cyster, S.D. Rosen, and L.T. Williams. 1998. A chemokine expressed in lymphoid high endothelial venules promotes the adhesion and chemotaxis of naive T lymphocytes. *Proc. Natl. Acad. Sci. U. S. A.* 95:258–63.
- Haario, H., M. Laine, A. Mira, and E. Saksman. 2006. DRAM: Efficient adaptive MCMC. *Stat. Comput.* 16:339–354.
- Hacein-Bey-Abina, S., C. Von Kalle, M. Schmidt, M.P. McCormack, N. Wulfraat, P. Leboulch, a Lim, C.S. Osborne, R. Pawliuk, E. Morillon, R. Sorensen, a Forster, P. Fraser, J.I. Cohen, G. de Saint Basile, I. Alexander, U. Wintergerst, T. Frebourg, a Aurias, D. Stoppa-Lyonnet, S. Romana, I. Radford-Weiss, F. Gross, F. Valensi, E. Delabesse, E. Macintyre, F. Sigaux, J. Soulier, L.E. Leiva, M. Wissler, C. Prinz, T.H. Rabbitts, F. Le Deist, a Fischer, and M. Cavazzana-Calvo. 2003. LMO2-associated clonal T cell proliferation in two patients after gene therapy for SCID-X1. *Science.* 302:415–9.
- Harder, T., and K.R. Engelhardt. 2004. Membrane domains in lymphocytes - from lipid rafts to protein scaffolds. *Traffic.* 5:265–75.
- He, X., X. He, V.P. Dave, Y. Zhang, X. Hua, E. Nicolas, W. Xu, B. a Roe, and D.J. Kappes. 2005. The zinc finger transcription factor Th-POK regulates CD4 versus CD8 T-cell lineage commitment. *Nature.* 433:826–33.
- Hebeisen, M., L. Baitsch, D. Presotto, P. Baumgaertner, P. Romero, O. Michielin, D.E. Speiser, and N. Rufer. 2013. SHP-1 phosphatase activity counteracts increased T cell receptor affinity. 123.
- Hernandez-Lopez, C. 2002. Stromal cell-derived factor 1/CXCR4 signaling is critical for early human T-cell development. *Blood.* 99:546–554.
- Hesse, M.D., A.Y. Karulin, B.O. Boehm, P. V Lehmann, and M. Tary-Lehmann. 2001. A T cell clone's avidity is a function of its activation state. *J. Immunol.* 167:1353–61.
- Hill, G.J., T.E. Shine, H.Z. Hill, and C. Miller. 1976. Failure of amygdalin to arrest B16 melanoma and BW5147 AKR leukemia. *Cancer Res.* 36:2102–7.
- Holst, J., A.L. Szymczak-Workman, K.M. Vignali, A.R. Burton, C.J. Workman, and D. a a Vignali. 2006. Generation of T-cell receptor retrogenic mice. *Nat. Protoc.* 1:406–17.
- Huseby, E.S., D. Liggitt, T. Brabb, B. Schnabel, C. Ohlén, and J. Goverman. 2001. A pathogenic role for myelin-specific CD8(+) T cells in a model for multiple sclerosis. *J. Exp. Med.* 194:669–76.
- Ichimura, T., P. a Fraser, and H.F. Cserr. 1991. Distribution of extracellular tracers in perivascular spaces of the rat brain. *Brain Res.* 545:103–13.
- Itano, B.A., P. Salmon, D. Kioussis, M. Tolaini, P. Corbella, and E. Robey. 1996. The Cytoplasmic Domain of CD4 Promotes the Development of CD4 Lineage T Cells By Andrea Itano, Patrick Salmon, Dimitris Kioussis,\* Mauro Tolaini,\* Paola Corbella,\* and Ellen Robey. 183.
- Janeway, C. a, and R. Medzhitov. 2002. Innate immune recognition. *Annu. Rev. Immunol.* 20:197–216.
- Johnson, L. a, R. a Morgan, M.E. Dudley, L. Cassard, J.C. Yang, M.S. Hughes, U.S. Kammula, R.E. Royal, R.M. Sherry, J.R. Wunderlich, C.-C.R. Lee, N.P. Restifo, S.L. Schwarz, A.P. Cogdill, R.J. Bishop, H. Kim, C.C. Brewer, S.F. Rudy, C. VanWaes, J.L. Davis, A. Mathur, R.T. Ripley, D. a Nathan, C.M. Laurencot, and S. a Rosenberg. 2009a. Gene therapy with human and mouse T-cell receptors mediates cancer regression and targets normal tissues expressing cognate antigen. *Blood.* 114:535–46.

- Johnson, L. a, R. a Morgan, M.E. Dudley, L. Cassard, J.C. Yang, M.S. Hughes, U.S. Kammula, R.E. Royal, R.M. Sherry, J.R. Wunderlich, C.-C.R. Lee, N.P. Restifo, S.L. Schwarz, A.P. Cogdill, R.J. Bishop, H. Kim, C.C. Brewer, S.F. Rudy, C. VanWaes, J.L. Davis, A. Mathur, R.T. Ripley, D. a Nathan, C.M. Laurencot, and S. a Rosenberg. 2009b. Gene therapy with human and mouse T-cell receptors mediates cancer regression and targets normal tissues expressing cognate antigen. *Blood*. 114:535–46.
- Johnson, L. a., B. Heemskerk, D.J. Powell, C.J. Cohen, R. a. Morgan, M.E. Dudley, P.F. Robbins, and S. a. Rosenberg. 2006. Gene Transfer of Tumor-Reactive TCR Confers Both High Avidity and Tumor Reactivity to Nonreactive Peripheral Blood Mononuclear Cells and Tumor-Infiltrating Lymphocytes. *J. Immunol*. 177:6548–6559.
- Joly, E., L. Mucke, and M.B. Oldstone. 1991. Viral persistence in neurons explained by lack of major histocompatibility class I expression. *Science*. 253:1283–5.
- Joly, E., and M.B. Oldstone. 1992. Neuronal cells are deficient in loading peptides onto MHC class I molecules. *Neuron*. 8:1185–90.
- June, C.H. 2007. Science in medicine Adoptive T cell therapy for cancer in the clinic. 117.
- Junt, T., E. Scandella, R. Forster, P. Krebs, S. Krautwald, M. Lipp, H. Hengartner, and B. Ludewig. 2004. Impact of CCR7 on Priming and Distribution of Antiviral Effector and Memory CTL. *J. Immunol*. 173:6684–6693.
- Junt, T., E. Scandella, and B. Ludewig. 2008. Form follows function: lymphoid tissue microarchitecture in antimicrobial immune defence. *Nat. Rev. Immunol*. 8:764–75.
- Kaech, S.M., S. Hemby, E. Kersh, and R. Ahmed. 2002. Molecular and functional profiling of memory CD8 T cell differentiation. *Cell*. 111:837–51.
- Kalia, V., S. Sarkar, S. Subramaniam, W.N. Haining, K. a Smith, and R. Ahmed. 2010. Prolonged interleukin-2 $\alpha$  expression on virus-specific CD8<sup>+</sup> T cells favors terminal-effector differentiation in vivo. *Immunity*. 32:91–103.
- Kang, S.S., J. Herz, J. V Kim, D. Nayak, P. Stewart-Hutchinson, M.L. Dustin, and D.B. McGavern. 2011. Migration of cytotoxic lymphocytes in cell cycle permits local MHC I-dependent control of division at sites of viral infection. *J. Exp. Med*. 208:747–59.
- Kennedy-Nasser, A. a, C.M. Bollard, and H.E. Heslop. 2009. Immunotherapy for epstein-barr virus-related lymphomas. *Mediterr. J. Hematol. Infect. Dis*. 1:e2009010.
- Kerfoot, S.M., and P. Kubes. 2002. Overlapping Roles of P-Selectin and  $\alpha$ 4 Integrin to Recruit Leukocytes to the Central Nervous System in Experimental Autoimmune Encephalomyelitis. *J. Immunol*. 169:1000–1006.
- Kessels, H.W., M.C. Wolkers, M.D. van den Boom, M.A. van der Valk, and T.N. Schumacher. 2001. Immunotherapy through TCR gene transfer. *Nat. Immunol*. 2:957–61.
- Kieback, E., and W. Uckert. 2010. Enhanced T cell receptor gene therapy for cancer. *Expert Opin. Biol. Ther*. 10:749–62.
- Kilgore, N.E., J.D. Carter, U. Lorenz, and B.D. Evavold. 2003. Cutting Edge: Dependence of TCR Antagonism on Src Homology 2 Domain-Containing Protein Tyrosine Phosphatase Activity. *J. Immunol*. 170:4891–4895.
- Killestein, J., M.J. Eikelenboom, T. Izeboud, N.F. Kalkers, H.J. Adèr, F. Barkhof, R. a. W. Van Lier, B.M.J. Uitdehaag, and C.H. Polman. 2003. Cytokine producing CD8<sup>+</sup> T cells are correlated to MRI features of tissue destruction in MS. *J. Neuroimmunol*. 142:141–148.
- Kim, J. V, S.S. Kang, M.L. Dustin, and D.B. McGavern. 2009. Myelomonocytic cell recruitment causes fatal CNS vascular injury during acute viral meningitis. *Nature*. 457:191–5.
- King, C.G., S. Koehli, B. Hausmann, M. Schmalzer, D. Zehn, and E. Palmer. 2012. T cell affinity regulates asymmetric division, effector cell differentiation, and tissue pathology. *Immunity*. 37:709–20.

- Kirak, O., E.-M. Frickel, G.M. Grotenbreg, H. Suh, R. Jaenisch, and H.L. Ploegh. 2010. Transnuclear mice with predefined T cell receptor specificities against *Toxoplasma gondii* obtained via SCNT. *Science*. 328:243–8.
- Kisielow, P., H.S. Teh, H. Blüthmann, and H. von Boehmer. 1988. Positive selection of antigen-specific T cells in thymus by restricting MHC molecules. *Nature*. 335:730–3.
- Kivisäkk, P., D.J. Mahad, M.K. Callahan, K. Sikora, C. Trebst, B. Tucky, J. Wujek, R. Ravid, S.M. Staugaitis, H. Lassmann, and R.M. Ransohoff. 2004. Expression of CCR7 in multiple sclerosis: implications for CNS immunity. *Ann. Neurol.* 55:627–38.
- Klein, L., M. Hinterberger, G. Wirnsberger, and B. Kyewski. 2009. Antigen presentation in the thymus for positive selection and central tolerance induction. *Nat. Rev. Immunol.* 9:833–44.
- Klump, H., B. Schiedlmeier, B. Vogt, M. Ryan, W. Ostertag, and C. Baum. 2001. Retroviral vector-mediated expression of HoxB4 in hematopoietic cells using a novel coexpression strategy. *Gene Ther.* 8:811–7.
- Kolumam, G. a, S. Thomas, L.J. Thompson, J. Sprent, and K. Murali-Krishna. 2005. Type I interferons act directly on CD8 T cells to allow clonal expansion and memory formation in response to viral infection. *J. Exp. Med.* 202:637–50.
- Komori, T., a Okada, V. Stewart, and F.W. Alt. 1993. Lack of N regions in antigen receptor variable region genes of TdT-deficient lymphocytes. *Science*. 261:1171–5.
- Kouskoff, V., K. Signorelli, C. Benoist, and D. Mathis. 1995. Cassette vectors directing expression of T cell receptor genes in transgenic mice. *J. Immunol. Methods*. 180:273–80.
- Krumbholz, M., D. Theil, F. Steinmeyer, S. Cepok, B. Hemmer, and M. Hofbauer. 2007. CCL19 is constitutively expressed in the CNS , up-regulated in neuroinflammation , active and also inactive multiple sclerosis lesions. 190:72–79.
- Ksiazek, T.G., D. Erdman, C.S. Goldsmith, S.R. Zaki, T. Peret, S. Emery, S. Tong, C. Urbani, J.A. Comer, W. Lim, P.E. Rollin, S.F. Dowell, A. Ling, C.D. Humphrey, W.-J. Shieh, J. Guarner, C.D. Paddock, P. Rota, B. Fields, J. DeRisi, J. Yang, N. Cox, J.M. Hughes, J.W. LeDuc, W.J. Bellini, and L.J. Anderson. 2003. A novel coronavirus associated with severe acute respiratory syndrome. *N. Engl. J. Med.* 348:1953–66.
- Kuerten, S., A. Schickel, C. Kerkloh, M.S. Recks, K. Addicks, N.H. Ruddle, and P. V Lehmann. 2012. Tertiary lymphoid organ development coincides with determinant spreading of the myelin-specific T cell response. *Acta Neuropathol.* 124:861–73.
- Kuhns, M.S., and M.M. Davis. 2008. The safety on the TCR trigger. *Cell*. 135:594–6.
- Kuhns, M.S., M.M. Davis, and K.C. Garcia. 2006. Deconstructing the form and function of the TCR/CD3 complex. *Immunity*. 24:133–9.
- Kunert, A., T. Straetemans, C. Govers, C. Lamers, R. Mathijssen, S. Sleijfer, and R. Debets. 2013. TCR-Engineered T Cells Meet New Challenges to Treat Solid Tumors: Choice of Antigen, T Cell Fitness, and Sensitization of Tumor Milieu. *Front. Immunol.* 4:363.
- Kursar, M., U.E. Höpken, M. Koch, A. Köhler, M. Lipp, S.H.E. Kaufmann, and H.-W. Mittrücker. 2005. Differential requirements for the chemokine receptor CCR7 in T cell activation during *Listeria monocytogenes* infection. *J. Exp. Med.* 201:1447–57.
- Kurts, C., M. Cannarile, I. Klebba, and T. Brocker. 2001. Cutting Edge: Dendritic Cells Are Sufficient to Cross-Present Self-Antigens to CD8 T Cells In Vivo. *J. Immunol.* 166:1439–1442.
- Kwidzinski, E., J. Bunse, O. Aktas, D. Richter, L. Mutlu, F. Zipp, R. Nitsch, and I. Bechmann. 2005. Indolamine 2,3-dioxygenase is expressed in the CNS and down-regulates autoimmune inflammation. *FASEB J.* 19:1347–9..
- Kyewski, B., and J. Derbinski. 2004. Self-representation in the thymus: an extended view. *Nat. Rev. Immunol.* 4:688–98.

- Labrecque, N., L.S. Whitfield, R. Obst, C. Waltzinger, C. Benoist, and D. Mathis. 2001. How much TCR does a T cell need? *Immunity*. 15:71–82.
- Lafaille, J.J. 2004. T-cell receptor transgenic mice in the study of autoimmune diseases. *J. Autoimmun.* 22:95–106.
- Lane, T.E., and M.P. Hosking. 2010. The pathogenesis of murine coronavirus infection of the central nervous system. *Crit. Rev. Immunol.* 30:119–30.
- Lee, D.T.S., Y.K. Wing, H.C.M. Leung, J.J.Y. Sung, Y.K. Ng, G.C. Yiu, R.Y.L. Chen, and H.F.K. Chiu. 2004. Factors associated with psychosis among patients with severe acute respiratory syndrome: a case-control study. *Clin. Infect. Dis.* 39:1247–9.
- Leen, A.M., C.M. Bollard, A.M. Mendizabal, E.J. Shpall, P. Szabolcs, J.H. Antin, N. Kapoor, S.-Y. Pai, S.D. Rowley, P. Kebriaei, B.R. Dey, B.J. Grilley, A.P. Gee, M.K. Brenner, C.M. Rooney, and H.E. Heslop. 2013. Multicenter study of banked third-party virus-specific T cells to treat severe viral infections after hematopoietic stem cell transplantation. *Blood*. 121:5113–23.
- Leen, A.M., G.D. Myers, U. Sili, M.H. Huls, H. Weiss, K.S. Leung, G. Carrum, R. a Krance, C.-C. Chang, J.J. Molldrem, A.P. Gee, M.K. Brenner, H.E. Heslop, C.M. Rooney, and C.M. Bollard. 2006. Monoculture-derived T lymphocytes specific for multiple viruses expand and produce clinically relevant effects in immunocompromised individuals. *Nat. Med.* 12:1160–6.
- Letourneur, F., and B. Malissen. 1989. Derivation of a T cell hybridoma variant deprived of functional T cell receptor alpha and beta chain transcripts reveals a nonfunctional alpha-mRNA of BW5147 origin. *Eur. J. Immunol.* 19:2269–74.
- Leung, R.K., K. Thomson, a Gallimore, E. Jones, M. Van den Broek, S. Sierro, a R. Alsheikhly, a McMichael, and a Rahemtulla. 2001. Deletion of the CD4 silencer element supports a stochastic mechanism of thymocyte lineage commitment. *Nat. Immunol.* 2:1167–73.
- Lin, M.T., S.A. Stohlman, and D.R. Hinton. 1997. Mouse hepatitis virus is cleared from the central nervous systems of mice lacking perforin-mediated cytolysis. *J. Virol.* 71:383–91.
- Lind, E.F., S.E. Prockop, H.E. Porritt, and H.T. Petrie. 2001. Mapping precursor movement through the postnatal thymus reveals specific microenvironments supporting defined stages of early lymphoid development. *J. Exp. Med.* 194:127–34.
- Linette, G.P., E. a Stadtmauer, M. V Maus, A.P. Rapoport, B.L. Levine, L. Emery, L. Litzky, A. Bagg, B.M. Carreno, P.J. Cimino, G.K. Binder-Scholl, D.P. Smethurst, A.B. Gerry, N.J. Pumphrey, A.D. Bennett, J.E. Brewer, J. Dukes, J. Harper, H.K. Tayton-Martin, B.K. Jakobsen, N.J. Hassan, M. Kalos, and C.H. June. 2013. Cardiovascular toxicity and titin cross-reactivity of affinity-enhanced T cells in myeloma and melanoma. *Blood*. 122:863–71.
- Link, A., T.K. Vogt, S. Favre, M.R. Britschgi, H. Acha-Orbea, B. Hinz, J.G. Cyster, and S. a Luther. 2007. Fibroblastic reticular cells in lymph nodes regulate the homeostasis of naive T cells. *Nat. Immunol.* 8:1255–65.
- Linnemann, C., B. Heemskerk, P. Kvistborg, R.J.C. Kluin, D. a Bolotin, X. Chen, K. Bresser, M. Nieuwland, R. Schotte, S. Michels, R. Gomez-Eerland, L. Jahn, P. Hombrink, N. Legrand, C.J. Shu, I.Z. Mamedov, A. Velds, C.U. Blank, J.B. a G. Haanen, M. a Turchaninova, R.M. Kerkhoven, H. Spits, S.R. Hadrup, M.H.M. Heemskerk, T. Blankenstein, D.M. Chudakov, G.M. Bendle, and T.N.M. Schumacher. 2013. High-throughput identification of antigen-specific TCRs by TCR gene capture. *Nat. Med.* 19:1534–41.
- Linnemann, C., T.N.M. Schumacher, and G.M. Bendle. 2011. T-cell receptor gene therapy: critical parameters for clinical success. *J. Invest. Dermatol.* 131:1806–16.
- Liu, C., T. Ueno, S. Kuse, F. Saito, T. Nitta, L. Piali, H. Nakano, T. Kakiuchi, M. Lipp, G. a Hollander, and Y. Takahama. 2005. The role of CCL21 in recruitment of T-precursor cells to fetal thymi. *Blood*. 105:31–9.



- Liu, M.T., H.S. Keirstead, and T.E. Lane. 2001. Neutralization of the Chemokine CXCL10 Reduces Inflammatory Cell Invasion and Demyelination and Improves Neurological Function in a Viral Model of Multiple Sclerosis. *J. Immunol.* 167:4091–4097.
- Liu, X., P. Nguyen, W. Liu, C. Cheng, M. Steeves, J.C. Obenauer, J. Ma, and T.L. Geiger. 2009. T cell receptor CDR3 sequence but not recognition characteristics distinguish autoreactive effector and Foxp3(+) regulatory T cells. *Immunity.* 31:909–20.
- Liu, Y., I. Teige, B. Birnir, and S. Issazadeh-Navikas. 2006. Neuron-mediated generation of regulatory T cells from encephalitogenic T cells suppresses EAE. *Nat. Med.* 12:518–25.
- Lo, J.C., R.K. Chin, Y. Lee, H. Kang, Y. Wang, J. V Weinstock, T. Banks, C.F. Ware, G. Franzoso, and Y. Fu. 2003. Differential regulation of CCL21 in lymphoid/nonlymphoid tissues for effectively attracting T cells to peripheral tissues. *J. Clin. Invest.* 112:1495–505.
- Love, P.E., J. Lee, and E.W. Shores. 2000. Critical Relationship Between TCR Signaling Potential and TCR Affinity During Thymocyte Selection. *J. Immunol.* 165:3080–3087.
- Luzyanina, T., J. Cupovic, B. Ludewig, and G. Bocharov. 2013. Mathematical models for CFSE labelled lymphocyte dynamics: asymmetry and time-lag in division. *J. Math. Biol.*
- Magnus, T., B. Schreiner, T. Korn, C. Jack, H. Guo, J. Antel, I. Ifergan, L. Chen, F. Bischof, A. Bar-Or, and H. Wiendl. 2005. Microglial expression of the B7 family member B7 homolog 1 confers strong immune inhibition: implications for immune responses and autoimmunity in the CNS. *J. Neurosci.* 25:2537–46.
- Marinkovic, T., A. Garin, Y. Yokota, Y. Fu, N.H. Ruddle, G.C. Furtado, and S.A. Lira. 2006. Interaction of mature CD3+CD4+ T cells with dendritic cells triggers the development of tertiary lymphoid structures in the thyroid. *J. Clin. Invest.* 116:2622–32.
- Matloubian, M., R.J. Concepcion, and R. Ahmed. 1994. CD4+ T cells are required to sustain CD8+ cytotoxic T-cell responses during chronic viral infection. *J. Virol.* 68:8056–63.
- Matloubian, M., C.G. Lo, G. Cinamon, M.J. Lesneski, Y. Xu, V. Brinkmann, M.L. Allende, R.L. Proia, and J.G. Cyster. 2004. Lymphocyte egress from thymus and peripheral lymphoid organs is dependent on S1P receptor 1. *Nature.* 427:355–60.
- Matthews, a. E., S.R. Weiss, M.J. Shlomchik, L.G. Hannum, J.L. Gombold, and Y. Paterson. 2001. Antibody Is Required for Clearance of Infectious Murine Hepatitis Virus A59 from the Central Nervous System, But Not the Liver. *J. Immunol.* 167:5254–5263.
- McGavern, D.B., and S.S. Kang. 2011. Illuminating viral infections in the nervous system. *Nat. Rev. Immunol.* 11:318–29.
- McGavern, D.B., and P. Truong. 2004. Rebuilding an Immune-Mediated Central Nervous System Disease: Weighing the Pathogenicity of Antigen-Specific versus Bystander T Cells. *J. Immunol.* 173:4779–4790.
- McIntosh, K., W.B. Becker, and R.M. Chanock. 1967. Growth in suckling-mouse brain of “IBV-like” viruses from patients with upper respiratory tract disease. *Proc. Natl. Acad. Sci. U. S. A.* 58:2268–73.
- McKeithan, T.W. 1995. Kinetic proofreading in T-cell receptor signal transduction. *Proc. Natl. Acad. Sci. U. S. A.* 92:5042–6.
- Medawar, P.B. 1948. Tests by tissue culture methods on the nature of immunity to transplanted skin. *Q. J. Microsc. Sci.* 89:239–52.
- Medzhitov, R., and C. a Janeway. 1998. Innate immune recognition and control of adaptive immune responses. *Semin. Immunol.* 10:351–3.
- Mempel, T.R., T. Junt, and U.H. von Andrian. 2006. Rulers over randomness: stroma cells guide lymphocyte migration in lymph nodes. *Immunity.* 25:867–9.
- Van der Merwe, P.A., and O. Dushek. 2011. Mechanisms for T cell receptor triggering. *Nat. Rev. Immunol.* 11:47–55.

- Michalek, R.D., and J.C. Rathmell. 2010. The metabolic life and times of a T-cell. *Immunol. Rev.* 236:190–202.
- Mitsuyasu, R.T., P.A. Anton, S.G. Deeks, D.T. Scadden, E. Connick, M.T. Downs, A. Bakker, M.R. Roberts, C.H. June, S. Jalali, A.A. Lin, R. Pennathur-das, and K.M. Hege. 2000. Plenary paper Prolonged survival and tissue trafficking following adoptive transfer of CD4 gene-modified autologous CD4  $\alpha$  and CD8  $\alpha$  T cells in human immunodeficiency virus – infected subjects. *Blood*. 96:785–793.
- Morgan, R. a, M.E. Dudley, J.R. Wunderlich, M.S. Hughes, J.C. Yang, R.M. Sherry, R.E. Royal, S.L. Topalian, U.S. Kammula, N.P. Restifo, Z. Zheng, A. Nahvi, C.R. de Vries, L.J. Rogers-Freezer, S. a Mavroukakis, and S. a Rosenberg. 2006a. Cancer regression in patients after transfer of genetically engineered lymphocytes. *Science*. 314:126–9.
- Morgan, R. a., M.E. Dudley, Y.Y.L. Yu, Z. Zheng, P.F. Robbins, M.R. Theoret, J.R. Wunderlich, M.S. Hughes, N.P. Restifo, and S. a. Rosenberg. 2003. High Efficiency TCR Gene Transfer into Primary Human Lymphocytes Affords Avid Recognition of Melanoma Tumor Antigen Glycoprotein 100 and Does Not Alter the Recognition of Autologous Melanoma Antigens. *J. Immunol.* 171:3287–3295.
- Morgan, R.A., N. Chinnasamy, D. Abate-Daga, A. Gros, P.F. Robbins, Z. Zheng, M.E. Dudley, S.A. Feldman, J.C. Yang, R.M. Sherry, G.Q. Phan, M.S. Hughes, U.S. Kammula, A.D. Miller, C.J. Hessman, A.A. Stewart, N.P. Restifo, M.M. Quezado, M. Alimchandani, A.Z. Rosenberg, A. Nath, T. Wang, B. Bielekova, S.C. Wuest, N. Akula, F.J. McMahon, S. Wilde, B. Mosetter, D.J. Schendel, C.M. Laurencot, and S.A. Rosenberg. 2013. Cancer regression and neurological toxicity following anti-MAGE-A3 TCR gene therapy. *J. Immunother.* 36:133–51.
- Moseman, E.A., and D.B. McGavern. 2013. The great balancing act: regulation and fate of antiviral T-cell interactions. *Immunol. Rev.* 255:110–24.
- Mueller, S.N., W. Heath, J.D. McLain, F.R. Carbone, and C.M. Jones. 2002. Characterization of two TCR transgenic mouse lines specific for herpes simplex virus. *Immunol. Cell Biol.* 80:156–63.
- Mueller, S.N., C.M. Jones, W. Chen, Y. Kawaoka, M.R. Castrucci, W.R. Heath, and F.R. Carbone. 2003. The Early Expression of Glycoprotein B from Herpes Simplex Virus Can Be Detected by Antigen-Specific CD8+ T Cells. *J. Virol.* 77:2445–2451.
- Mueller, S.N., W. a Langley, G. Li, A. García-Sastre, R.J. Webby, and R. Ahmed. 2010. Qualitatively different memory CD8+ T cells are generated after lymphocytic choriomeningitis virus and influenza virus infections. *J. Immunol.* 185:2182–90.
- Müller, A.J., O. Filipe-Santos, G. Eberl, T. Aebischer, G.F. Späth, and P. Bousso. 2012. CD4+ T cells rely on a cytokine gradient to control intracellular pathogens beyond sites of antigen presentation. *Immunity*. 37:147–57.
- Murphy, J.B., and E. Sturm. 1923. Conditions Determining the Transplantability of Tissues in the Brain. *J. Exp. Med.* 38:183–97.
- Nakano, H., and M.D. Gunn. 2001. Gene Duplications at the Chemokine Locus on Mouse Chromosome 4: Multiple Strain-Specific Haplotypes and the Deletion of Secondary Lymphoid-Organ Chemokine and EBI-1 Ligand Chemokine Genes in the plt Mutation. *J. Immunol.* 166:361–369.
- Nauerth, M., B. Weißbrich, R. Knall, T. Franz, G. Dössinger, J. Bet, P.J. Paszkiewicz, L. Pfeifer, M. Bunse, W. Uckert, R. Holtappels, D. Gillert-marien, M. Neuenhahn, A. Krackhardt, and M.J. Reddehase. 2013. TCR-ligand koff rate correlates with the protective capacity of antigen-specific CD8+ T cells for adoptive transfer. *Sci. Transl. Med.* 5:192ra87.
- Nika, K., C. Soldani, M. Salek, W. Paster, A. Gray, R. Etzensperger, L. Fugger, P. Polzella, V. Cerundolo, O. Dushek, T. Höfer, A. Viola, and O. Acuto. 2010. Constitutively active Lck kinase in T cells drives antigen receptor signal transduction. *Immunity*. 32:766–77.
- Noor, S., A.S. Habashy, J.P. Nance, R.T. Clark, K. Nemati, M.J. Carson, and E.H. Wilson. 2010. CCR7-dependent immunity during acute *Toxoplasma gondii* infection. *Infect. Immun.* 78:2257–63.

- Noor, S., and E.H. Wilson. 2012. Role of C-C chemokine receptor type 7 and its ligands during neuroinflammation. *J. Neuroinflammation*. 9:77.
- Olmos, S., S. Stukes, and J.D. Ernst. 2010. Ectopic activation of Mycobacterium tuberculosis-specific CD4<sup>+</sup> T cells in lungs of CCR7<sup>-/-</sup> mice. *J. Immunol*. 184:895–901.
- Osman, G.E., S. Cheunsuk, S.E. Allen, E. Chi, H.D. Liggitt, L.E. Hood, and W.C. Ladiges. 1998. Expression of a type II collagen-specific TCR transgene accelerates the onset of arthritis in mice. *Int. Immunol*. 10:1613–22.
- Ott, M.G., M. Schmidt, K. Schwarzwaelder, S. Stein, U. Siler, U. Koehl, H. Glimm, K. Kühlcke, A. Schilz, H. Kunkel, S. Naundorf, A. Brinkmann, A. Deichmann, M. Fischer, C. Ball, I. Pilz, C. Dunbar, Y. Du, N. a Jenkins, N.G. Copeland, U. Lüthi, M. Hassan, A.J. Thrasher, D. Hoelzer, C. von Kalle, R. Seger, and M. Grez. 2006. Correction of X-linked chronic granulomatous disease by gene therapy, augmented by insertional activation of MDS1-EVI1, PRDM16 or SETBP1. *Nat. Med*. 12:401–9.
- Owen, J.J., and M.A. Ritter. 1969. Tissue interaction in the development of thymus lymphocytes. *J. Exp. Med*. 129:431–42.
- Owens, T., I. Bechmann, and B. Engelhardt. 2008. Perivascular spaces and the two steps to neuroinflammation. *J. Neuropathol. Exp. Neurol*. 67:1113–21.
- Oxenius, a, M.F. Bachmann, R.M. Zinkernagel, and H. Hengartner. 1998. Virus-specific MHC-class II-restricted TCR-transgenic mice: effects on humoral and cellular immune responses after viral infection. *Eur. J. Immunol*. 28:390–400.
- Oxenius, a, R.M. Zinkernagel, and H. Hengartner. 1998. Comparison of activation versus induction of unresponsiveness of virus-specific CD4<sup>+</sup> and CD8<sup>+</sup> T cells upon acute versus persistent viral infection. *Immunity*. 9:449–57.
- Palmer, E., and D. Naeher. 2009. Affinity threshold for thymic selection through a T-cell receptor-co-receptor zipper. *Nat. Rev. Immunol*. 9:207–13.
- Pao, L.I., K. Badour, K. a Siminovitch, and B.G. Neel. 2007. Nonreceptor protein-tyrosine phosphatases in immune cell signaling. *Annu. Rev. Immunol*. 25:473–523.
- Parkhurst, M.R., J.C. Yang, R.C. Langan, M.E. Dudley, D.-A.N. Nathan, S. a Feldman, J.L. Davis, R. a Morgan, M.J. Merino, R.M. Sherry, M.S. Hughes, U.S. Kammula, G.Q. Phan, R.M. Lim, S. a Wank, N.P. Restifo, P.F. Robbins, C.M. Laurencot, and S. a Rosenberg. 2011. T cells targeting carcinoembryonic antigen can mediate regression of metastatic colorectal cancer but induce severe transient colitis. *Mol. Ther*. 19:620–6.
- Parra, B., D.R. Hinton, N.W. Marten, C.C. Bergmann, M.T. Lin, C.S. Yang, and S. a Stohlman. 1999. IFN-gamma is required for viral clearance from central nervous system oligodendroglia. *J. Immunol*. 162:1641–7.
- Pashenkov, M., M. Söderström, and H. Link. 2003. Secondary lymphoid organ chemokines are elevated in the cerebrospinal fluid during central nervous system inflammation. *J. Neuroimmunol*. 135:154–160.
- Patsoukis, N., J. Brown, V. Petkova, F. Liu, L. Li, and V. a Boussiotis. 2012. Selective effects of PD-1 on Akt and Ras pathways regulate molecular components of the cell cycle and inhibit T cell proliferation. *Sci. Signal*. 5:ra46.
- Pearce, E.L., and H. Shen. 2007. Generation of CD8 T Cell Memory Is Regulated by IL-12. *J. Immunol*. 179:2074–2081.
- Pender, M.P., K.B. Nguyen, P. a McCombe, and J.F. Kerr. 1991. Apoptosis in the nervous system in experimental allergic encephalomyelitis. *J. Neurol. Sci*. 104:81–7.
- Perlman, S., G. Evans, and a Afifi. 1990. Effect of olfactory bulb ablation on spread of a neurotropic coronavirus into the mouse brain. *J. Exp. Med*. 172:1127–32.
- Pesic, M., I. Bartholomäus, N.I. Kyratsous, and V. Heissmeyer. 2013. Technical advance 2-photon imaging of phagocyte-mediated T cell activation in the CNS. 123.
- Peterson, E.J., M.L. Woods, S. a Dmowski, G. Derimanov, M.S. Jordan, J.N. Wu, P.S. Myung, Q.H. Liu, J.T. Pribila, B.D. Freedman,

- Y. Shimizu, and G. a Koretzky. 2001. Coupling of the TCR to integrin activation by Slap-130/Fyb. *Science*. 293:2263–5.
- Petrie, H.T., and J.C. Zúñiga-Pflücker. 2007. Zoned out: functional mapping of stromal signaling microenvironments in the thymus. *Annu. Rev. Immunol.* 25:649–79.
- Pewe, L., G.F. Wu, E.M. Barnett, R.F. Castro, and S. Perlman. 1996. Cytotoxic T cell-resistant variants are selected in a virus-induced demyelinating disease. *Immunity*. 5:253–62.
- Pewe, L., S. Xue, and S. Perlman. 1997. Cytotoxic T-cell-resistant variants arise at early times after infection in C57BL/6 but not in SCID mice infected with a neurotropic coronavirus. *J. Virol.* 71:7640–7.
- Piccio, L., B. Rossi, E. Scarpini, C. Laudanna, C. Giagulli, a. C. Issekutz, D. Vestweber, E.C. Butcher, and G. Constantin. 2002. Molecular Mechanisms Involved in Lymphocyte Recruitment in Inflamed Brain Microvessels: Critical Roles for P-Selectin Glycoprotein Ligand-1 and Heterotrimeric Gi-Linked Receptors. *J. Immunol.* 168:1940–1949.
- Pinkoski, M.J., M. Hobman, J. a Heibein, K. Tomaselli, F. Li, P. Seth, C.J. Froelich, and R.C. Bleackley. 1998. Entry and trafficking of granzyme B in target cells during granzyme B-perforin-mediated apoptosis. *Blood*. 92:1044–54.
- Pipkin, M.E., J. a Sacks, F. Cruz-Guilloty, M.G. Lichtenheld, M.J. Bevan, and A. Rao. 2010. Interleukin-2 and inflammation induce distinct transcriptional programs that promote the differentiation of effector cytolytic T cells. *Immunity*. 32:79–90.
- Pöllinger, B., G. Krishnamoorthy, K. Berer, H. Lassmann, M.R. Bösl, R. Dunn, H.S. Domingues, A. Holz, F.C. Kurschus, and H. Wekerle. 2009. Spontaneous relapsing-remitting EAE in the SJL/J mouse: MOG-reactive transgenic T cells recruit endogenous MOG-specific B cells. *J. Exp. Med.* 206:1303–16.
- Pope, C., S.-K. Kim, a. Marzo, K. Williams, J. Jiang, H. Shen, and L. Lefrancois. 2001. Organ-Specific Regulation of the CD8 T Cell Response to *Listeria monocytogenes* Infection. *J. Immunol.* 166:3402–3409.
- Prlic, M., G. Hernandez-Hoyos, and M.J. Bevan. 2006. Duration of the initial TCR stimulus controls the magnitude but not functionality of the CD8+ T cell response. *J. Exp. Med.* 203:2135–43.
- Quah, B.J.C., H.S. Warren, and C.R. Parish. 2007. Monitoring lymphocyte proliferation in vitro and in vivo with the intracellular fluorescent dye carboxyfluorescein diacetate succinimidyl ester. *Nat. Protoc.* 2:2049–56.
- Rahemtulla, A., W.P. Fung-Leung, M.W. Schilham, T.M. Kündig, S.R. Sambhara, A. Narendran, A. Arabian, A. Wakeham, C.J. Paige, and R.M. Zinkernagel. 1991. Normal development and function of CD8+ cells but markedly decreased helper cell activity in mice lacking CD4. *Nature*. 353:180–4.
- Raj, V.S., H. Mou, S.L. Smits, D.H.W. Dekkers, M. a Müller, R. Dijkman, D. Muth, J. a Demmers, A. Zaki, R. a M. Fouchier, V. Thiel, C. Drosten, P.J.M. Rottier, A.D.M.E. Osterhaus, B.J. Bosch, and B.L. Haagmans. 2013. Dipeptidyl peptidase 4 is a functional receptor for the emerging human coronavirus-EMC. *Nature*. 495:251–4.
- Ramakrishna, C., S. a Stohlman, R.D. Atkinson, M.J. Shlomchik, and C.C. Bergmann. 2002. Mechanisms of Central Nervous System Viral Persistence: the Critical Role of Antibody and B Cells. *J. Immunol.* 168:1204–1211.
- Rangel-Moreno, J., J.E. Moyron-Quiroz, L. Hartson, K. Kusser, and T.D. Randall. 2007. Pulmonary expression of CXC chemokine ligand 13, CC chemokine ligand 19, and CC chemokine ligand 21 is essential for local immunity to influenza. *Proc. Natl. Acad. Sci. U. S. A.* 104:10577–82.
- Ransohoff, R.M., and B. Engelhardt. 2012. The anatomical and cellular basis of immune surveillance in the central nervous system. *Nat. Rev. Immunol.* 12:623–35.
- Ransohoff, R.M., P. Kivisäkk, and G. Kidd. 2003. Three or more routes for leukocyte migration into the central nervous system. *Nat. Rev. Immunol.* 3:569–81.
- Reese, T.S., and M.J. Karnovsky. 1967. Fine structural localization of a blood-brain barrier to exogenous peroxidase. *J. Cell Biol.* 34:207–17.

- Reis e Sousa, C. 2006. Dendritic cells in a mature age. *Nat. Rev. Immunol.* 6:476–83.
- Reis e Sousa, C., S. Hieny, T. Scharton-Kersten, D. Jankovic, H. Charest, R.N. Germain, and A. Sher. 1997. In vivo microbial stimulation induces rapid CD40 ligand-independent production of interleukin 12 by dendritic cells and their redistribution to T cell areas. *J. Exp. Med.* 186:1819–29.
- Robbins, P.F., Y.F. Li, M. El-Gamil, Y. Zhao, J. a. Wargo, Z. Zheng, H. Xu, R. a. Morgan, S. a. Feldman, L. a. Johnson, a. D. Bennett, S.M. Dunn, T.M. Mahon, B.K. Jakobsen, and S. a. Rosenberg. 2008. Single and Dual Amino Acid Substitutions in TCR CDRs Can Enhance Antigen-Specific T Cell Functions. *J. Immunol.* 180:6116–6131.
- Robbins, P.F., R. a Morgan, S. a Feldman, J.C. Yang, R.M. Sherry, M.E. Dudley, J.R. Wunderlich, A. V Nahvi, L.J. Helman, C.L. Mackall, U.S. Kammula, M.S. Hughes, N.P. Restifo, M. Raffeld, C.-C.R. Lee, C.L. Levy, Y.F. Li, M. El-Gamil, S.L. Schwarz, C. Laurencot, and S. a Rosenberg. 2011. Tumor regression in patients with metastatic synovial cell sarcoma and melanoma using genetically engineered lymphocytes reactive with NY-ESO-1. *J. Clin. Oncol.* 29:917–24.
- Rosen, S.D. 2004. Ligands for L-selectin: homing, inflammation, and beyond. *Annu. Rev. Immunol.* 22:129–56.
- Rosenberg, S. a. 2008. Cancer Immunotherapy Cricothyroidotomy. 1072–1073.
- Rossi, F.M. V, S.Y. Corbel, J.S. Merzaban, D. a Carlow, K. Gossens, J. Duenas, L. So, L. Yi, and H.J. Ziltener. 2005. Recruitment of adult thymic progenitors is regulated by P-selectin and its ligand PSGL-1. *Nat. Immunol.* 6:626–34.
- Rot, A., and U.H. von Andrian. 2004. Chemokines in innate and adaptive host defense: basic chemokinese grammar for immune cells. *Annu. Rev. Immunol.* 22:891–928.
- Roth, E., and H. Pircher. 2004. IFN- Promotes Fas Ligand- and Perforin-Mediated Liver Cell Destruction by Cytotoxic CD8 T Cells. *J. Immunol.* 172:1588–1594.
- Rothenberg, E. V, J.E. Moore, and M. a Yui. 2008. Launching the T-cell-lineage developmental programme. *Nat. Rev. Immunol.* 8:9–21.
- Rouvier, E., M.F. Luciani, and P. Golstein. 1993. Fas involvement in Ca(2+)-independent T cell-mediated cytotoxicity. *J. Exp. Med.* 177:195–200.
- Rowe, C.L., S.C. Baker, M.J. Nathan, and J.O. Fleming. 1997. Evolution of mouse hepatitis virus: detection and characterization of spike deletion variants during persistent infection. *J. Virol.* 71:2959–69.
- Rudd, C.E., A. Taylor, and H. Schneider. 2009. CD28 and CTLA-4 coreceptor expression and signal transduction. *Immunol. Rev.* 229:12–26.
- San José, E., a Borroto, F. Niedergang, a Alcover, and B. Alarcón. 2000. Triggering the TCR complex causes the downregulation of nonengaged receptors by a signal transduction-dependent mechanism. *Immunity.* 12:161–70.
- Sanderson, N.S.R., M. Puntel, K.M. Kroeger, N.S. Bondale, M. Swerdlow, N. Iranmanesh, H. Yagita, A. Ibrahim, M.G. Castro, and P.R. Lowenstein. 2012. Cytotoxic immunological synapses do not restrict the action of interferon- $\gamma$  to antigenic target cells. *Proc. Natl. Acad. Sci. U. S. A.* 109:7835–40.
- Sato, T., S. Ohno, T. Hayashi, C. Sato, K. Kohu, M. Satake, and S. Habu. 2005. Dual functions of Runx proteins for reactivating CD8 and silencing CD4 at the commitment process into CD8 thymocytes. *Immunity.* 22:317–28.
- Scandella, E., B. Bolinger, E. Lattmann, S. Miller, S. Favre, D.R. Littman, D. Finke, S. a Luther, T. Junt, and B. Ludewig. 2008. Restoration of lymphoid organ integrity through the interaction of lymphoid tissue-inducer cells with stroma of the T cell zone. *Nat. Immunol.* 9:667–75.
- Scandella, E., K. Fink, T. Junt, B.M. Senn, E. Lattmann, R. Forster, H. Hengartner, and B. Ludewig. 2007. Dendritic Cell-Independent B Cell Activation During Acute Virus Infection: A Role for Early CCR7-Driven B-T Helper Cell Collaboration. *J. Immunol.* 178:1468–1476.

- Schenkel, J.M., K. a Fraser, V. Vezys, and D. Masopust. 2013. Sensing and alarm function of resident memory CD8<sup>+</sup> T cells. *Nat. Immunol.* 14:509–13.
- Schmid, D. a, M.B. Irving, V. Posevitz, M. Hebeisen, A. Posevitz-Fejfar, J.-C.F. Sarria, R. Gomez-Eerland, M. Thome, T.N.M. Schumacher, P. Romero, D.E. Speiser, V. Zoete, O. Michielin, and N. Rufer. 2010. Evidence for a TCR affinity threshold delimiting maximal CD8 T cell function. *J. Immunol.* 184:4936–46.
- Schodin, B. a, T.J. Tsomides, and D.M. Kranz. 1996. Correlation between the number of T cell receptors required for T cell activation and TCR-ligand affinity. *Immunity.* 5:137–46.
- Scholten, K.B.J., D. Kramer, E.W.M. Kueter, M. Graf, T. Schoedl, C.J.L.M. Meijer, M.W.J. Schreurs, and E. Hooijberg. 2006. Codon modification of T cell receptors allows enhanced functional expression in transgenic human T cells. *Clin. Immunol.* 119:135–45.
- Schulz, O., and C. Reis e Sousa. 2002. Cross-presentation of cell-associated antigens by CD8alpha<sup>+</sup> dendritic cells is attributable to their ability to internalize dead cells. *Immunology.* 107:183–9.
- Schumann, K., T. Lämmermann, M. Bruckner, D.F. Legler, J. Polleux, J.P. Spatz, G. Schuler, R. Förster, M.B. Lutz, L. Sorokin, and M. Sixt. 2010. Immobilized chemokine fields and soluble chemokine gradients cooperatively shape migration patterns of dendritic cells. *Immunity.* 32:703–13.
- Sedgwick, J.D., S. Schwender, H. Imrich, R. Dörries, G.W. Butcher, and V. ter Meulen. 1991. Isolation and direct characterization of resident microglial cells from the normal and inflamed central nervous system. *Proc. Natl. Acad. Sci. U. S. A.* 88:7438–42.
- Sha, W.C., C.A. Nelson, R.D. Newberry, D.M. Kranz, J.H. Russell, and D.Y. Loh. 1988. Positive and negative selection of an antigen receptor on T cells in transgenic mice. *Nature.* 336:73–6.
- Shrestha, B., and M.S. Diamond. 2007. Fas ligand interactions contribute to CD8<sup>+</sup> T-cell-mediated control of West Nile virus infection in the central nervous system. *J. Virol.* 81:11749–57.
- Shrestha, B., M.A. Samuel, S. Michael, and M.S. Diamond. 2006. CD8<sup>+</sup> T Cells Require Perforin To Clear West Nile Virus from Infected Neurons CD8<sup>2</sup> T Cells Require Perforin To Clear West Nile Virus from Infected Neurons. 80.
- Shui, J.-W., J.S. Boomer, J. Han, J. Xu, G. a Dement, G. Zhou, and T.-H. Tan. 2007. Hematopoietic progenitor kinase 1 negatively regulates T cell receptor signaling and T cell-mediated immune responses. *Nat. Immunol.* 8:84–91.
- Singer, A., S. Adoro, and J.-H. Park. 2008. Lineage fate and intense debate: myths, models and mechanisms of CD4- versus CD8-lineage choice. *Nat. Rev. Immunol.* 8:788–801.
- Sixt, M., B. Engelhardt, F. Pausch, R. Hallmann, O. Wendler, and L.M. Sorokin. 2001. Endothelial cell laminin isoforms, laminins 8 and 10, play decisive roles in T cell recruitment across the blood-brain barrier in experimental autoimmune encephalomyelitis. *J. Cell Biol.* 153:933–46.
- Skulina, C., S. Schmidt, K. Dornmair, H. Babbe, A. Roers, K. Rajewsky, H. Wekerle, R. Hohlfeld, and N. Goebels. 2004. Multiple sclerosis: brain-infiltrating CD8<sup>+</sup> T cells persist as clonal expansions in the cerebrospinal fluid and blood. *Proc. Natl. Acad. Sci. U. S. A.* 101:2428–33.
- Smith, C.M., N.S. Wilson, J. Waithman, J. a Villadangos, F.R. Carbone, W.R. Heath, and G.T. Belz. 2004. Cognate CD4(+) T cell licensing of dendritic cells in CD8(+) T cell immunity. *Nat. Immunol.* 5:1143–8.
- Smith-Garvin, J.E., G. a Koretzky, and M.S. Jordan. 2009. T cell activation. *Annu. Rev. Immunol.* 27:591–619.
- Soneoka, Y., P.M. Cannon, E.E. Ramsdale, J.C. Griffiths, G. Romano, S.M. Kingsman, and A.J. Kingsman. 1995. A transient three-plasmid expression system for the production of high titer retroviral vectors. *Nucleic Acids Res.* 23:628–33.
- Speiser, D.E., D. Kyburz, U. Stübi, H. Hengartner, and R.M. Zinkernagel. 1992. Discrepancy between in vitro measurable and in vivo virus neutralizing cytotoxic T cell reactivities. Low T cell receptor specificity and avidity sufficient

- for in vitro proliferation or cytotoxicity to peptide-coated target cells but not for in vivo prot. *J. Immunol.* 149:972–80.
- Spranger, S., I. Jeremias, S. Wilde, M. Leisegang, L. Stärck, B. Mosetter, W. Uckert, M.H.M. Heemskerk, D.J. Schendel, and B. Frankenberger. 2012. TCR-transgenic lymphocytes specific for HMMR/Rhamm limit tumor outgrowth in vivo. *Blood.* 119:3440–9.
- Stärck, L., K. Popp, H. Pircher, and W. Uckert. 2014. Immunotherapy with TCR-redirected T cells: comparison of TCR-transduced and TCR-engineered hematopoietic stem cell-derived T cells. *J. Immunol.* 192:206–13.
- Stefanová, I., B. Hemmer, M. Vergelli, R. Martin, W.E. Biddison, and R.N. Germain. 2003. TCR ligand discrimination is enforced by competing ERK positive and SHP-1 negative feedback pathways. *Nat. Immunol.* 4:248–54.
- Steffen, B.J., E.C. Butcher, and B. Engelhardt. 1994. Evidence for involvement of ICAM-1 and VCAM-1 in lymphocyte interaction with endothelium in experimental autoimmune encephalomyelitis in the central nervous system in the SJL/J mouse. *Am. J. Pathol.* 145:189–201.
- Stein, J. V., a Rot, Y. Luo, M. Narasimhaswamy, H. Nakano, M.D. Gunn, a Matsuzawa, E.J. Quackenbush, M.E. Dorf, and U.H. von Andrian. 2000. The CC chemokine thymus-derived chemotactic agent 4 (TCA-4, secondary lymphoid tissue chemokine, 6Ckine, exodus-2) triggers lymphocyte function-associated antigen 1-mediated arrest of rolling T lymphocytes in peripheral lymph node high endothelial venules. *J. Exp. Med.* 191:61–76.
- Steinman, R.M. 1991. The dendritic cell system and its role in immunogenicity. *Annu. Rev. Immunol.* 9:271–96.
- Steinman, R.M., S. Turley, I. Mellman, and K. Inaba. 2000. The induction of tolerance by dendritic cells that have captured apoptotic cells. *J. Exp. Med.* 191:411–6.
- Stetson, D.B., M. Mohrs, V. Mallet-Designé, L. Teyton, and R.M. Locksley. 2002. Rapid expansion and IL-4 expression by Leishmania-specific naive helper T cells in vivo. *Immunity.* 17:191–200.
- Stiles, L.N., M.P. Hosking, R. a Edwards, R.M. Strieter, and T.E. Lane. 2006. Differential roles for CXCR3 in CD4+ and CD8+ T cell trafficking following viral infection of the CNS. *Eur. J. Immunol.* 36:613–22.
- Stohlman, S. a, C.C. Bergmann, M.T. Lin, D.J. Cua, and D.R. Hinton. 1998. CTL effector function within the central nervous system requires CD4+ T cells. *J. Immunol.* 160:2896–904.
- Stone, J.D., A.S. Chervin, and D.M. Kranz. 2009. T-cell receptor binding affinities and kinetics: impact on T-cell activity and specificity. *Immunology.* 126:165–76.
- Sun, G., X. Liu, P. Mercado, S.R. Jenkinson, M. Kyriiotou, L. Feigenbaum, P. Galéra, and R. Bosselut. 2005. The zinc finger protein cKrox directs CD4 lineage differentiation during intrathymic T cell positive selection. *Nat. Immunol.* 6:373–81.
- Sun, J.C., M. a Williams, and M.J. Bevan. 2004. CD4+ T cells are required for the maintenance, not programming, of memory CD8+ T cells after acute infection. *Nat. Immunol.* 5:927–33.
- Thomas, S., H.J. Stauss, and E.C. Morris. 2010. Molecular immunology lessons from therapeutic T-cell receptor gene transfer. *Immunology.* 129:170–7.
- Toft-Hansen, H., R. Buist, X.-J. Sun, a. Schellenberg, J. Peeling, and T. Owens. 2006. Metalloproteinases Control Brain Inflammation Induced by Pertussis Toxin in Mice Overexpressing the Chemokine CCL2 in the Central Nervous System. *J. Immunol.* 177:7242–7249.
- Torti, N., S.M. Walton, T. Brocker, T. Rülcke, and A. Oxenius. 2011. Non-hematopoietic cells in lymph nodes drive memory CD8 T cell inflation during murine cytomegalovirus infection. *PLoS Pathog.* 7:e1002313.
- Townsend, A., and H. Bodmer. 1989. Antigen recognition by class I-restricted T lymphocytes. *Annu. Rev. Immunol.* 7:601–24.
- Trajkovic, V., O. Vuckovic, S. Stosic-Grujicic, D. Miljkovic, D. Popadic, M. Markovic, V. Bumbasirevic, A. Backovic, I. Cvetkovic, L. Harhaji, Z. Ramic, and M. Mostarica Stojkovic.

2004. Astrocyte-induced regulatory T cells mitigate CNS autoimmunity. *Glia*. 47:168–79.
- Tran, E.H., K. Hoekstra, N. van Rooijen, C.D. Dijkstra, and T. Owens. 1998. Immune invasion of the central nervous system parenchyma and experimental allergic encephalomyelitis, but not leukocyte extravasation from blood, are prevented in macrophage-depleted mice. *J. Immunol.* 161:3767–75.
- Treanor, B. 2012. B-cell receptor: from resting state to activate. *Immunology*. 136:21–7.
- Turner, S.J., P.C. Doherty, J. McCluskey, and J. Rossjohn. 2006. Structural determinants of T-cell receptor bias in immunity. *Nat. Rev. Immunol.* 6:883–94.
- Uckert, W., and T.N.M. Schumacher. 2009. TCR transgenes and transgene cassettes for TCR gene therapy: status in 2008. *Cancer Immunol. Immunother.* 58:809–22.
- Udaka, K., T.J. Tsomides, P. Walden, N. Fukusen, and H.N. Eisen. 1993. A ubiquitous protein is the source of naturally occurring peptides that are recognized by a CD8+ T-cell clone. *Proc. Natl. Acad. Sci. U. S. A.* 90:11272–6.
- Uematsu, Y., S. Ryser, Z. Dembić, P. Borgulya, P. Krimpenfort, a Berns, H. von Boehmer, and M. Steinmetz. 1988. In transgenic mice the introduced functional T cell receptor beta gene prevents expression of endogenous beta genes. *Cell*. 52:831–41.
- Valitutti, S., M. Dessing, K. Aktories, H. Gallati, and A. Lanzavecchia. 1995a. Sustained signaling leading to T cell activation results from prolonged T cell receptor occupancy. Role of T cell actin cytoskeleton. *J. Exp. Med.* 181:577–84.
- Valitutti, S., S. Müller, M. Cella, E. Padovan, and A. Lanzavecchia. 1995. Serial triggering of many T-cell receptors by a few peptide-MHC complexes. *Nature*. 375:148–51.
- Valitutti, S., S. Müller, M. Salio, and A. Lanzavecchia. 1997. Degradation of T cell receptor (TCR)-CD3-zeta complexes after antigenic stimulation. *J. Exp. Med.* 185:1859–64.
- Varma, R., G. Campi, T. Yokosuka, T. Saito, and M.L. Dustin. 2006. T cell receptor-proximal signals are sustained in peripheral microclusters and terminated in the central supramolecular activation cluster. *Immunity*. 25:117–27.
- Veillette, A., S. Latour, and D. Davidson. 2002. Negative regulation of immunoreceptor signaling. *Annu. Rev. Immunol.* 20:669–707.
- Viola, a, and a Lanzavecchia. 1996. T cell activation determined by T cell receptor number and tunable thresholds. *Science*. 273:104–6.
- Wakim, L.M., and M.J. Bevan. 2011. Cross-dressed dendritic cells drive memory CD8+ T-cell activation after viral infection. *Nature*. 471:629–32.
- Walter, B.A., V.A. Valera, S. Takahashi, K. Matsuno, and T. Ushiki. 2006. Evidence of antibody production in the rat cervical lymph nodes after antigen administration into the cerebrospinal fluid. *Arch. Histol. Cytol.* 69:37–47.
- Walter, E. a, P.D. Greenberg, M.J. Gilbert, R.J. Finch, K.S. Watanabe, E.D. Thomas, and S.R. Riddell. 1995. Reconstitution of cellular immunity against cytomegalovirus in recipients of allogeneic bone marrow by transfer of T-cell clones from the donor. *N. Engl. J. Med.* 333:1038–44.
- Wilson R.K., Lai E, Concannon P, Barth RK, Hood LE. Structure, organization and polymorphism of murine and human T-cell receptor alpha and beta chain gene families. *Immunolog. Reviews* 101, 149-172 (1988)
- Weiss, S.R., and S. Navas-Martin. 2005. Coronavirus pathogenesis and the emerging pathogen severe acute respiratory syndrome coronavirus. *Microbiol. Mol. Biol. Rev.* 69:635–64.
- Wherry, E.J., S.-J. Ha, S.M. Kaech, W.N. Haining, S. Sarkar, V. Kalia, S. Subramaniam, J.N. Blattman, D.L. Barber, and R. Ahmed. 2007. Molecular signature of CD8+ T cell exhaustion during chronic viral infection. *Immunity*. 27:670–84.



- Whitmire, J.K., N. Benning, and J.L. Whitton. 2006. Precursor Frequency, Nonlinear Proliferation, and Functional Maturation of Virus-Specific CD4+ T Cells. *J. Immunol.* 176:3028–3036.
- Wilde, S., D. Sommermeyer, B. Frankenberger, M. Schiemann, S. Milosevic, S. Spranger, H. Pohla, W. Uckert, D.H. Busch, and D.J. Schendel. 2009. Dendritic cells pulsed with RNA encoding allogeneic MHC and antigen induce T cells with superior antitumor activity and higher TCR functional avidity. *Blood.* 114:2131–9.
- Wilson, E.H., T.H. Harris, P. Mrass, B. John, E.D. Tait, G.F. Wu, M. Pepper, E.J. Wherry, F. Dzierzinski, D. Roos, P.G. Haydon, T.M. Laufer, W. Weninger, and C. a Hunter. 2009. Behavior of parasite-specific effector CD8+ T cells in the brain and visualization of a kinesis-associated system of reticular fibers. *Immunity.* 30:300–11..
- Worbs, T., T.R. Mempel, J. Böhler, U.H. Von Andrian, and R. Förster. 2007. CCR7 ligands stimulate the intranodal motility of T lymphocytes in vivo. 204:489–495.
- Wurbel, M. -a. 2001. Mice lacking the CCR9 CC-chemokine receptor show a mild impairment of early T- and B-cell development and a reduction in T-cell receptor gamma delta + gut intraepithelial lymphocytes. *Blood.* 98:2626–2632.
- Yasuda, T., K. Bundo, A. Hino, K. Honda, A. Inoue, M. Shirakata, M. Osawa, T. Tamura, H. Nariuchi, H. Oda, T. Yamamoto, and Y. Yamanashi. 2007. Dok-1 and Dok-2 are negative regulators of T cell receptor signaling. *Int. Immunol.* 19:487–95.
- Yasutomo, K., C. Doyle, L. Miele, C. Fuchs, and R.N. Germain. 2000. The duration of antigen receptor signalling determines CD4+ versus CD8+ T-cell lineage fate. *Nature.* 404:506–10.
- Yednock, T.A., C. Cannon, L.C. Fritz, F. Sanchez-Madrid, L. Steinman, and N. Karin. 1992. Prevention of experimental autoimmune encephalomyelitis by antibodies against alpha 4 beta 1 integrin. *Nature.* 356:63–6.
- Yee, C., P. a Savage, P.P. Lee, M.M. Davis, and P.D. Greenberg. 1999. Isolation of high avidity melanoma-reactive CTL from heterogeneous populations using peptide-MHC tetramers. *J. Immunol.* 162:2227–34.
- Yoon, H., T.S. Kim, and T.J. Braciale. 2010. The cell cycle time of CD8+ T cells responding in vivo is controlled by the type of antigenic stimulus. *PLoS One.* 5:e15423.
- Yu, Q., B. Erman, a. Bhandoola, S.O. Sharrow, and a. Singer. 2003. In Vitro Evidence That Cytokine Receptor Signals Are Required for Differentiation of Double Positive Thymocytes into Functionally Mature CD8+ T Cells. *J. Exp. Med.* 197:475–487.
- Zeh, H.J., D. Perry-Lalley, M.E. Dudley, S. a Rosenberg, and J.C. Yang. 1999. High avidity CTLs for two self-antigens demonstrate superior in vitro and in vivo antitumor efficacy. *J. Immunol.* 162:989–94.
- Zehn, D., S.Y. Lee, and M.J. Bevan. 2009. Complete but curtailed T-cell response to very low-affinity antigen. *Nature.* 458:211–4.
- Zhang, N., and M.J. Bevan. 2011. CD8(+) T cells: foot soldiers of the immune system. *Immunity.* 35:161–8.
- Zhao, Y., Z. Zheng, P.F. Robbins, H.T. Khong, S. a. Rosenberg, and R. a. Morgan. 2005. Primary Human Lymphocytes Transduced with NY-ESO-1 Antigen-Specific TCR Genes Recognize and Kill Diverse Human Tumor Cell Lines. *J. Immunol.* 174:4415–4423.
- Zhong, S., K. Malecek, L. a Johnson, Z. Yu, E. Vega-Saenz de Miera, F. Darvishian, K. McGary, K. Huang, J. Boyer, E. Corse, Y. Shao, S. a Rosenberg, N.P. Restifo, I. Osman, and M. Krogsgaard. 2013. T-cell receptor affinity and avidity defines antitumor response and autoimmunity in T-cell immunotherapy. *Proc. Natl. Acad. Sci. U. S. A.* 110:6973–8.
- Zhou, J., D.R. Hinton, S.A. Stohlman, C. Liu, L. Zhong, and N.W. Marten. 2005. Maintenance of CD8+ T cells during acute viral infection of the central nervous system requires CD4+ T cells but not interleukin-2. *Viral Immunol.* 18:162–9.
- Zinselmeyer, B.H., S. Heydari, C. Sacristán, D. Nayak, M. Cammer, J. Herz, X. Cheng, S.J. Davis, M.L. Dustin, and D.B. McGavern. 2013. PD-1 promotes immune exhaustion by

- inducing antiviral T cell motility paralysis. *J. Exp. Med.* 210:757–74.
- Zuklys, S., G. Balciunaite, a. Agarwal, E. Fasler-Kan, E. Palmer, and G. a. Hollander. 2000. Normal Thymic Architecture and Negative Selection Are Associated with Aire Expression, the Gene Defective in the Autoimmune-Polyendocrinopathy-Candidiasis-Ectodermal Dystrophy (APECED). *J. Immunol.* 165:1976–1983.
- Züst, R., L. Cervantes-Barragán, T. Kuri, G. Blakqori, F. Weber, B. Ludewig, and V. Thiel. 2007. Coronavirus non-structural protein 1 is a major pathogenicity factor: implications for the rational design of coronavirus vaccines. *PLoS Pathog.* 3:e109.

## 9.2 Figure legend

<b>Figure 1.</b> T cell development. ....	11
<b>Figure 2.</b> Generation of TCR diversity by somatic recombination of TCR gene segments. ...	16
<b>Figure 3.</b> Components of TCR signalosome and their interactions. ....	24
<b>Figure 4.</b> Structure of the brain meninges and blood vessels. ....	37
<b>Figure 5.</b> Generation of MHV s598-specific hybridoma cells. ....	59
<b>Figure 6.</b> Characterization of the s598-specific TCR. ....	60
<b>Figure 7.</b> Analysis of s598-specific transgenic founder mice. ....	61
<b>Figure 8.</b> Comparison of transgenic TCR expression in three different founder lines. ....	63
<b>Figure 9.</b> In vitro functionality of Spiky transgenic splenocytes. ....	64
<b>Figure 10.</b> Distribution of MHV in the CNS and concomitant upregulation of CCR7 ligands. ....	78
<b>Figure 11.</b> CNS-resident cellular components involved in the production of CCR7 ligands. ....	81
<b>Figure 12.</b> CCR7 ligands control MHV CNS infection and prevent severe disease. ....	83
<b>Figure 13.</b> Activation and recruitment of MHV-specific CD8 <sup>+</sup> T cells to the infected CNS. ....	85
<b>Figure 14.</b> CCR7-proficient T cells protect against MHV induced neuroinflammation. ....	86
<b>Figure 15.</b> Expression of CCR7 ligands in the CNS controls CD8 <sup>+</sup> T cell recruitment and function. ....	87
<b>Figure S16.</b> Chemokine CXCR3 is not necessary for the control of MHV induced inflammation. ....	91
<b>Figure S17.</b> Functionality of CNS-infiltrating Spiky transgenic CD8 <sup>+</sup> T cells. ....	92
<b>Figure 18.</b> Endogenous CD8 <sup>+</sup> T cell responses during MHV infection. ....	109
<b>Figure 19.</b> Characteristics of retrogenic s598-specific CD8 <sup>+</sup> T cells. ....	111
<b>Figure 20.</b> Tunable expression of s598-specific TCR. ....	113
<b>Figure 21.</b> TCR expression levels critically determine CD8 <sup>+</sup> T cell activation threshold and intensity of the proliferative response. ....	115
<b>Figure 22.</b> Model-based analysis of TCR-density-dependent CD8 <sup>+</sup> T cell performance. ....	117
<b>Figure 23.</b> In vivo protective capacity of TCR retrogenic CD8 <sup>+</sup> T cells. ....	119

### 9.3 Abbreviations

7AAD	Aminoactinomycin D
ADAP	Adhesion and degranulation promoting adapter protein
AIRE	Autoimmune regulator
ALT	Alanine aminotransferase
Apaf	Apoptotic protease activating factor
APC	Antigen presenting cell
ATT	Adoptive T cell therapy
B6	C57BL/5
BCR	B cell receptor
BRS	Basic residue rich sequence
BSS	Balanced Salt Solution
CAM	Cell adhesion molecule
CCL	CC chemokine ligand
CCR	CC chemokine receptor
cDNA	Complementary deoxyribonucleic acid
CDR	Complementary determining region
CEACAM1a	Carcinoembryonic antigen-related cell adhesion molecule
CFSE	Carboxyfluorescein succinimidyl ester
CNS	Central nervous system
CSF	Cerebrospinal fluid
cTEC	Cortical thymic epithelial cell
CTL	Cytotoxic T lymphocyte
CTLA	Cytotoxic T lymphocyte antigen
CXCR	C-X-C chemokine receptor
DC	Dendritic cell

---

DMEM	Dulbecco's Modified Eagle's minimal essential medium
EAE	Experimental autoimmune encephalitis
EBV	Epstein-Barr Virus
EC	Endothelial cell
EDTA	Ethylenediaminetetraacetic acid
ERGIC	Endoplasmic reticulum Golgi intermediate complex
ERK	Extracellular signal-regulated kinases
EYFP	Enhanced Yellow Florescent Protein
FADD	Fas-Associated protein with Death Domain
FCS	Fetal calf serum
FITC	Fluorescein isothiocyanate
FRC	Fibroblastic Reticular Cells
GFP	Green fluorescent protein
GM-CSF	Granulocyte-macrophage colony-stimulating factor
HAT	Hypoxanthine-aminopterin-thymidine
HCoV	Human Coronavirus
HEPES	2-[4-(2-hydroxyethyl)piperazin-1-yl]ethanesulfonic acid
HEV	High endothelial venul
HSC	Hematopoietic stem cells
ICAM1	Intercellular adhesion molecule 1
ICOS	Inducible T-cell co-stimulator
IFN-g	Interferon-g
IL	Interleukin
IS	Immunological synapse
ITAM	immunereceptortyrosin based activation motif
ITK	Interleukin-2-inducible T-cell kinase
LAT	Linker for Activation
LCK	Lymphocyte-specific protein tyrosine kinase

LCMV	Lymphocytic choriomeningitis virus
LFA1	Lymphocyte associated antigen 1
LN	Lymph node
MAPK	Mitogen-activated protein kinases
MART-I	Melanoma antigen recognized by T-cells
MCMV	Murine cytomegalovirus
Mers-Cov	The Middle East respiratory syndrome coronavirus
MESF	Molecules of equivalent soluble fluorochrome
MHC	major histocompatibility complex
MHV	Mouse hepatitis virus
MMPs	Matrix metalloproteinases
mRNA	Messenger Ribonucleic acid
MS	Multiple sclerosis
mTEC	Medullary thymic epithelial cell
MTOC	Microtubule-organizing center
NEAA	Non essential amino acids
NF-kB	Nuclear factor kappa-light-chain-enhancer of activated B cell
NFAT	Nuclear factor of activated T-cells
PAG	Phosphoprotein associated with glycosphingolipid
PAMP	Pathogen associated molecular pattern
PBS	Phosphate buffered saline
PCR	Polymerase chain reaction
PD-1	Programmed death 1
PDPN	Podoplanin
PE	Phycoerythrin
PEG	Polyethylene Glycol
PerCP	Peridinin Chlorophyll protein
pfu	Plaque forming unit

---

PKCq	Protein kinase C theta type
PMA	Phorbolmyristate acetate
PNAd	Peripheral-node addressin
PRR	Pattern recognition receptor
PSGL1	Platelet selectin glycoprotein ligand
PTP CD45	Protein tyrosine phosphatases
PTPN22	Protein tyrosine phosphatase, non-receptor type 22 (lymphoid)
RAG	Recombination activating gene
Rg	Retrogenic mice
RPMI	Roswell Park Memorial Institute medium
RSS	Recombination signal sequence
S1P1	Sphingosine-1-phosphate receptor 1
SARS-CoV	Severe acute respiratory syndrome
SLO	Secondary lymphoid organ
SLP76	SH2-domain-containing leukocyte protein of 76kDa
SMAC	Supramolecular adhesion complex
SRC	proto-oncogene tyrosine-protein kinase
TBP	TATA-binding protein
TCR	T cell receptor
TGF-b	Tumor growth factor b
TNF	Tumor necrosis factor
TNFRSF	Tumor necrosis factor receptor superfamily
VCAM	Vascular cell adhesion molecule
ZAP70	Zeta-chain-associated protein kinase 70

## 9.4 Acknowledgments

Being on my own in the “big world” taught me an important lesson: It doesn’t matter in life what material wealth you possess - it comes and goes all the time. What matters are the skills and knowledge you bring with yourself wherever you go; what matters are the people you know who share with you both the happiness and the sorrow and help you make the best of both. Therefore, I am grateful to all people I have met during my PhD journey who helped me to learn, to change, to experience and to laugh.

Like for all big decisions in life I have asked my Dad’s opinion which lab in Switzerland I should choose for my PhD. He told me: “Go to St. Gallen, it sounds like the Professor that runs the lab is a true mentor and he will teach you good science and guide you through your research.” And as always, my Dad was right. I have chosen not only a great mentor and scientist, but also a great person. I am beyond grateful to my mentor Burkhard Ludewig for all the support and motivation that kept me going when it was tough. Words cannot fully express my gratitude for past five years, but I am happy I have got the extra time in your lab to try to express them through my work.

I would like to thank my ETH supervisor Wolf-Dietrich Hardt for great advice and support of my work over the past five years. I am very grateful to Annette Oxenius for accepting to join my thesis committee in the later stage, and also for all the support for my PhD work.

My dear Rita, thank you for always being there for me. Thank you for your brilliant technical help and your most reassuring, supportive and caring attitude. You always made me feel safe!



Lucas, I always admired your scientific thinking and your calmness. Thank you for your most amazing work that made Spiky proud of being in the story together with your microscopy. And thank you for your help in and out of the lab.

My dear Sonja, you have contributed so much to me as a scientist and as a person. Along with all the things you have done for me, teaching me how to inject i.v. and translating my summary to German will be “written in stone” and I will always mention and remember you for this.

I would like to thank my “amigos” Cristina and Christian for being great support in the lab, fantastic collaborators and even greater friends.

Dear Ursula, thank you for always being so kind and taking such great care of all our administrative needs. And thank you for the talk we had that day, it meant the world to me.

Harinda Wewelwala, thank you for taking such good care of Spiky and making sure that I have something to eat during long weekend experiments.

Dear Fabienne, thank you so much for helping with mice work and always being so swift and well organized.

Mario, thank you for proof-reading my writings. I enjoy our chatting and picking up the differences between our two languages.

Elke, thank you for your great advice and your care.

Other members of IMMBIO: Urs, Hung-Wei, Flurin, Annalisa and Marichita, thank you for making every lab day better and more enjoyable.

Further, I am thankful to collaborators who greatly contributed to my work. Gennady Bocharov for modelling my data, making complicated mathematics understandable to a biologist like myself and for most helpful and exciting discussions. Lilian Stärck for bringing the world of retrogenic mice to me and helping me establish the system in our lab. Moreover, thank you for introducing the non-scientific side of Berlin to me - I have greatly enjoyed it.

I am extremely grateful to our former lab members Veronika, Eveline, Luisa, Qian, Roland, Matthias, Ronald, Monika, Eva and Karin. It was a great pleasure working with you all.

Veronika, thank you for supporting my baby steps into TCR cloning and lab techniques. I enjoyed our discussions on scientific and non-scientific topics a lot. I miss you so much. Your Rosalie is blooming beautifully.

Eveline, thank you for being there for me. I enjoyed our RNA isolation almost equally as our margarita time. I miss you here.

Luisa, thank you for bringing me into immunology. I still keep the first ICS protocol you gave me and remember the first experiment we did together staying till 2 a.m.. You primed me and like a well-behaved T cell I have kept going like that. We all miss you.

Finally, I am beyond grateful to my family, my Mom, Dad and my brother for supporting my dream, being understanding for all the missed holidays, motivating me, being my strength and putting the example to me how to never-ever give up.

Thank you, Daddy for teaching me to always give the best of myself and providing me with all I needed to live my dream. I will miss our discussions, I will miss your way of thinking and your lectures on life and science and above all I will miss you!

I promise you – I will never stop questioning and exploring - just like you taught me!

## **9.5 Curriculum Vitae**